Doctorate Thesis

博士論文

# Graphics by Computational Acoustic Fields

(計算機音響場によるグラフィクス表現)

Yoichi Ochiai

落合 陽一

# Graphics by Computational Acoustic Fields

Beyond symbolic machines towards field oriented programmable matters

Yoichi Ochiai

School of Interdisciplinary Information Studies, The University of Tokyo

Abstract

We propose a method for realizing a new expression of Computer Graphics that expands their malleability towards physical materials in the real world. Our method utilizes an acoustic field that is calculated, generated, and controlled by computers. By applying such computational acoustic fields and physical phenomena around the field, we can transform the characteristics of real-world objects. These altered materials have a malleability that is similar to the Computer Graphics model. This concept is also applicable to other methods (e.g., self-actuation, hybrid methods) that consider programmable matters.

The resulting system can be applied to display technologies such as Computer Graphics, Entertainment Computing, and Human Interfaces. We develop an optical programmable screen whose view angle can be set between 2 and 175°. Various expressions can be obtained by controlling the view angle dynamically. We then derive a haptic transformation that can modify uneven surfaces by up to 50 μm by controlling the thickness of the squeeze film effect. Finally, we present an acoustic levitation method that can levitate objects of up to 1 g (7.8 g/cm$^3$) and move particles at up to 72 cm/s using ultrasonic phased arrays.

This thesis introduces the theory and design of general Computational Fields, with a specific emphasis on Computational Acoustic Fields. We implement and evaluate three types of systems based on acoustic fields. The first changes the optical state of a colloidal screen by 3D acoustic fields, the second applies a haptic transformation to physical material under time-divided 2D acoustic fields, and the third uses acoustic manipulation in a 3D acoustic potential field. Like materials in Computer Graphics, the characteristics of real-world materials can be altered by Computational Fields. Finally, we discuss the advantages and limitations of our method.

Thesis Supervisor:

Jun Rekimoto

Professor of Interdisciplinary Information Studies

The University of Tokyo

# 計算機音響場によるグラフィクス表現

環境型プログラマブルマターの実現に向けて

落合陽一

東京大学大学院学際情報学府総合分析情報学コース

要旨

コンピュータグラフィクス表現における可塑性を現実の物体にも与えるような新たな表現手法を本論文で提案する．提案手法を実現するため，計算機によって計算され，生成され，制御された音響場である計算機音響場を用いて，音響場と音響場に付随する物理現象を応用することで実世界の事物の物理的性質を変化させる．提案手法によって駆動された実世界の事物はコンピュータグラフィクス表現のような可塑性を持ち，音響場の制御によって見た目や手触り，三次元位置などを動的に変更することができる．このような音響場を制御することによる環境型のプログラマブルマターというコンセプトは近年増えつつある他のプログラマブルマターに関する手法を整理する上でも有用である．

本論文で得られた成果はディスプレイ技術や，コンピュータグラフィクス表現，エンターテイメントコンピューティングやヒューマンインターフェースの発展に寄与すると考えられる．本論文の２章で紹介する２度から１７５度までプログラム可能な視野角を持つ光学的スクリーンは複数光源を用いた３D 表現や時分割重畳による質感表現 (1 次元 BRDF 表現＋２次元画像の重畳 ) に応用可能である。また３章で紹介するアナログな物体の手触りをスクイーズ膜効果によって変える研究では，50um 分の凹凸の触覚を消したり書き換えたりできることを示し，共振周波数制御によって人間が触れても安定的に触覚提示が行えるようなディスプレイを開発した．それに加え４章ではフェーズドアレイ技術を用いて音響浮揚技術を３次元的に拡大し，既存のワークスペースを拡張したほか，最大１g (7.8 g/cm$^3$) のものを浮揚させ，７２cm/ 秒のスピードで動かすことに成功した. これは新たなディスプレイ表現やマニピュレーション用途に応用可能である．

本論文の構成は下記のようなものになる．まず一般的に計算機を用いた物理場の制御における理論とデザイン手法をまとめる．これは現状用いられている物理場の制御に関してグラフィクスやインターフェース用途の観点からまとめたものである．その後計算機音響場と本論文で用いる性質について述べる．その後，２章でコロイド溶液を用いたスクリーンの開発，３章でスクイーズ膜効果を用いた触覚変容技術の開発，４章で３次元音響浮揚技術とそれを用いたグラフィクス技術について述べる．各２，３，４章に個別に議論は含むが，５章にてより一般的な議論を述べた後，６章の結論にて結ぶ.

博士指導教官 :

暦本純一　教授

東京大学学際情報学府

# Graphics by Computational Acoustic Fields

Beyond symbolic machines towards field oriented programmable matters

Yoichi Ochiai

The following people served as readers for this thesis:

Thesis Reader

Jun Rekimoto
Professor of Interdisciplinary Information Studies,
The University of Tokyo

Thesis Reader

Ken Sakamura
Professor of Interdisciplinary Information Studies,
The University of Tokyo

Thesis Reader

Noboru Koshizuka
Professor of Interdisciplinary Information Studies,
The University of Tokyo

Thesis Reader

Takeo Igarashi
Professor of Department of Computer Science,
Graduate School of Information Science and Technology,
The University of Tokyo

Thesis Reader

Hiroyuki Shinoda
Professor of Department of Complexity Science and Engineering,
Graduate School of Frontier Sciences,
The University of Tokyo

## Contents 5

**List of Figures ( Chapter1 )**

**List of Figures ( Chapter2 )**

**List of Figures ( Chapter3 )**



**List of Figures ( Chapter4 )**

**List of Figures (Chapter 5)**

## List of Tables

## Acknowledgement

This thesis has several projects and every project has involved a team of collaborators.
First, I would like to thank Jun Rekimoto for providing the support and inspiration to pursue this work. He has been an insightful advisor, and this work could not have been completed anywhere besides Rekimoto Laboratory.
Second, I would like to thank Takayuki Hoshi for discussion and collaboration to pursue this work. This work could not have been completed without him.
Third, I would like to thank my thesis readers. I am grateful to Ken Sakamura, Noboru Koshizuka, Takeo Igarashi, and Hiroyuki Shinoda for their advise and comments for this thesis.
Fourth, I would like to thank my major collaborators on the project. I am grateful to Alexis Oyama for discussion with him that inspire me to develop colloidal display. I owe many thanks to Masaya Takasaki and Daisuke Yamaguchi for developing Diminished Haptics. Discussion with Hiromi Nakamura and Shogo Yamashita plays very important role in organizing the concept of Computational Fields.
Several chapters of this thesis are based on work that has been coauthored and previously published. Chapters 2,4 was written with Takayuki Hoshi and Jun Rekimoto. Chapter 3 was written with Takayuki Hoshi and Daisuke Yamaguchi.
This project has been funded by JSPS (Kakenhi 25-9313).
My greatest supporters through this process – Three years of my life – have been my fiancé Ayumi who put my individual productivity in perspective as the joy of their lives lights up smaller accomplishments like this thesis along the path of living. Thank you. You are the most important people to me and have kept me balanced in these years at The University of Tokyo. I love you all without bounds, and this work is dedicated to you. May our lives be filled with insight, joy and love.

# 謝辞

本論文を書き上げるにあたり，様々な方々のご協力とご指導を頂きました．心より御礼申し上げます．東京大学大学院情報学環暦本純一教授には，本論文の指導はもとより，2011 年度から修士課程および博士課程と 4 年間の長きにわたり，研究テーマについての考え方，研究室での生活の仕方までご助言いただきました．これらの研究は氏の寛大な指導の下以外では成し得ず，また修士課程博士課程での氏のご指導なくしては著者は研究の道に進むことはなかったと考えます．公私共々お忙しい中本当にたくさんのご指導を頂きました．ここに深く感謝し，重ねて御礼申し上げます．

同大学大学院情報学環坂村健教授と越塚登教授には，博士論文審査委員でのご指導とともに，本研究の節目には必ず客観的で的確なご指導をいただき，また著者に活を入れる温かなご助言をいただきました．深く感謝申し上げます．また，同大学情報学環総合分析情報学コースの先生方からも同様に，毎年の研究の節目である博士コロキアムで多大なご助言をいただきました．皆様に御礼申し上げます．博士論文審査委員として論文構成についてご指導頂きました東京大学大学院新領域創成科学研究科複雑理工学専攻　篠田裕之教授には，定量的な記述についてまた，専門的な見地から暖かいご指導を賜りました．また同じく博士論文審査委員として論文構成についてご指導頂きました東京大学大学院情報理工学系研究科コンピュータ科学専攻五十嵐健夫教授には，論文全体や章の構成，細部に至るまできめ細かなご助言とご指導を賜りました．より専門的な知見から本研究の広がりや，関連研究との位置づけについて詳細なご助言をいただきました．深く感謝いたします．

また本研究を行うにあたり，名古屋工業大学星貴之テニュアトラック助教には投稿論文の執筆のご指導のみならず，実装，研究手法等，公私共々大変お世話になりました．ここに深く感謝いたします．また，２章，３章，４章の研究の元になった投稿論文での共著者である埼玉大学工学部工学科の高崎正也教授および山口大介助教にも大変お世話になりました．ここに深く感謝いたします．それに加え，２章の投稿論文の共著者であるアレックスオオヤマ氏，１章に関わるディスカッションを共に行った同研究室の中村裕美博士，山下聖悟氏にもここに深く感謝いたします．

上に挙げた方々以外にも研究活動を行うにあたり，様々な方にご助言とご助力をいただきました．東京大学大学院情報学環暦本研究室メンバーである研究員，秘書と学生の皆様には常日頃から大変ご迷惑をおかけしましたが，いつも寛大な皆様のおかげで博士論文を書き上げることができました．最後に，研究活動を行うにあたり，心の支えとなってくださった家族と婚約者である亜由美に感謝いたします．皆様ありがとうございました．

*This work is dedicated to my family*

# 1.Introduction: Research towards Computational Fields

*"The ultimate display would, of course, be a room within which the computer can control the existence of matter. A chair displayed in such a room would be good enough to sit in. Handcuffs displayed in such a room would be confining, and a bullet displayed in such a room would be fatal. With appropriate programming such a display could literally be the Wonderland into which Alice walked."*

*Ivan E. Sutherland, The Ultimate Display, 1965.*

## 1.1. Introduction

In 1965, Ivan Sutherland stated that the ultimate display is a room that can control the existence of matter [1] (Figure 1.2). We strongly agree with his vision, and envision that digital resources should be accessible as freely as non-digital resources (e.g., physical objects). We also believe that non-digital material should be as malleable as digital material (e.g., data) in digital resources (e.g., computers).

Continuous efforts are being made to extend user interfaces (UIs) toward seamless interaction between digital resources and the real world. Conventional methods of real-world oriented UIs involve filling the gap between the physical existence of digital resources and data in digital resources. For example, Graphical UIs (GUIs) have a gap between their screens and the physical world [2] (Figure 1.1(b)). There is a difference between the shape of screens and shape of the digital content on the screens. To overcome this restriction, two approaches have been discussed since the 1990s. The first overlays information onto matter (Tangible Bits (Figure 1.1(c), Figure 1.3) [5] and projection augmented reality (AR) [6] (Figure 1.1(c))), and the second overlays information on the human side (known as "looking through the computer" (Figure 1.1(d), Figure 1.4) [7][8]]).

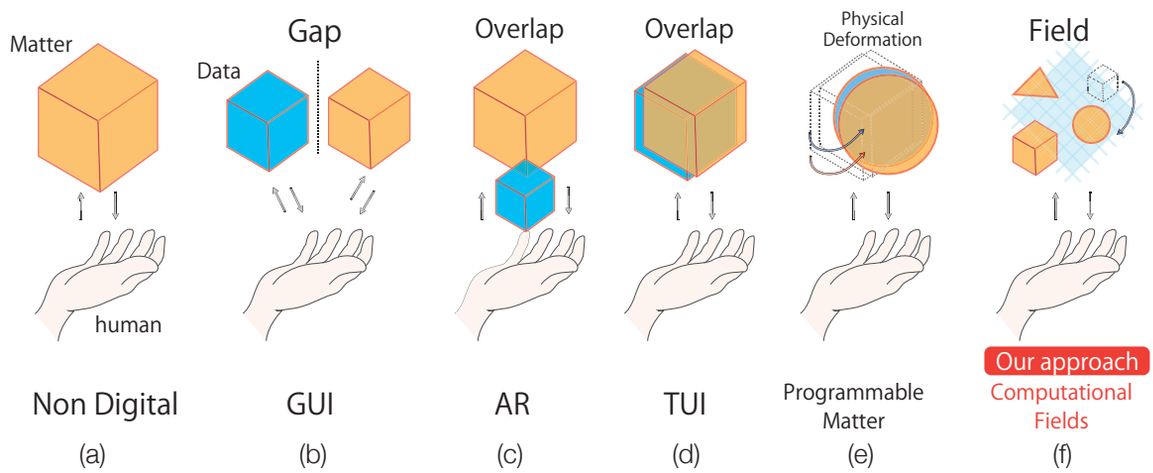


Figure 1.1: Conventional UIs and our approach: Computational Fields. Blue cubes represent data in digital resources, orange cube represent the physical shape in real world. GUI has the difference between physical shape of hardware and graphics in the screen. AR overlaps graphics onto matters via screen. Physical shape of TUI represent data in digital resources. Programmable matter changes its physical shape corresponding to data in digital resources. Computational Fields is the methods to realize programmable matter by environmental actuation utilizing the field quantities.

These approaches aim to increase the accessibility of information in digital resources. They are not restricted to visual approaches, but also include kinetic motion and can display other sensations such as sound, haptic, odor, and so on. Recently, some concepts have been proposed that would allow physical matter in the real world to be controlled by digital resources (Figure 1.1(e)) [10][11][12][13]. These concepts increase the accessibility of digital resources.

In this chapter, we introduce the concept of “Computational Fields” to classify a means of environmental actuation (Figure 1.1(f)). We define the framework of Computational Fields to consider the actuation of “Fields” in which physical quantities (e.g., light, electricity, magnetism, and acoustics) are simulated, generated, and controlled by digital resources. The method of handling field quantities is not new, but this framework enables us to clarify how to alter the physical environment by appropriate field design (Figure 1.5). The framework is also useful for summarizing the increasing interest in “field-oriented programmable matter,” which is a kind of programmable matter [10][11][12][13] whose distribution is driven by Computational Fields. In this thesis, we focus on Computational Acoustic Fields. To clarify the characteristics of Computational Acoustic Fields, we first introduce the framework of general Computational Fields.

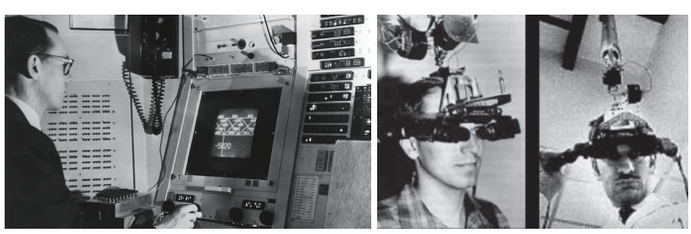

Figure 1.2: SketchPad and Ultimate Display [1]

Figure 1.3: Example of TUI [5]

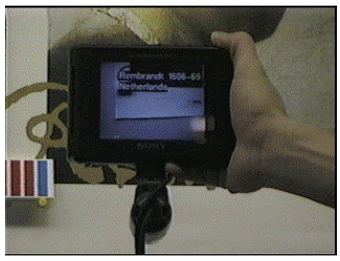

Figure 1.4: NaviCam [2]

There are two methods for enhancing the programmability of the real world: self-actuation and environmental actuation (Figure 1.6). Our idea is a type of environmental actuation. Self-actuation suffers from restrictions in the shape and size of the target objects that implement the actuation modules. The space needed to implement an actuator increases the volume of the system, and this increases the awareness of the machines. In contrast, environmental actuation requires no specific physical modules. In this case, energy is distributed in space, and matter is affected by this distribution. This idea leads to our vision Computational Fields, which focus on fields instead of matter.

Environmental actuation itself is not new. However, in terms of realizing programmable matter, it is useful to consider the unified concept of calculating, generating, and controlling fields. It is also important to discuss the different characteristics of field quantities. The framework of Computational Fields operates similarly to the “graphics pipeline” in Computer Graphics. Establishing a design method for field-oriented programmable matter is a new concept, and it is therefore necessary to compare different approaches (e.g., differences in controllable materials, noncontact forces, control methods).

We believe that field-oriented programmable matter is one means of realizing Calm Technology [3], i.e., a technology that informs us but does not demand our focus or attention. Mark Weiser suggested the vision of Calm Technology in 1996 [3]. Some two decades on, our daily lives are surrounded by computers [5]. As Weiser pointed out, calmness is a fundamental challenge for all technological design for the next 50 years; we are now facing issues related to calmness. We also agree with his vision, and his statement that

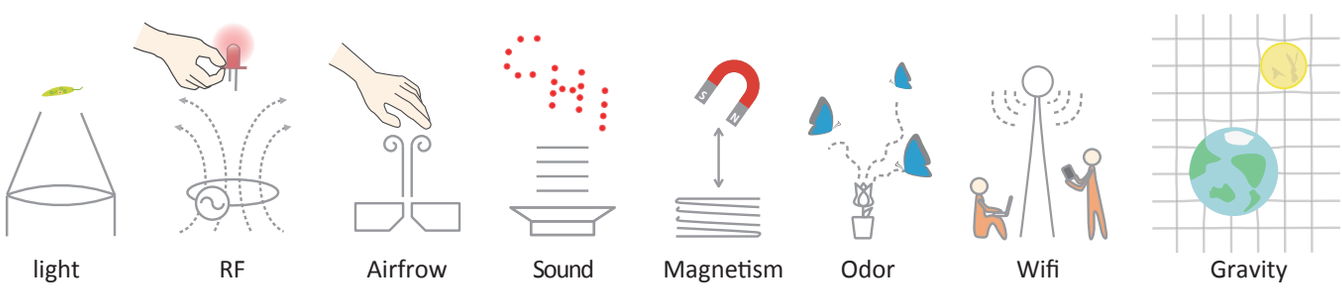


Figure 1.5: Examples included in our vision: Computational Fields. Technologies and Fields are drawn in gray. We describe mainly (a)-(e) in this thesis. (f)-(h) situations are described in discussion part. (a): optical manipulation of euglena, (b): LED remotely powered by RF, (c): tactile stimulation by air-jet, (d): levitation graphics by acoustic potential field, (e): magnetic force, (f): butterflies attracted by fragrant flower (g): humans searching wifi area (h): celestial bodies governed by gravity.

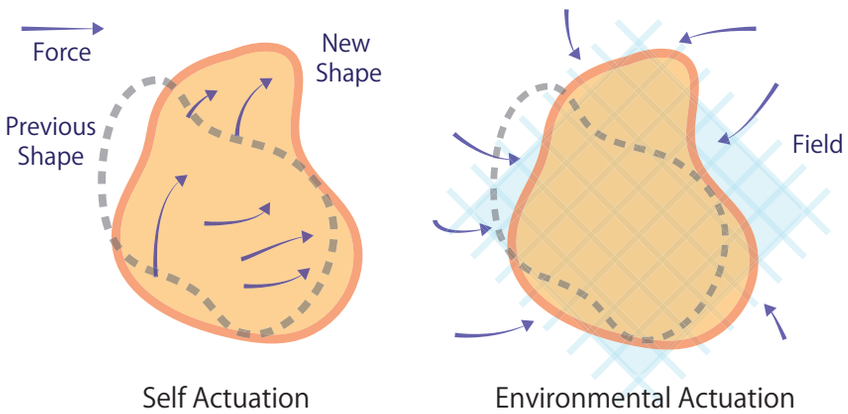


Figure 1.6: Self-actuated versus environmental actuation.

what matters is not technology itself, but its relationship to us—we believe technology can contribute towards the ideal of calmness. A vision designed with an appropriate combination of scientific aspects, technology, design, and implementation can drive us toward a solution for calmness, i.e., awareness of ubiquitous computers [3]. We believe this problem can be solved if ubiquitous or pervasive computers can alter the real world to be "programmable" by hidden and separated actuators. In this case, the technology itself (digital resources or machines) is hidden, and the actuation targets are mixed with other non-digital objects. These are not distinguishable until they are actuated or activated, and therefore do not require our attention unnecessarily.

Naturally, physical media (photons, vibrations of air) are required to transmit information between computers and humans. The means of transmitting information has been implemented in two approaches. The first considers actuators to directly stimulate humans, and the second considers actuators to move and/or alter physical matter, with humans interacting with these objects (which we define as programmable matter). In both approaches, remoteness is one of the keys to realizing calmness, because digital content is separated from the specific hardware by remote technologies. Remote technologies such as optical, acoustic, olfactory, and recent noncontact tactile displays have been developed for the first approach. For the second approach, most actuation technologies still require contact for actuation and/or support, although the possibility of environmental actuation for a UI has recently been demonstrated. We redefine these environmental actuation technologies to realize environmentally actuated programmable matter in a unified manner, the so-called Computational Fields. In the first approach, light, sound, odor, and force fields are generated and designed. In the second approach, physical matter is manipulated by the designed force field. In other words, we focus on the fields rather than the actuators and matter. By separating programmable matter into matter and fields, the range of selectivity of the programmable matter (combination of material and motion) is

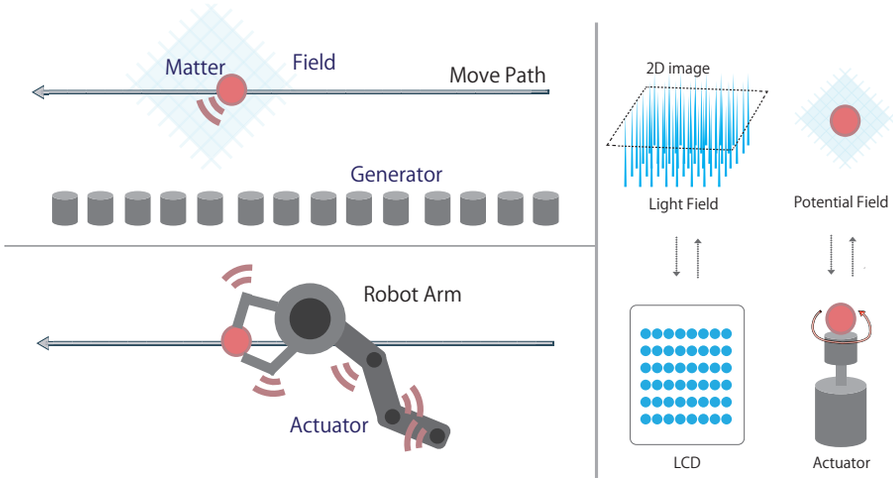


Figure 1.7: (Left) Comparison of conventional actuation versus field actuation ( movement of matter along same move path) and (right) conventional interface versus Computational Fields.

increased. Moreover, separation of matter and fields reduces the awareness of specific machines (e.g., display hardware, robots) (Figure 1.7). This contributes to the realization of calmness in machines.

Real-world oriented interaction consists of input (sensing) and output (displaying). For the input, existing technologies are based on the fields of physical quantities (e.g., light field, magnetic field). For the output, whereas visual displays are described as light-field generators, most technologies for the actuation of objects still require contact. We therefore focus on actuation technologies to complete our concept of Computational Fields, and expand the capability of actuation by including noncontact methods. We then focus on how to control the real-world object.

To implement and apply the process of Computational Fields, we simplify the actuation methods (Figure 1.7, left). For example, we demonstrate the manipulation process. Conventional robotic actuation (e.g., robot arms) requires many actuators to obtain a degree of freedom (DOF). However, the Computational Fields approach is a simple actuation process, and its control method is not complex. Computational Fields cannot manipulate objects in a complex manner, but this method has the advantages of calmness and selectivity of actuation materials.

The relationship between the Computational Fields and conventional actuation interfaces (using embodied actuators, e.g., attached motor, solenoid) is similar to that between the light-field and liquid crystal displays (LCDs) (Figure 1.7, right). Light fields [27] have more programmability than LCDs. However, from a single viewpoint, the final rendered image (2D) is the same.

| | Force type | Study | Principle | Workspace | Object or target | Number of objects |
|---|---|---|---|---|---|---|
| Contact | Acoustic | ShiverPad [25] | Ultrasonic vibration | 49x49 $mm^2$ | Finger | 1 |
| | | Diminished Haptics [26] (Chapter 3) | Ultrasonic vibration | 14x14 $mm^2$ | Finger | 1 |
| | Magnetic | Pico [17] | Electro magnet | 305x610 $mm^2$ | Magnetic objects | 3 |
| | Electric | TesraTouch [28] | Electrostatic force | 316x254 $mm^2$ | Finger | 1 |
| | Mechanical | inFORM [15] | Linear actuator | 381x381 $mm^2$ | Ball, tablet, etc. | 1 |
| Noncontact | Acoustic | Noncontact tactile display [29][89] | Radiation pressure | 180x180x150 $mm^3$ | Hand | 1 |
| | | Poppable Display [22](Chapter 2) | Radiation pressure | 80 mm in diameter | Soap film | 1 |
| | | Ultra-tangibles [21] | Radiation pressure | 150x90 $mm^2$ | Balls | 2 |
| | | Pixie Dust [24](Chapter 4) | Acoustic levitaiotn | 1000x1000 $mm^2$ | Polystyrene particles | Mass of particles |
| | Magnetic | FingerFlux [20] | Electro magnet | 370.5x234 $mm^2$ | Magnet on finger | 1 |
| | | Magnetic fluid artwork [30] | Electro magnet | 600x600x130 $mm^3$ | Magnetic fluid | Fluid |
| | | ZeroN [30] | Electro magnet | 380x380x90 $mm^3$ | Magnetic sphere | 1 |
| | Aerodynamic | Airjet haptic feedback [31] | Airjet | 360x360x300 $mm^3$ | Hand-held tool | 1 |
| | | AIREAL [32] | Vortex of air | 1000 mm & 75 deg | Hand | 1 |

The values in this table are based on the reported values in the reffered papers.

Table 1.1: Type of forces used in related approaches and projects we developped in this research

In the present research, we offer three contributions to the computer science community. The first is to provide a new vision in realizing programmable matter, defining the problems to be solved, and comparing the proposed and conventional approaches. The second is to provide a Computational Fields design method for theoretical and human-centered methods. The third is to implement, apply, and evaluate system examples based on computational acoustic and magnetic fields. The structure of this chapter is as follows: we introduce the concept in the Introduction, provide a survey of related works (Table 1.1), describe the design method, formulation, and characteristic of Computational Acoustic Fields, and summarize the contributions of this thesis.

Some conventional studies can be categorized into computational fields. These studies are also the target of this paper. The role of this study is to introduce the design concept and theoretical definitions to the human–computer interface (HCI) communities in order to discuss the research concept, scalability, implementation, and evaluation in a unified manner. We believe that our concept, design, implementation, and discussion will contribute to enhancing the vision of HCI.

## 1.2. Related Approaches

We will discuss three topics: 1) interface visions toward real-world-oriented interactions [12]; 2) actuation technologies, which are used or available in these interfaces; and 3) light fields as an example of an information-filled space.

### 1.2.1.Deformable UIs

Many types of UI have been proposed. For example, Project FEELEX aims to combine visual and haptic information in a single device [9]. Programmable matter [10] mimics an original object using millions of microrobots. Poupyrev et al. investigated and discussed animated interfaces that can dynamically change their physical properties [11]. Radical

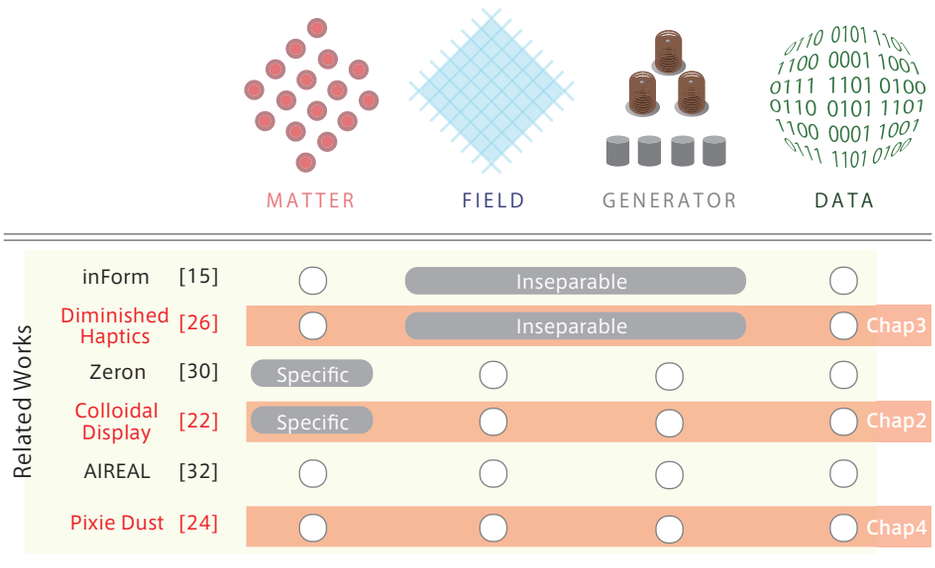


Figure 1.8: Considered components for the design methods.

Atoms [12] is an extension of Tangible Bits in which all digital information has a physical manifestation [5]. Smart Material Interfaces [13] use smart materials to display properties that can be altered by external stimuli.

Note that these studies have focused on physical matter in conventional approaches. In other words, information is stored inside the physical matter and displayed by altering part of or the entire shape, movement, position, color, or other property. In contrast, our Computational Fields vision aims to fill space (outside the physical matter) with information. This vision explores a new application space of UIs, and intersects with some conventional ideas.

Actuation technologies provide a means of deforming devices. The visions described above are implemented using both self-actuation and environmental actuation. Some examples of self-actuation include arrays of linear actuators (FEELEX [9], LUMEN [11], Recompose [14], and inFORM [15]), air-pump actuators (PneUI [16]), shape memory alloys (SMI [13]), and electromagnets (programmable matter [10]). Most environmental actuation technologies use electromagnets (Pico [17], ZeroN [18]).

To fill a space with information, we would prefer actuation technologies that do not require physical contact to transport forces, such as magnetism. We explain noncontact actuation technologies in the next subsection.

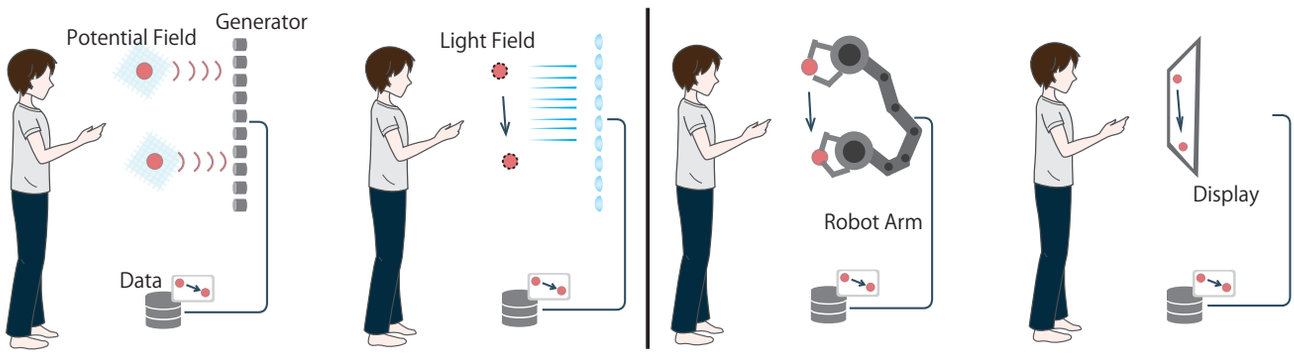


Figure 1.9: Interaction between a human and a generator: (left) human, matter, field, and generator; and (right) conventional study, robot arm, and GUI.

### 1.2.2.Noncontact Actuation Technologies

Compared with contact actuation technologies such as robot-arm manipulation, noncontact actuation technologies are relatively weak, and some of them suffer from specific restrictions. Acknowledging these drawbacks, noncontact actuation technologies still have a desirable advantage: the work space is not occupied by bulky robot arms, which can be unsafe for users. In UIs, there are two main types of noncontact force: magnetism and ultrasonic force.

Many tabletop interfaces have been developed that use an electromagnet array (e.g., Pico [17], Tamable looper [19], FingerFlux [20]). ZeroN [18] levitates and manipulates a magnetic sphere by precisely controlling an electromagnet and an XY stage.

Ultrasonic traveling waves are used in Ultra-tangibles [21] to press and move objects, and Colloidal Display (Chapter 2) [22] uses such waves to deform and break a soap-film screen. Ultrasonic standing waves are used in lapillus bug [23] to levitate and transport objects, and in Pixie Dust (Chapter 4) [24] to control a potential energy distribution in midair and create graphics by filling it with small particles. In later chapters, we specifically treat Computational Acoustic Fields. However, we first treat various Computational Field types to describe the contrast between Computational Acoustic Fields and other fields.

## 1.3. Design

In designing the Computational Fields and Environmental Actuated Interfaces, four components were considered (Figure 1.8): Matter (actuated object), Field (computational field of physical quantity), Generator (device to control Field), and Data (digital resources). In

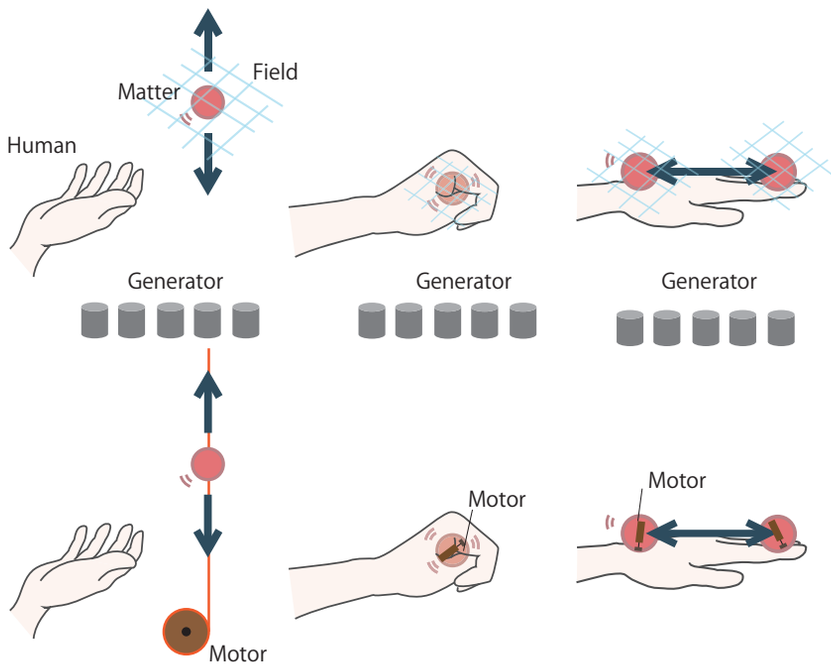


Figure 1.10: Example of actuations: (top) field, and (bottom) actuator.

addition, we have to consider the human senses to design suitable human interfaces.

Fields of physical quantities that directly stimulate human sensory organs can be used as UIs without matter (e.g., light, sound, smell, heat). In contrast, fields of physical quantities that do not directly stimulate human sensory organs require Matter through which the Human can receive Data from the Fields (e.g., magnetic, ultrasonic, and electromagnetic fields). The former is inherently a human interface obtained by Computational Fields, and we discuss the latter hereafter.

In conventional techniques such as ZeroN [18], Ultra-tangibles [21], Colloidal Display (Chapter 2) [22], and lapillus bug [23], Matter is actuated by Fields that are controlled by Generators. Pixie Dust (Chapter 4) [24] uses real-world-oriented computer graphics with acoustically levitated particles (Matter) according to the concept of a computational potential field (Figure 1.8 (upper left)), an ultrasonic field generated by ultrasonic phased arrays (Generators). Here, we treat not only Computational Acoustic Fields, but also general Computational Fields by including various types of Fields. This provides a generalized concept of Fields with which to design UIs.

Note that Sensors (devices to monitor the field) could be considered to complete the whole interaction, in addition to the components listed above. Optical sensing methods (sensors of a light field) are typically used in conventional HCI studies. Sensors of Fields used for actuation can also be used to detect user input. Both are included in the human

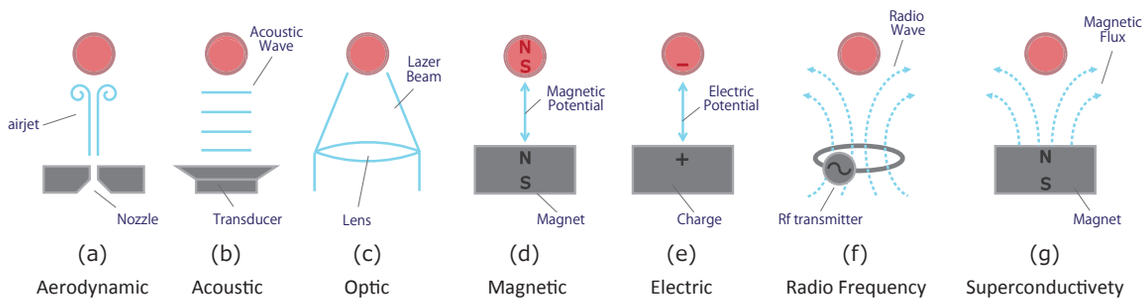


Figure 1.11: Description of the powers.

interfaces around Computational Fields, and so we do not need to discuss Sensors.

### 1.3.1.Relationship between Components

Our key idea is to redefine objects actuated by noncontact forces as a combination of Matter and Fields. We focus on Fields rather than Matter. This idea increases the programmability of actuation, because the design of Fields is not restricted. With this idea, we can now discuss noncontact actuation in a manner similar to that of light fields.

Fields need to interact with matter to be sensed by Humans. In this process, the fields of physical quantities determine the restrictions on the physical properties of Matter. For example, in an acoustic force, the weight density and compression ratio of Matter is essential in determining the actuation force. In a magnetic field, the magnetic permeability coefficient of Matter must be nonzero to allow actuation forces to be generated. The details are explained in chapter 1.4.

### 1.3.2.Design Factor with Human Interactions

When computational fields are transformed into UIs, we must assume one of two conditions: 1) Humans can directly recognize the Field, and 2) Humans cannot recognize the Field (Figure 1.9).

| | Propagation | Origin of force | Limitation | Pressure * | Area * | Force * |
|---|---|---|---|---|---|---|
| Aerodynamic | ~ 10 m/s * | Wind pressure | Easy to diffuse | 60 Pa | 100×100 $mm^2$ | 0.6 N |
| Acoustic [29][34][35] | Sound speed | Radiation pressure | None | 100 Pa | sinc (φ20 mm) | 0.01 N |
| Optical | Light speed | Radiation pressure | None | 0.0008 Pa | φ 1 mm | $6\times10^{-8}$ N |
| Electric | Light speed | Electric force | High voltage (100 V ~) | 110 Pa | 10×10 $mm^2$ | 0.01 N |
| Magnetic | Light speed | Magnetic force | Magnetic object | 400 kPa | 10×10 $mm^2$ | 40 N |
| Radio-frequency [36] | Light speed | Eddy currents | Conductive and non-magnetic object | 400 Pa | φ 5.2 cm | 3.4 N |
| Superconducting | Light speed | Meissner effect | Low temperature and superconductive obj. | 400 kPa | 10×10 $mm^2$ | 40 N |

Noncontact forces mentioned in "Levitation in Physics [33] " and their characteristics. * Typical value

Table 1.2: Noncontact technologies and their limitations.

In the first case, the field design must ensure that the properties of the physical quantities are compatible with human perception. In the second case, in the field design, the noncontact Force is important in transmitting information to Humans via Matter.

The actuation programmability is not lost, regardless of Matter, Field, and Generator (Figure 1.10). This feature enables us to design various interactions using the same combination of Matter, Field, and Generator.

## 1.4. Formulation

We now describe our concept of “computational fields” in a theoretical sense. For simplicity and practicality, we assume stationary conditions. First, a generalized description is given. Second, the candidate physical quantities available in our daily life are discussed. Finally, acoustic and magnetic fields are introduced as examples.

To manipulate objects in midair, Generators control the spatial distribution of some types of physical quantities. The force that acts on a small sphere is determined by the interaction between the sphere and the physical quantity. We will find it useful to consider the potential energy density of the physical quantity, because the gradient of the distribution of potential energy density provides the force that acts on the sphere. The force F [N] acting on a small sphere is expressed as

$$\mathrm{F} = -V\nabla U(\mathrm{p}_1,\mathrm{p}_2,...,\mathrm{x},\mathrm{y},\mathrm{z}) \quad (1.1)$$

where V [$m^3$] is the volume of the sphere, U ($p_1$, $p_2$,..., x, y, z) [$J/m^3$] is the potential energy density, $p_1$, $p_2$,... are parameters related to the sphere, and (x, y, z) is the position of the sphere. The number and type of parameters depend on the physical quantity. This equation tells us that we need only consider the spatial distribution of the potential energy density U (Figure 1.14).

Noncontact forces were discussed by Brandt [33]. Although he focused on levitation, his discussion is also useful for our purpose. Seven types of levitation technologies are available: aerodynamic, acoustic, optical, electric, magnetic, radio-frequency, and superconducting levitation (Figure 1.11). Among these, the technologies with possible applications in our daily lives are acoustic and magnetic technologies (Table 1.2). In this thesis, we utilize acoustic fields in a semi-contact manner (chapter 3: squeeze film effects) and noncontact manner (chapter 2,4: radiation pressure and standing waves). We now describe the theoretical basis for the examples of chapters 2, 3, and 4.

We show two actual examples: the mathematical descriptions of the potential energy density of the acoustic and magnetic fields. The acoustic potential energy density is expressed as

$$U = -B\langle K_a \rangle + (1-\gamma)\langle P_a \rangle \quad (1.2)$$

where Ka [J/m$^3$] and Pa [J/m$^3$] are the kinetic and potential energy densities of ultrasound, respectively. < > indicates the time average. B and γ are defined as,

$$B \equiv \frac{3(\rho - \rho_0)}{2\rho + \rho_0} \gamma \equiv \frac{\beta}{\beta_0} \quad (1.3)$$

Where ρ [kg/m$^3$] and $\rho_0$ [kg/m$^3$] are the weight densities of the sphere and the medium, respectively. β [N/m$^2$] and $\beta_0$ [N/m$^2$] are the compression ratios of the sphere and the medium, respectively. There are two parameters related to the sphere: $p_1 = \rho$ and $p_2 = \beta$.

The magnetic potential energy density is given as,

$$U = -\frac{1}{2}(\mu - \mu_0)H^2 \quad (1.4)$$

where μ [H/m] and $\mu_0$ [H/m] are the magnetic permeability coefficients of the sphere and the medium, respectively. H [A/m] is the magnetic field strength. There is one parameter related to the sphere: $p_1 = \mu$.

We now describe the potential energy distribution of the acoustic and magnetic fields. There are other possibilities that could be calculated to generate Computational Fields (e.g., light, electricity, superconductivity). Methods of controlling these field quantities have been proposed over many years. Different fields are described in different theoreti-

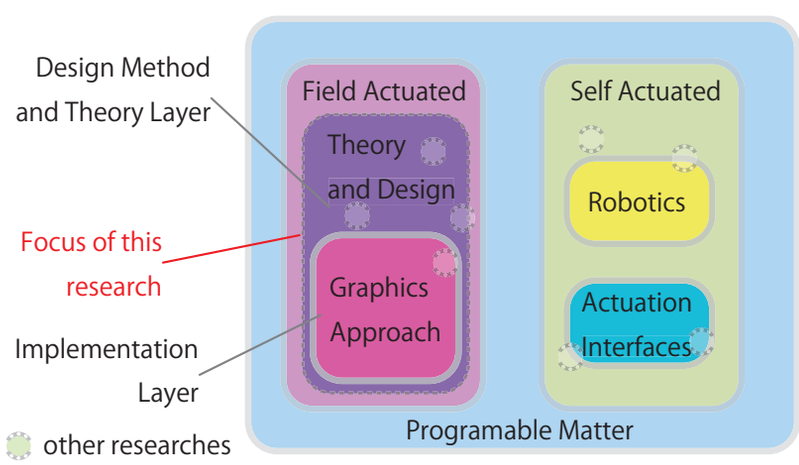


Figure 1.12: Position and Focus of This study

cal descriptions. Figure 1.13 shows the implementation of Generators. Figure 1.13 (left) is a Magnetic Field generator, and Figure 1.13 (right) is an Acoustic Field generator. These generators can generate Computational Field distributions that are similar to the simulated results (e.g., Figure 1.14 ).

These Computational Fields have different size and energy characteristics, as illustrated in Table 1.2. Light Fields and Electromagnetic Fields can effect change over distances of order nm–µm, whereas Acoustic Fields operate on µm–mm orders. There are various fields that can be handled with a computer and generators. To realize graphical applications for display and UIs, we choose a Computational Acoustic Field to realize our concept of Environmental Actuated Programmable Matter (Figure 1.12) because of its dimensional and energetic order.

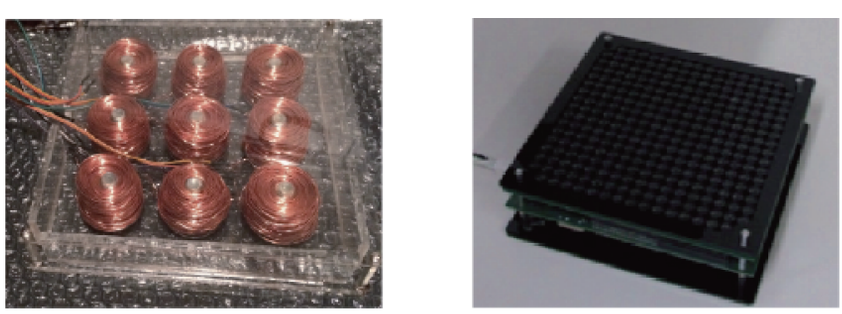

Figure 1.13: (left) Computational Magnetic Field Generators (right) Computational Acoustic Field Generator

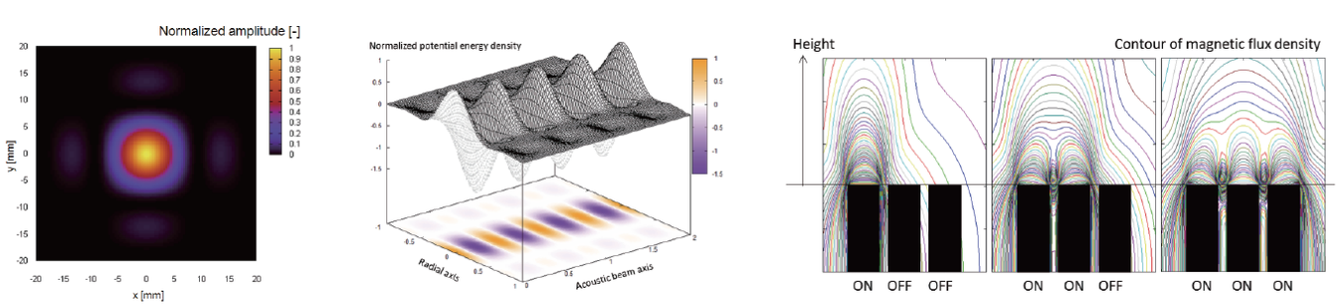


Figure 1.14: (left) Simulated Results in Acoustic Fields (right) Simulated Result in Magnetic Fields

## 1.5. Computational Acoustic Fields

We now describe the characteristics of Computational Acoustic Fields. We specifically consider ultrasonic acoustic waves to utilize human interfaces. Human auditory sensors cannot recognize ultrasound frequencies. Because of this high-frequency characteristic, we can form directional beams for use in human interfaces without recognizing the existence of these acoustic beams.

Considering human sensory characteristics, changes over μm–cm distances are recognized as shape changes in daily life. Shape changes of the order of nm can affect only color, whereas changes over the order of a meter are too large for daily use. Shape transforms at the μm order are recognized as texture changes both in haptics (roughness) and optics (reflection). Changes of mm–cm orders are recognized as shape and position changes. We focus on five transformations: reflective texture (Chapter 2), haptic texture (Chapter 3), the shape of a 2.5D screen (Chapter 2), the position of a levitated object (Chapter 4), and the distribution of levitated objects (Chapter 4).

We use four phenomena of ultrasonic acoustic fields in our projects: capillary waves, squeeze film effects, radiation pressure, and standing waves.

Capillary Wave: We remotely actuate a colloidal film to generate capillary waves on its surface. Capillary waves on the colloidal screen are of μm order, and can change the optical reflective texture of the film (Figure 1.16).

Squeeze Film Effect: We externally actuate material by ultrasonic transducers. When a user touches the actuated material, the squeeze film effect occurs between the material and the user's finger. The air film levitates the finger from the surface of the pasted material to the order of several μm (Figure 1.17).

Radiation Pressure: We remotely actuate a colloidal film to utilize it as a 2.5D display. Radiation pressure can be generated at the focal point of an ultrasonic phased array (Figure 1.18).

Standing Waves: We remotely generate standing waves at the focal points of ultrasonic waves, and use them to levitate objects. By changing the distribution of focal points, we can change the position and distribution of the levitated objects (Figure 1.19).

An explanation of these phenomena is shown in Figure 1.15.

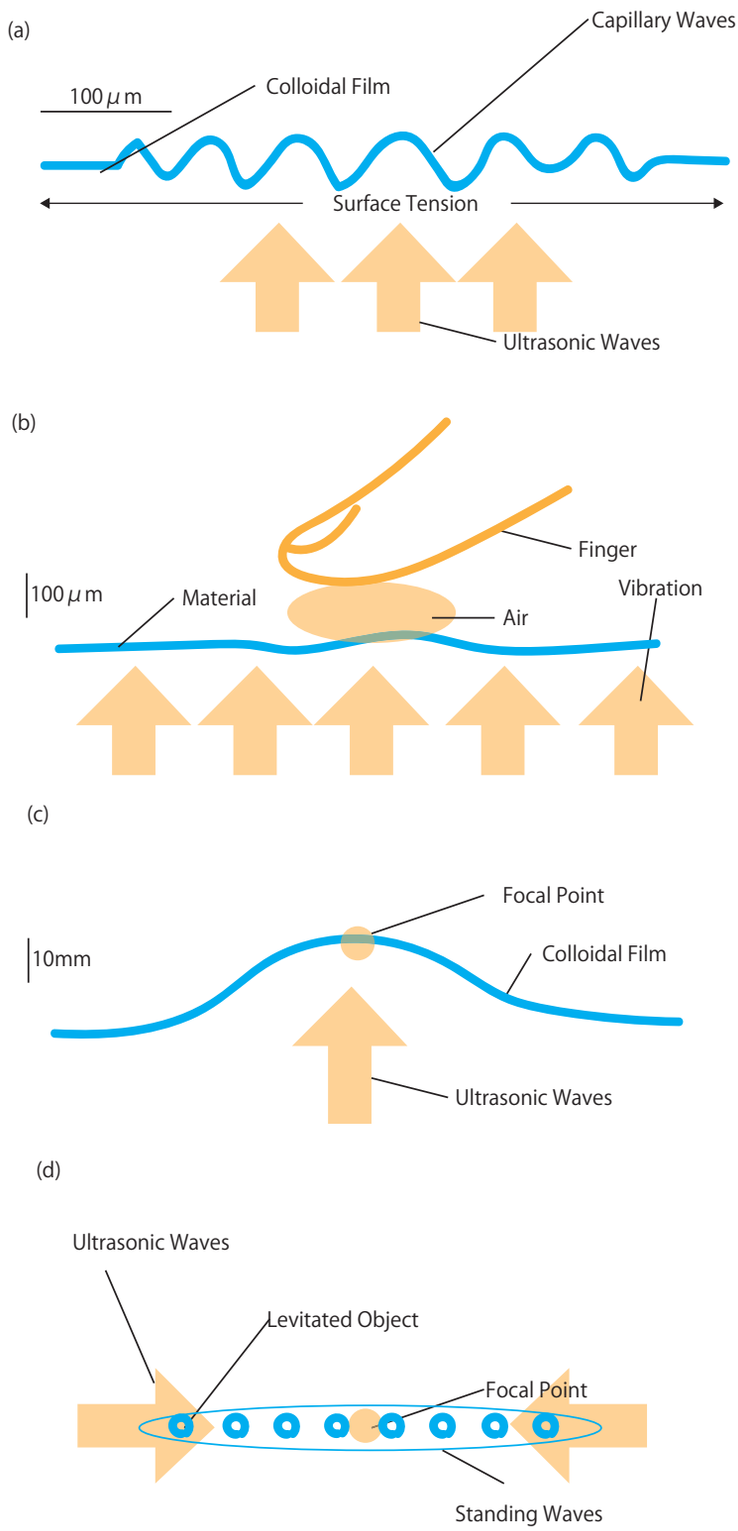


Figure 1.15: Explanations of Four Phenomena (a) Capillary waves on colloidal film (b) squeeze film effect (c) deformation of colloidal film (d) standing waves

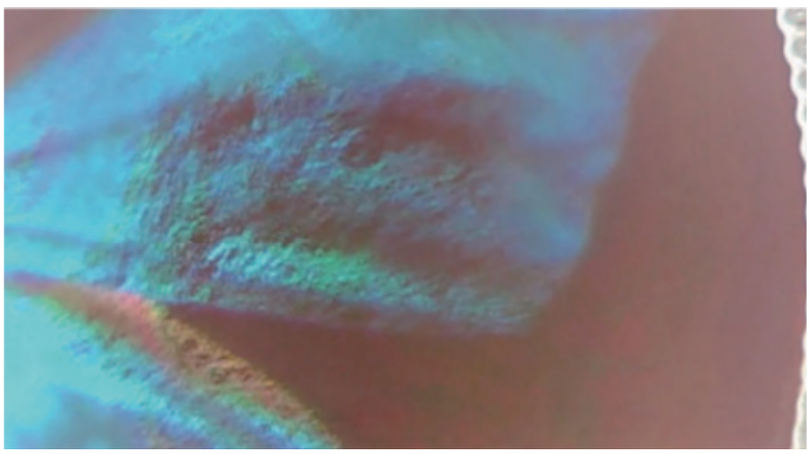

Figure 1.16: Colloidal Screen activated by 3D acoustic field.

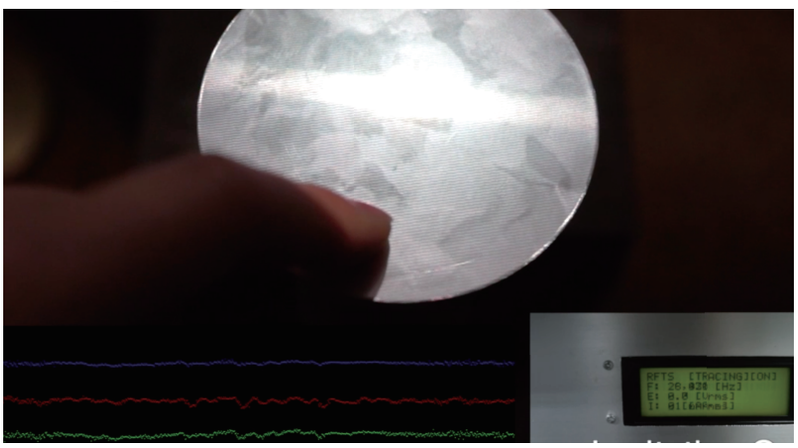

Figure 1.17: Metal Plate activated by time-division 2D acoustic field.

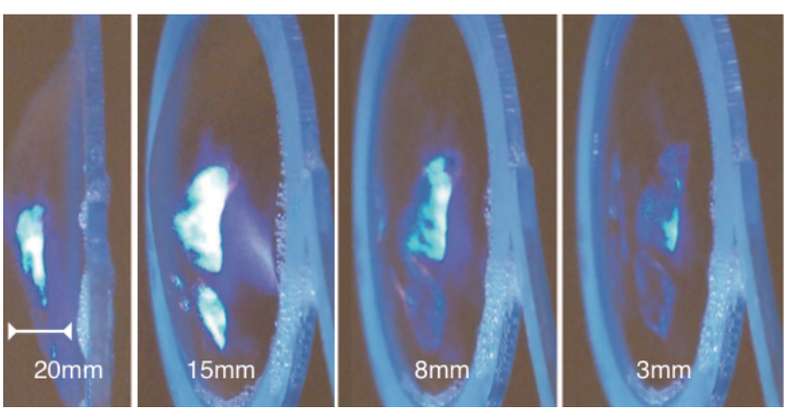


Figure 1.18: 2.5D shape change on colloidal film by acoustic radiation pressure

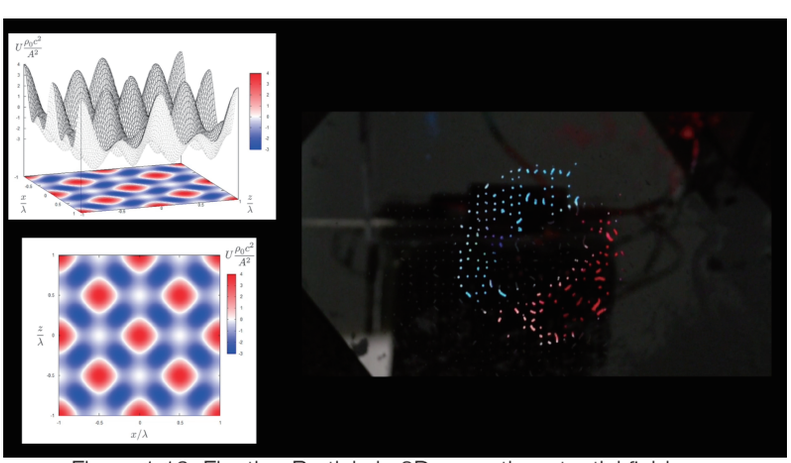

Figure 1.19: Floating Particle in 3D acoustic potential field

## 1.6. Contributions of this study

We now describe the contributions and position of this study (Figure 1.12).

In the following chapters, we apply a Computational Acoustic Field to realize the malleability of Computer Graphics (e.g., programmability of optical state, shape, haptic state, and 3D position) in real-world objects. The common feature of these studies is that the actuated objects do not have actuators, and are driven by Computational Acoustic Fields. We provide examples of how to implement field-oriented programmable matter towards this graphical approach. Computational Fields are not a new concept, but using this topic as a general term is useful to classify and compare the field of physical quantities and to discuss how to utilize them in graphics and human interfaces.

This thesis has a three-layered hierarchical structure. At the top layer, we introduce the concept of Computational Fields, in which fields of physical quantities are controlled by computers to alter the real world. This concept is useful to summarize research on field-oriented programmable matter (methods of Environmental Actuation). In this layer, we introduce the characteristics of Computational Acoustic Fields and the phenomena that we use in our projects.

In the middle layer, we focus on noncontact and environmental actuation technologies, which have not been discussed from the viewpoint of fields. We list and compare noncontact actuation technologies and environmental actuation technologies. In chapter 1, we discuss and classify acoustic fields and other field quantities from the viewpoint of graphics applications and human interfaces. In chapter 4, we discuss these field manipulation techniques from the viewpoint of manipulation and levitation methods.

In the bottom layer, we implement three prototype systems for environmental actuation based on acoustic fields. We consider the optical control of a colloidal screen (Figure 1.16), haptic transformation (Figure 1.17), and acoustic manipulation (Figure 1.19). Our results are applicable to display technologies in various areas.

In chapter 2, we introduce an optical programmable screen with a view angle that can be programmed from 2–175°. Conventional studies on screens with dynamic optical properties have not explored applications combined with projected images. Our results overcome the limitation on screen characteristics, enabling us to change the optical characteristics and shape of the screen. Our results can be applied to various expressions (e.g., 3D expression, BRDF material expression) by controlling the view angle dynamically.

In chapter 3, we describe a haptic modification system that can modify uneven surfaces by up to 50 μm by controlling the thickness of the squeeze film effect. This project explores the design space around the haptic modification of real-world textures via the

squeeze film effect. For this purpose, we develop a transducer and a resonance tracing system that can matches the amplitude of vibration against the user's touch. This technology is applicable to new material samples that can modify their haptic characteristics.

In chapter 4, we present an acoustic levitation method that can levitate objects of up to 1 g (7.8 g/cm$^3$). This method can move particles and small objects at up to 72 cm/s. We expand a standing wave-based acoustic manipulation method to 3D manipulation by employing ultrasonic phased arrays instead of a single transducer. The manipulation workspace is expanded to one million times that of conventional studies. We explore the design space of this manipulation method with an emphasis on graphics applications. Our results are applicable to levitated displays and the animation of physical objects.

We believe that these prototype systems and methods obtained by Computational Acoustic Fields will contribute to expanding graphics expressions, and will be applicable to UIs, displays, computer graphics, and entertainment computing.

# 2.Project on Colloidal Screens

*In this chapter, we describe a method to change the optical state and 2.5 D shape of colloidal screen by computational 3D acoustic field. This project is aimed to realize malleability on optical and shape transformation of real world object like computer graphics in the digital world by applying computational acoustic fields. In this chapter we utilize capillary waves on colloidal screen to change the reflectance state and employ acoustic radiation pressure to deform the colloidal screen(Figure 2.1).*

## 2.1. Introduction

All over the world, screens are used to display various digital contents, such as movies, presentations, and shows, and are essential in the field of entertainment. The fundamental process utilized to display content on a screen is as follows: digital content is created, the content is rendered, and the content is shown on a screen via a projector. A significant amount of information (e.g.. material expression, light field information) is lost when the content is shown on a static surface because ordinary screens are rigid and static and the texture of the screen cannot change dynamically corresponding to the contents. However, in the digital world, we can dynamically specify an object's texture by modifying its light and bump maps. Consequently, in our research, we are attempting to take the first step in bringing digital to physical by applying this computer graphics concept to screens in the real world. In this project we define texture as optical characteristics of material and small bump on surface.

We propose to control the optical characteristics of screens in order to reproduce the realistic appearance of contents, and thereby provide a new entertainment systems option. To realize this concept, we choose a colloidal film and excite it with an

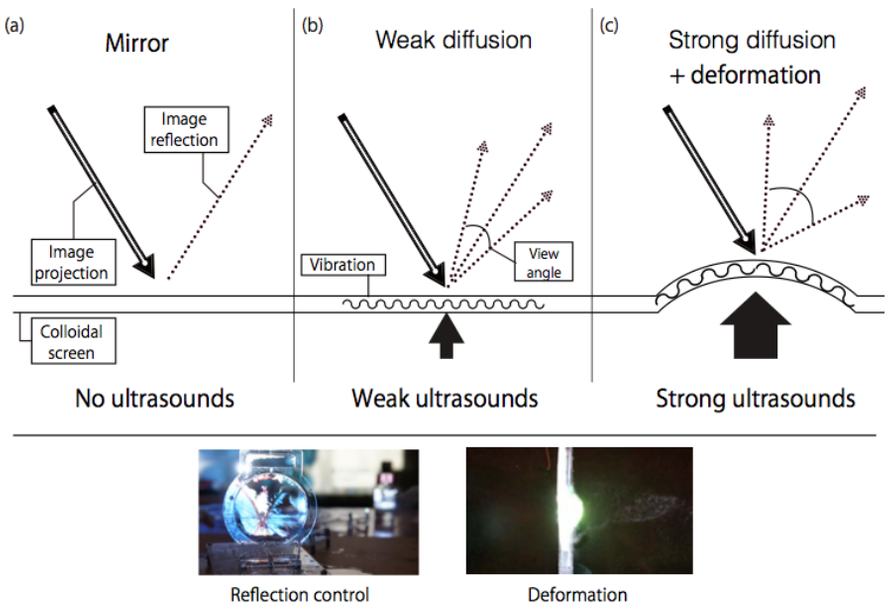


Figure 2.1: The image is projected (black arrow with line) from the top. The ultrasonic waves (black arrow) hit the membrane to reflect the image (light dotted arrow). Note that there are two types of effects related to the intensity of ultrasound: A weak ultrasound mainly changes the viewing angle while a stronger ultrasound additionally changes the shape of the screen.

ultrasonic wave (Figure 2.1). The ultrasonic wave induces a minute wave (known as a "capillary wave") on the colloidal film that leads to an expansion of the viewing angle. To the best of our knowledge, ours is the first approach to utilize this phenomenon to control the optical characteristics of a screen. We can control the vibration of the screen at high frequency. In addition to expanding the viewing angle, we can induce an optical illusion to reproduce glitter by means of time division control. This method is combination of 1D BRDFs expression and 2D projected images.

The main application of colloidal screen [37] is control of reflection and texture. In addition, colloidal film is a unique material, which imbues a screen made from it with flexible characteristics such as screen deformation, physical popping, and actual screen reconstitution. The possibility exists for these features to be applied in entertainment computing.

The remainder of this chapter is organized as follows. In Section 2.2, we cite related research and discuss the reason why our research is relevant. In Section 2.3, we explain the theory underpinning our work. In Section 2.4, we give an overview of our system, including system requirements. In Section 2.5, we discuss an evaluation conducted by means of a laser experiment, and discuss prototype applications de-

veloped in Section 2.6 (Application for 3D expression), 2.7 (Application for deformable display) and 2.8 (application for material expression). Finally, we discuss the limitations of our proposed system, in Section 2.9, and conclude by looking at possible future work, in Section 2.10.

## 2.2. Related Work

In our study, we dynamically change the shape and texture of the screen (Figure 2.1). Therefore, in this section, we cite researches that are relevant to active screens, and which either change the spatial position or the texture of an object. We then look at how our research relates to these relevant research efforts.

### 2.2.1. Texture Displays

In this subsection, we look at research done to control the surface textures of an active screen.

In [38], Raffle et al. proposed Super Cilia Skin (Figure 2.2), a conceptual interactive surface comprising thousands of cilia-sized actuators, and actually developed 128 magnetic cilia. Coelho and Maes [39] subsequently presented Sprout I/O, which expanded on the concept using Teflon actuators as cilia-like structures, which can actually bend and stretch, for the surface.

Furukawa et al. presented FurDisplay, a surface constructed of fur and controlled with a vibrating motor [40]. When the surface of FurDisplay is activated, the hair stands upright. By detecting capacitance change, it promotes interaction of people and fur. These researches are related to our research because they express the physical texture using actuation. They are good for wearable computing and interactive architecture, but the range of expression of textures are restricted and they are limited in terms of size and the limited ability provided by actuators for control.

Research is also being conducted on dynamic texture display. Hullin et al. developed Dynamic BRDF Display (Figure 2.3), which changes the reflection parameter of the surface of water by vibrating it using actuators [41]. This can diffuse reflection and blur images. This research can express BRDF that cannot be expressed in an LCD

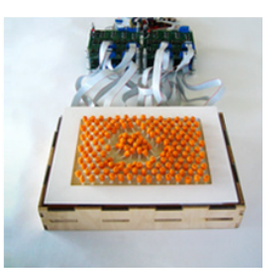

Figure 2.2: Super Cilla Skin[38]

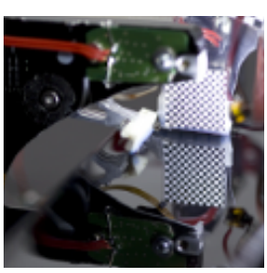

Figure 2.3: Dynamic BRDF Display[41]

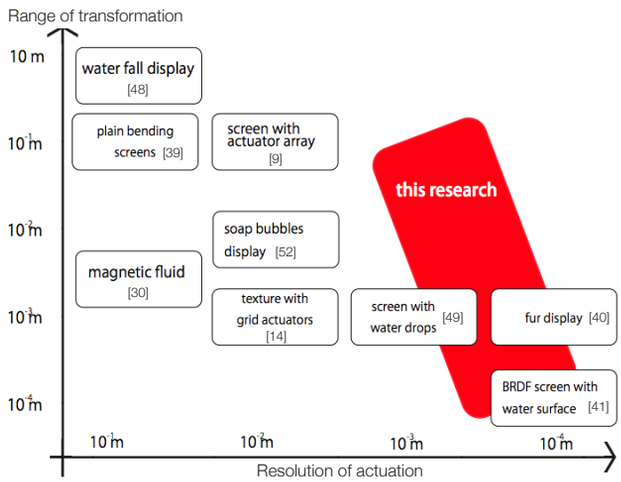


Figure 2.4: Position of our research corresponding to other relevant researches. Vertical axis represents the amount of transformation dealt to the object while the horizontal axis represents the resolution of actuation. Notice how our research (red) covers the areas that have not been explored yet.

display such as that presented by Koike et al. [42]. Although it is a pioneering research, it has not explored the design space with projecting image. Then we focus on the controlling BRDF and combining with 2D projection in this project.

### 2.2.2. Deformable Screens

Research geared towards controlling the spatial position of an active screen is also being actively pursued. Many of the systems researched were first used for tactile presentation [43]. For example, the system that Cholewiak et al. [43] developed in 1981 was used as a tactile skin display and utilized several actuators. The system displayed the vibratory stimulation using several cylindrical actuators that moved up and down. There are also other systems with similar mechanisms to that used by Cholewiak et al. [43]; for example, the deformable actuated screen “Project FEELEX” [9], which constructs 3D forms on the surface of the screen using an actuator array set under the screen. In addition, LUMEN, proposed by Poupyrev et al. [44], comprised actuated dot matrix LEDs—physical pixels shown in RGB and H (height). Leithinger et al. [14] also proposed an interactive deformable screen called Recompose.

Other researches dealing with control of the spatial positions of displays also exist. There are image projection technologies that use fog as a screen, such as the systems proposed by Rakkolainen et al. (Figure 2.6) [46] and Lee et al. [47]. These technologies display images in the air using a fog screen and a camera. This is projected

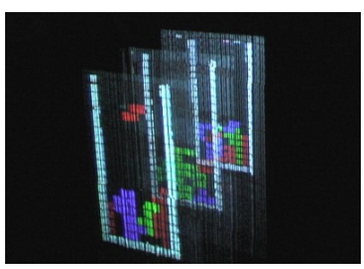

Figure 2.5: Water display [49]

Figure 2.6: Fog screen [46]

in the air as a result of fog's diffusivity characteristics.

Research on displays using water is also being conducted. Sugihara et al. [48] used fountain as a deformable water screen. Barnum et al. [49](Figure 2.5) developed a screen that uses the water drops in the air. Water drops have lens-like characteristics. By using these characteristics, they were able to project an image onto the water drops. They made a water drop sequence in the air and projected the image corresponding to the spatial position by synchronizing the projector with the water bulbs, and applied their technology to create a multilayer screen. Other interesting artworks include those presented by Suzuki et al. [50], which uses underwater air bubbles, and Kodama et al. [30], which uses magnetic liquid.

Displays have also been made using soap bubbles. Bubble Cosmos [51] is a technology that constructs a screen in the air by confining fog in a bubble; and Shaboned Display [52] turns a bubble into a pixel. Bubbles have also been used as a musical instrument [53].

### 2.2.3. Position of this study

Our research is positioned as shown in Figure 2.4. The size of the changes on the vertical and horizontal axes represents the resolution of actuation. For example, since a dynamic BRDF [41] changes the surface texture by detailed vibration, the resolution of actuation is high and the size of change is small. Researches on dynamic textures with small actuators are not high-resolution and the size of spatial change is limited.

Using this rationale, we positioned our research in the area colored in red. The actuator resolution of our research is high when the spatial change is small and low when the spatial change is large. No research equivalent to this domain exists. Our research contribution is high because we use the same hardware settings to accomplish many of the features achieved in related research.

## 2.3. Theory

In this section, we describe the theory underpinning the colloidal screen technology. First, we describe the capillary waves that are induced on the soap film, then introduce the reflection model of the colloidal display, and finally, describe the ultrasounds.

### 2.3.1. Capillary waves on soap film

The diffusion on the ultrasound-activated colloidal film is caused by the capillary waves, which are dominated by surface tension. The dispersion relation of the waves on the interface is described by following equation [54].

(a)

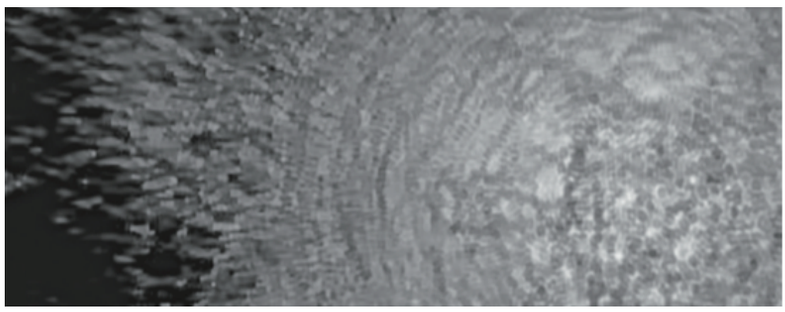

(b)

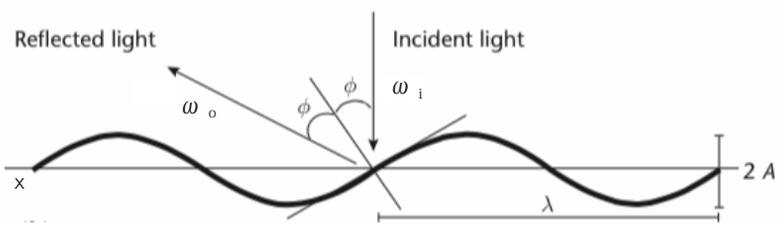


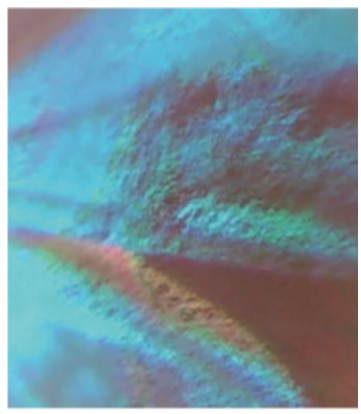

(c)

Figure 2.7: (a) Magnified (200x) Activated Colloidal Surface (b)Model of Colloidal Screen (c) Magnified Colloidal Screen with Projection(4x)

$$\lambda = \left( \frac{8\pi\sigma}{\rho f^2} \right)^{\frac{1}{3}} \qquad (2.1)$$

where σ is the surface tension, ρ is the density of the colloidal solution and f is the excitation frequency. Wavelength λ is estimated from Equation (2.1). The surface tension of colloidal liquid σ is 0.07275 N/m (20 deg C). Suppose the surface tension of colloidal liquid to be 1/2 of water and density to be the same as water 1000kg/m$^3$. In this situation, with 40kHz ultrasounds, the wavelength λ is 2π/k=83μm.

These minute waves (Figure 2.7(a)) occur on the ultrasound-activated colloidal film and diffuse the light on the surface.

These minute waves (see Figure 2.7(a)) diffuse light. For simplicity, assume that the activated capillary wave is a sine wave. Figure 2.7(b) shows the relationship between the viewing angle and capillary wave. $\omega_i$ is incident light, $\omega_o$ is reflected light. The capillary wave g(x, t) is

$$g(x,t) = A\sin(kx - \omega_r t) \qquad (2.2)$$

where x is the distance along the x-axis (parallel to colloidal surface); t is the time; A is the capillary-wave amplitude; k is the wave number, with k = 2π/λ; and $\omega_r$ is the angular frequency, with $\omega_r$ = 2πf. When the incident light ($\omega_i$) is vertical to the colloidal film, from above Equation 2.2, the reflection angle ϕ is

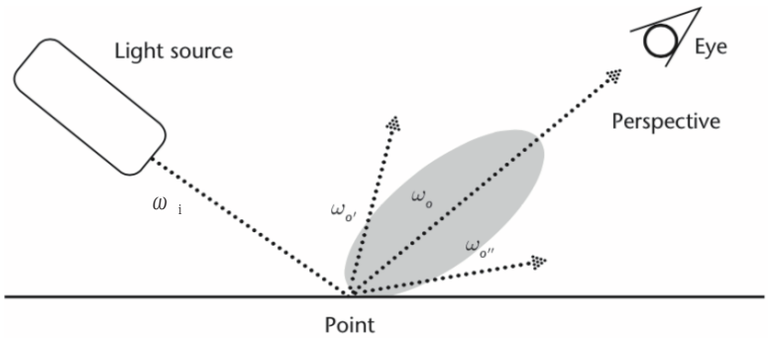

Figure 2.8: Reflection Model of Colloidal Screen

$$\phi = \operatorname{arc\,cot}\left( \frac{-1}{Ak\cos(kx - \omega_r t)} \right). \quad (2.3)$$

Then, the colloidal display's viewing angle θ is 4ϕ(figure shows only half view angle). With our setup, the viewing angle is determined by A, which we assume is in proportion to the ultrasound's intensity.

### 2.3.2. Reflection of Screen

Let us now look at the reflection model of the colloidal screen. The film surface reflection model used in the colloidal display is the bidirectional reflectance distribution function (BRDF). The BRDF expression is shown in Figure 2.8.

$$f_r(\omega_i, \omega_o) = \frac{dL_r(\omega_o)}{dE_i(\omega_i)} = \frac{dL_r(\omega_o)}{L_i(\omega_i)\cos\theta_i d\omega_i} \quad (2.4)$$

where r is the reflected light, $\omega_i$ is the incident light's direction, $\omega_o$ is the reflected light's direction, d is the differential, L is the radiance ($L_i$ is radiance of incident light. $L_r$ is radiance of reflected light), and E is the irradiance ($E_i$ is irradiance of incident light, $E_r$ is irradiance of reflected light). Furthermore, we can ignore the bidirectional transmittance distribution function by specifying the surface's state to obtain the BRDF only and to obtain a front projection. We ignore the radiation and absorption at the colloidal display.

There are two states that we utilize in this colloidal screen; "mirror" and "diffuse". A colloidal film doesn't have diffuse reflection on its ordinary state (without ultrasonic vibration); it's similar to a mirror. As with a mirror, the light emitted from the light source reaches the eyes in perspective (see Figure 2.8). So, the viewer sees only a dot or a light source on the mirror surface. We call this the mirror (specular) state.

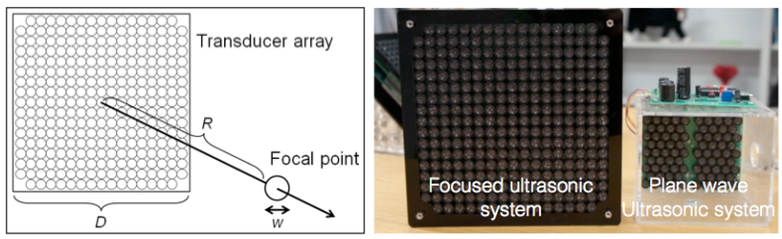


Figure 2.9: Equipments for ultrasonic vibration

We can project images on this surface by expanding the reflected light's viewing angle in the presence of $\omega_o$ in the BRDF model. In Figure 2.8, the expanded range of reflection for $\omega_o$ is from $\omega_{o'}$ to $\omega_{o''}$. The perspective light source that covers $\omega_o$ causes the image to appear on the film. We call this the diffuse state.

We control the reflectance distribution on the basis of the theory we described in the previous section. On the basis of the principle of energy conservation, we express the relationship between $L_r$ and $L_i$ as

$$\int_{H_o^2} f_r(\omega_i, \omega_o) d\sigma^{\perp}(\omega_o) \leq 1 \text{ for all } \omega_i \in H_i^2 \quad (2.5)$$

where H means all directions in a hemisphere. We transform this to

$$\int_{H_o^2} dL_r(\omega_o) \leq L_i, \ \omega_o \in H_o^2. \quad (2.6)$$

This equation represents the tradeoff between the viewing angle and the projected image's brightness. This indicates that we can display an image with high brightness when $\omega_o$ is a narrow distribution.

### 2.3.3. Ultrasonic Waves

The phased array focusing technique is used to achieve a high-intensity ultrasound wave. The focal point of the ultrasound is generated by setting adequate phase delays of multiple transducers. In addition, the focal point can be moved to an arbitrary position by controlling the phase delays [29].

The acoustic radiation pressure, a nonlinear phenomenon of ultrasound, acts when the ultrasound becomes high-intensity. When an ultrasound beam is reflected vertically at the soap film, it is subjected to a constant vertical force in the direction of the incident beam. Assuming a plane wave, the acoustic radiation pressure P [Pa] is described as

$$P = \alpha E = \alpha \frac{p^2}{\rho c^2} \qquad (2.7)$$

where c [m/s] is the sound speed, p [Pa] is the RMS sound pressure of the ultrasound, and ρ [kg/m$^3$] is the density of the medium. α is a constant that depends on the reflection coefficient of the soap film. In a case where there is total reflection, its value is two.

The phased array focusing technique is used to deform the screen within a localized area and activate the screen with more intensity.

The focal point of the ultrasound is generated by setting adequate phase delays in the multiple transducers. In addition, the focal point can be moved to an arbitrary position by controlling the phase delays. A trade-off exists between the spatial resolution and the array size. Theoretically, the spatial distribution of ultrasound generated from a rectangular transducer array approximates the shape of a sinc function [29]. The width of the main lobe (w [m]) is parallel to the side of the rectangular and is written as

$$w = \frac{2\lambda R}{D} \qquad (2.8)$$

where λ [m] is the wavelength, R [m] is the focal length, and D [m] is the side length of the rectangular array (Figure 2.9(left)). Our system can control the spatial position of focus and it contributes to activate the films partially.

## 2.4. Design

In this section, we look at the design requirements for the colloidal display and give an overview of the system.

| Projector | LCD or DLP | |
|---|---|---|
| Screen | Colloidal Solution | Soap |
| | Size of Membrane | 8cm in diameter |
| Ultrasound | Transducers | 285pics |
| | Focus Control | Phased Array |
| | Frequency | 40kHz |
| | Size of Focal Point | 2cm at distance of 20cm |

Table 2.1: Specifications of Components

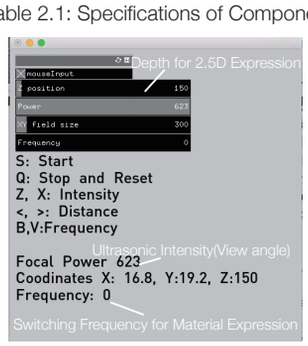


Figure 2.10: Control Interfaces

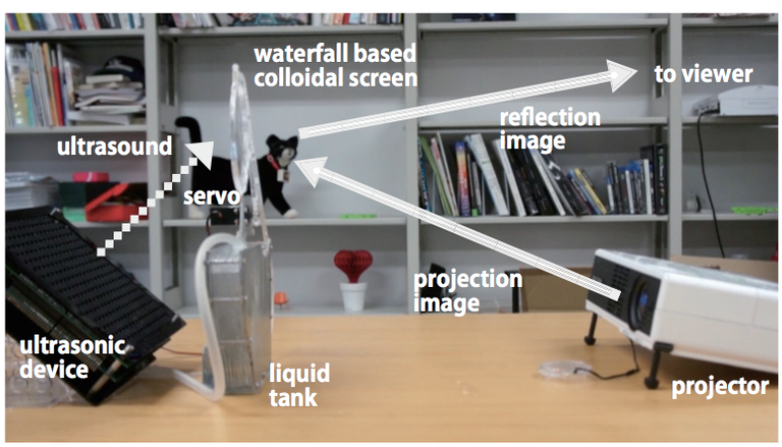


Figure 2.11: System Overview

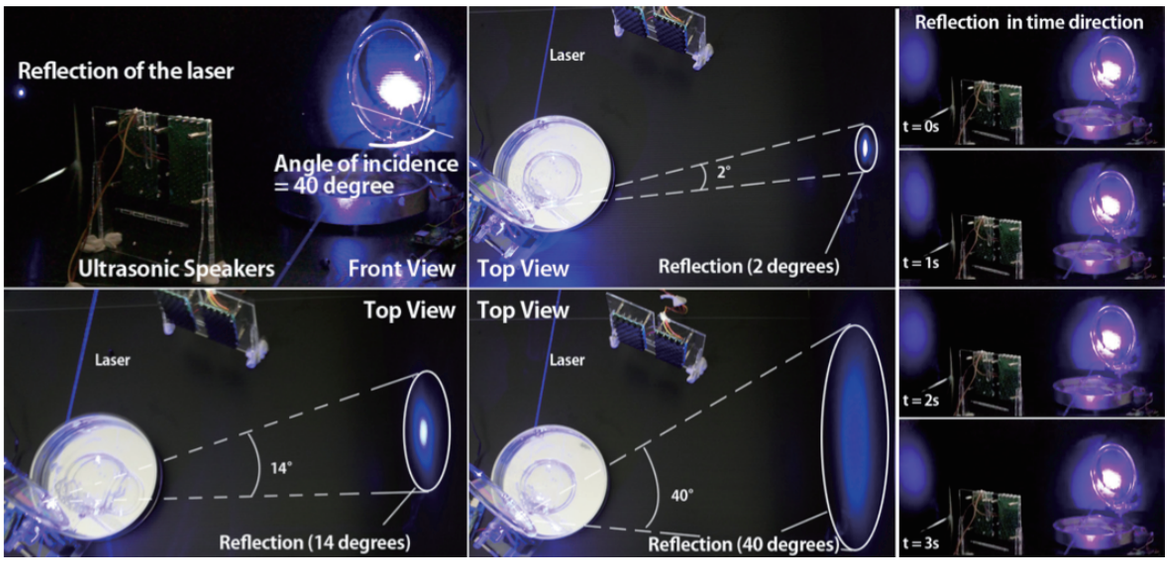


Figure 2.12: Laser experiment example of wave form modulation. Different types of waves create different view angles. High intensity wave: 40 degrees, middle intensity wave: 14 degrees, and low intensity wave: 2 degrees.

### 2.4.1. System Requirements

The concept underlying our system is changing the appearances of images by switching the screen's reflectance at high frequency. Therefore, the system has to satisfy the following requirements:

*-The film must be light and soft enough for its optical properties to be changed using vibration.*

*-The ultrasonic systems must be operated at high frequency.*

*-Colloidal frames must continuously supply the colloidal solution to the colloidal membrane, resulting in an extension of the membrane's life with high stability against the powerful ultrasonic waves.*

To satisfy these requirements, we use a strong ultrasonic actuator power speaker to vibrate the screen remotely and use colloid film that, although it is made from light material that is weak and fragile, has a high surface tension and is flexible.

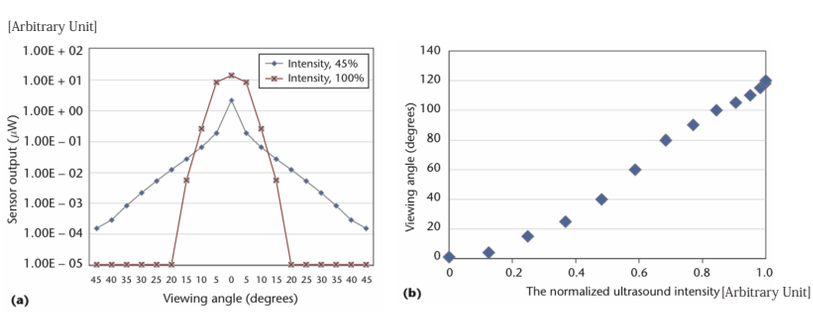


Figure 2.13: Evaluating screen reflection. (a) The relationship between the brightness and angle. The red line denotes a small viewing angle and is brighter than the blue line; the blue line denotes a wider viewing angle with low brightness. (b) The relationship between the viewing angle and the normalized ultrasound intensity.

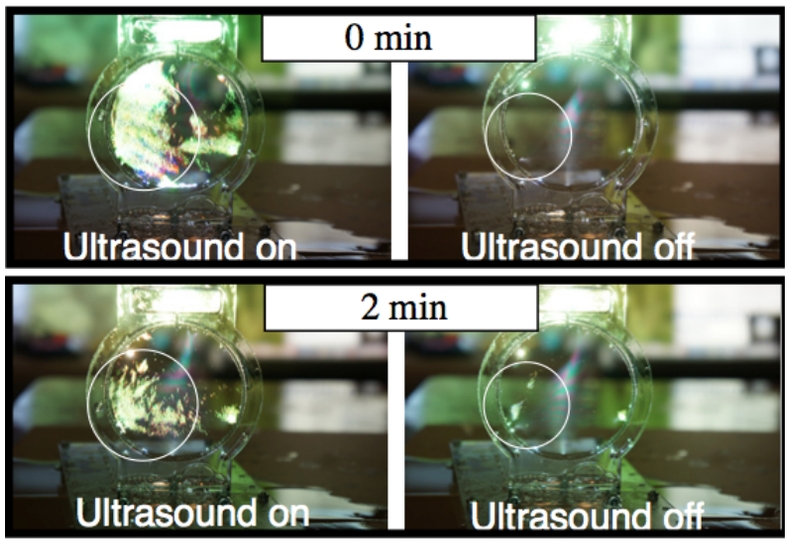

Figure 2.14: Stability experiment

Ultrasonic waves directly affect the reflection of the film, so if we switch the ultrasonic waves on/off, to human eyes, it appears as if a switch is being made from transparent to opaque.

### 2.4.2. System Overview

- *LCD or DLP projector, such as a video equipment, which emits light.*
- *Colloidal film*
- *Film's frame with waterfall system and the mechanism to replace the film*
- *Equipments for ultrasonic vibration.*

Figure 2.11 shows one of the configuration that uses these components. Projector's light goes to the film and film's frame. Ultrasound waves are produced from the speaker simultaneously and hit the film, vibrating it. When the film is broken, it is replaced by servo-motors. The specifications of each part are described in Table 2.1.

## 2.5. Evaluation

### 2.5.1. Laser Experiment

The colloidal screen's view angle varies when the intensity of the ultrasonic wave is changed or modulated. Figure 2.12 displays experimental results obtained using different ultrasonic waves. However, the same effect can be seen when the intensity and the focus length are changed. The view angle become wider corresponding to the intensity of ultrasonic waves. Looking at the BRDF equation, Equation (2.4) (Section 2.3.2), it is obvious that this means that it is changing parameter $\omega_o$. We are able to control this parameter from 2 - 87.5° . Because the screen is vibrated intensely, the laser's reflection is not consistent. This is shown in Figure 2.12(Right), where t is

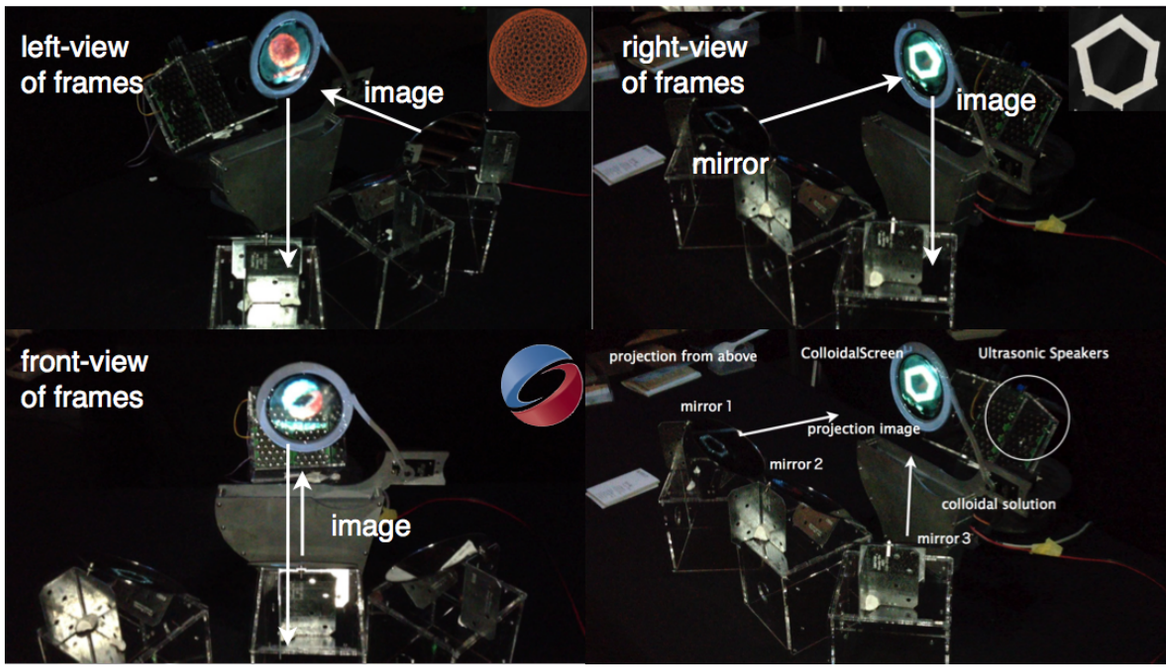


Figure 2.15: (Multi-view Screen) Three different images from different perspectives are shown. The top-left image viewed from the left, the bottom-left from the center, and the top-right from the right.

time. There are slight differences in each image but the shape of the laser reflection is similar.

The graph of the brightness on each angle is shown in Figure 2.13. It shows that the narrow reflection angle (with low ultrasonic intensity) is bright in the center of the reflection and the brightness diminishes in the neighborhood of the center of the reflection. In contrast, the wide reflection angle (with high ultrasonic intensity) results in a gentle decrease in brightness.

This result shows that we can control the view angle and distribution of the brightness by changing the intensity of the ultrasonic wave. It indicates that the colloidal screen solves the problem of screen selection and enlarges the application of the projector screen.

### 2.5.2. Stability

In this subsection, we describe the retention time along with the stability of the colloid film. In our experiment, the colloidal film kept its membrane stable for three minutes on average when the ultrasonic waves were applied. The key component is water; the less water there is in the membrane, the more noisy the image. Figure 2.14 shows how the image quality changes with time. Observing the circle on the four images, it can be seen that the images on the left devolve into the images on the right over time. This is because as time passes the water evaporates, causing the transmission characteristics to be reduced, which results in the image being disturbed. The main reason for this disturbance of the display is failure to control the reflection characteristic.

## 2.6. Applications for 3D expression

We developed several prototypes that utilize the characteristics of the colloidal screen. In this section, we describe four sample applications of the colloidal screen that use different optical properties. The multi-view screen uses the view angle, the plane-based 3D screen uses the transparency, the deformable screen uses the phase array to change the shape, and the bump mapped screen uses deformation with specifications.

In this subsection we describe the unique display applications utilizing soap bubbles unique characteristic firstly. After that we describe BRDF material expression on colloidal screen.

### 2.6.1. Multi-view Screen

We developed a display to show multiple images from multiple angles using the characteristics of the colloidal screen. The principle of operation depends on the characteristics of reflectance distribution of $\omega_o$ for multiple light sources, as shown in Figure 2.8. Different projection sources provide several different images for each angle. The images are being multiplexed at the same time but one image can only be seen in one direction.

In this application, five components are needed: different directional light source, colloidal solution, frame for the membrane, film replacement mechanism, and ultrasonic oscillation. The installation position is shown in Figure 2.15.

We projected the image from above and decomposed a single image into three images by angling the three mirrors in different directions. We also set an ultrasonic oscillator behind the screen to operate it. The result is shown in Figure 2.15. There are three images: one from the left, one from the center, and one from the right. We set

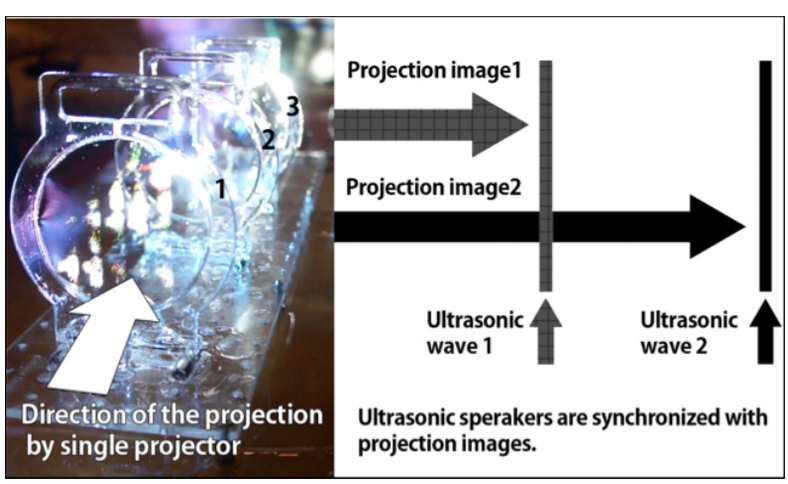


Figure 2.16: (Plane based 3D screen) The transparency alternates within the 3 screens.


Figure 2.17: Overview of poppable display.

the left edge at r = 0 degrees and the mirrors at positions r = 45, 90, and 135 degrees. We adjusted the colloidal screen so that the reflection angle was 40 degrees (by ultrasonic modulation). The actual transition of the images is shown on the right side of Figure 2.15. The transition is smooth and there are no image overlaps.

### 2.6.2. Plane-based 3D screen

In this subsection, we describe the development of a 3D display using multiple planes (Figure 2.16). LCD displays have a problem when it comes to viewing multiple layers; because of polarization, it is not possible to display multiple planes at the same time. In this respect, the colloidal display has several advantages. This colloidal screen can display more than one plane at the same time, and the image is very bright.

We setup multiple sets of colloidal screen and ultrasonic speakers with ultrasonic oscillations synchronized with the projector. The installation position is shown in Figure 2.16. Each colloidal screen had an ultrasonic speaker that set its transparency. Toggling the transparency of each screen was achieved by simply turning the speakers on and off. The system was able to show three different images on each colloidal screen by controlling the transparency of each screen synchronized with the projector's images. This is effectively a 20 Hz time division plane-based 3D screen with a single projector. (it operates 60Hz on 3 screens)

## 2.7. Applications for Deformable Display

Screens are essential to entertainment as they display various digital contents such as movies, presentations, and shows. Typical screens are rigid and static, and allow no physical user interaction corresponding to the displayed contents. In this research, we attempt to enable physical interactions with a display. A colloidal screen [37] (shown in Figure 2.1) is expanded to be “poppable” for this purpose. The transparency of the colloidal screen is controlled by ultrasound waves, and the screen is deformed by changing the intensity of these waves.

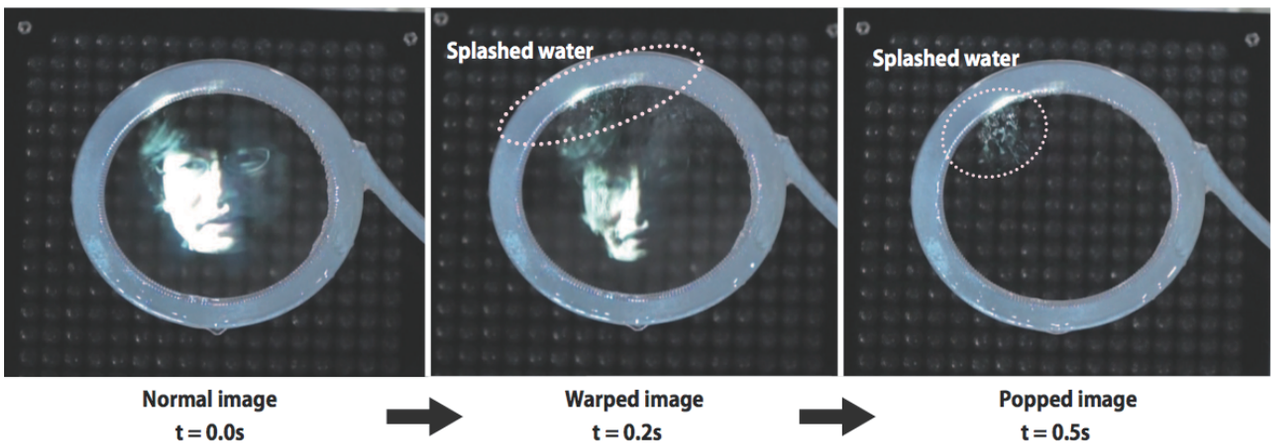


Figure 2.18: Deforming & Image popping. When the ultrasonic focal points hits the membrane, image on the bubble screen is warped and membrane splashes the water. After that, bubble screen pops in 0.3-2 seconds.

Here we propose to add application of “physical effect” in display interaction and entertainment computing using this technology. “Pop” and “deform” interaction on display has a potential to computer entertainment. There are many “analog” toys and games that pops balloons, deform images, and break something. These games and toys have surprise and amusement. Poppable display is a digital display that enables such physical interactions: popping, deforming, and breaking. Adding to that, these physical effects are repeatable by replacing the soap films. Soap films are unique material which allows the object to pass through (shown in Figure 2.19). Digital toys might be applicable soon with a portable projector and there are a lot of toys using soap bubbles. This research will contribute to combine the essential enjoyment of soap bubbles and computer entertainment.

### 2.7.1. Application Setup

This application has four components: a projector; a tank of soap solution; a frame;

Figure 2.19: Cutting into colloidal screen

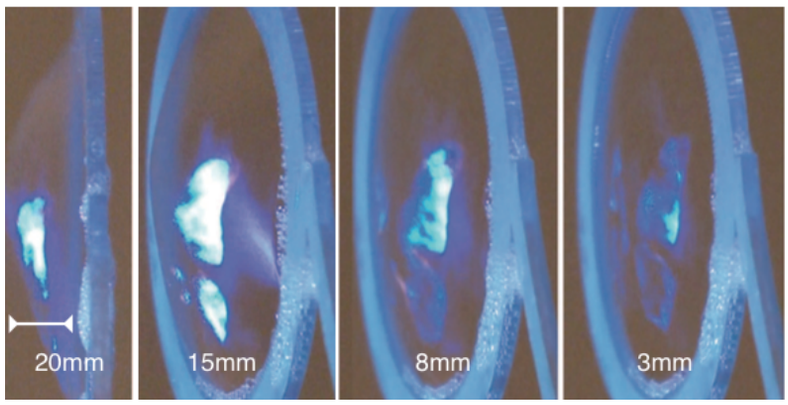


Figure 2.20: Deformation of the screen of up to 20mm.

and the mechanism to replace the film, an ultrasonic excitation device. All devices are same as Figure 2.11.

The projector light is focused on the film and the film's frame. Ultrasound waves are produced from the speaker simultaneously and hit the film, vibrating it. Then the image is projected on the colloidal screen.

A higher-intensity ultrasound wave pops out and breaks the film. When the film is broken, it is replaced by the servomotors.

### 2.7.2. Physical Effects & Interactions

#### 2.7.2.1. Poppingimage

In this system we propose physical and visual effect of popping. We can pop the bubble screen by focusing the ultrasonic waves in high intensity. In Figure 2.18 we

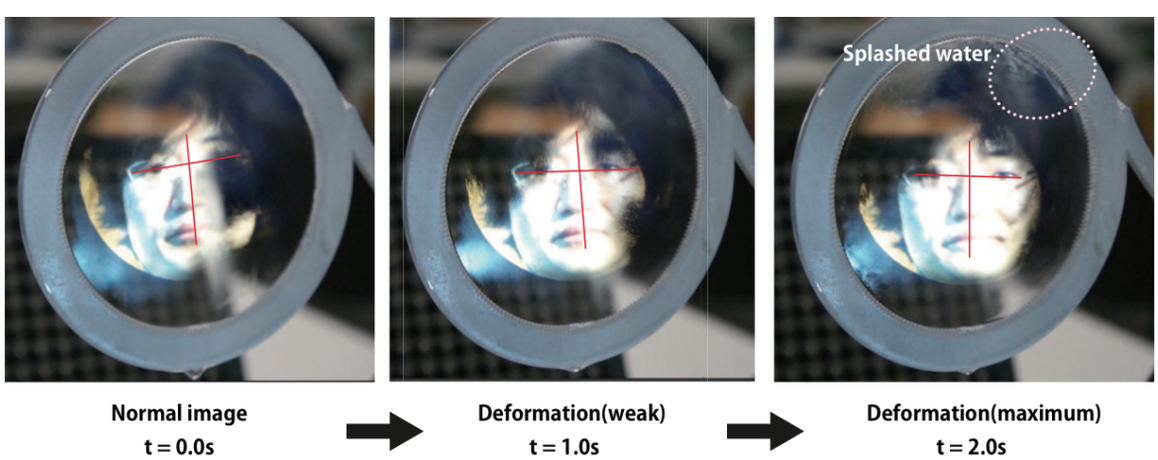


Figure 2.21: Image Deformation. The focal point moves back side of screen to front side. Red lines indicate the deformation of screen. Red lines connect eye to eye and nose to mouse.

show how it pops.

When the ultrasonic focal points hits the membrane, image on the bubble screen is warped and membrane splashes the water. After that, bubble screen pops in 0.3-2 seconds. It is faster to break when the focal point hits the membrane around the edge of the frame. This system replaces the membrane in 5 seconds.

This physical effect can be applied to games, especially using this system as a target. Moreover, it enhances the effect of video projection such as bumping or bursting.

#### 2.7.2.2. Insert object into the image

Soap film is an unique material which allows the object to pass through it. In Figure 2.19 we show a knife cutting into the screen. The object must be wet. Ultrasonic focal point should be set at far opposite side of the frame.

This interaction can be expanded in the future to allow the user to literally cut the screen. Further more, this system propose interaction such as tearing, breaking and sticking with screens. If the object is wet enough, it would not affect the membrane's lifetime. However if we insert the object without wet surface, the soap film quickly pop out.

#### 2.7.2.3. Deforming Animation

In this application we propose deforming animation. We can deform the bubble screen by moving the focal point of the ultrasonic wave. In Figure 2.21, we show how it can deform the face that is projected.

This physical effect can be applied to many entertainment such as imitating a force field. Moreover, by projecting the face image, it has a potential to enhance the chat's communication or interaction by deforming the screen

## 2.8. Applications for Material Expressions

In this chapter, we used ultrasonic phased arrays to excite the colloidal films in order to change reflectance of a colloidal screen by capillary waves. We've extended this mechanism to the material display application by determining how to reproduce a material's reflectance and evaluating the reproduced appearances. Moreover by alternating the soap film's reflectance at high speed through time division multiplexing, we can generate different materials' reflectance on colloidal screen and made the display more realistic.

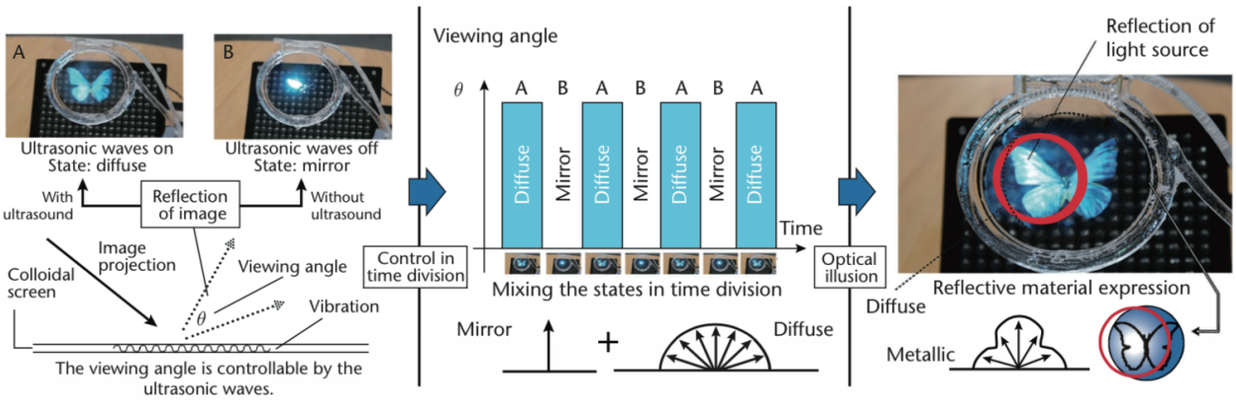


Figure 2.22: How applications for material expression work. At the left, the bold arrow represents the image from the projector. Applying ultrasound waves to the soap film changes the projected image's reflectance. When we apply the waves, the film bounces the projected image at an angle. We can control this viewing angle's range. In the figure, A denotes when the ultrasound is on, displaying the diffuse state, and B represents when the ultrasound is off, displaying the mirror (specular) state. By alternating these two states at high speed (20Hz to 800Hz), the display presents an optical illusion that expresses different materials, such as metals.

### 2.8.1. Alternating Reflectance

In the real world, the light emitted from the source reflects on an object's texture, resulting in our ability to simultaneously view both the object's reflection and texture. In this application we aim to mimic this by using a projector as both the light source and image source. Traditional screens show only the image source; we can show both sources. The projector acts as a light source in the mirror state and as an image source in the diffuse state.

By quickly alternating between the two states in 20Hz to 800Hz, we can show an image with specific reflectance (see Figure 2.22). The transition time from the mirror state (ultrasound off) to the diffuse state (ultrasound on) is short and from the diffuse state to the mirror state is relatively long because activation process is driven by ultrasonic vibration in contrast return process is driven by surface tension. This creates a difference between images displayed with different ultrasound frequencies, as we show later.(Figure 2.25)

To control an image's brightness, we use multiple parameters: the projector's luminance, the image's brightness, the screen's reflection distribution, and the ratio of alternating the reflection states.

### 2.8.2. Controllable Parameters

The display lets us control three parameters related to texture appearance: reflection

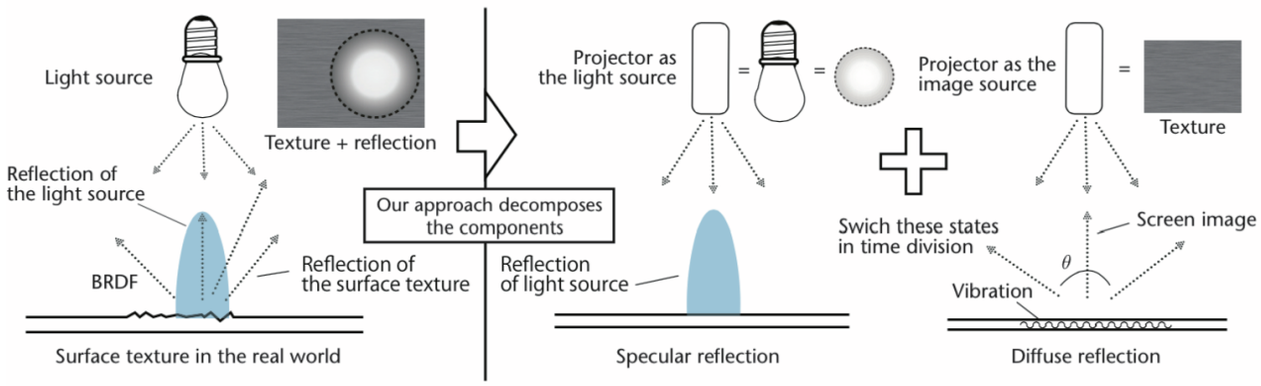


Figure 2.23: Mimicking a real-world texture by controlling the ratio of the mirror and diffuse states. BRDF stands for bi-directional reflectance distribution function.

(through the viewing angle and timing), projection brightness, and the projected images. (Figure 2.24)

We vary the screen's viewing angle by modulating the frequency of the ultrasound device's output intensity. The texture also changes the screen image's brightness when the projector's brightness and the digital image's brightness are given. If we change the image's contrast, the texture's appearance changes. This method is similar to the mix of image-based rendering techniques used in computer graphics.

### 2.8.3. Screen Images

Figure 2.25 shows the results for five viewing angles of four states:

- *The mirror state,*
- *20-Hz ultrasound modulation,*
- *800-Hz ultrasound modulation, and*

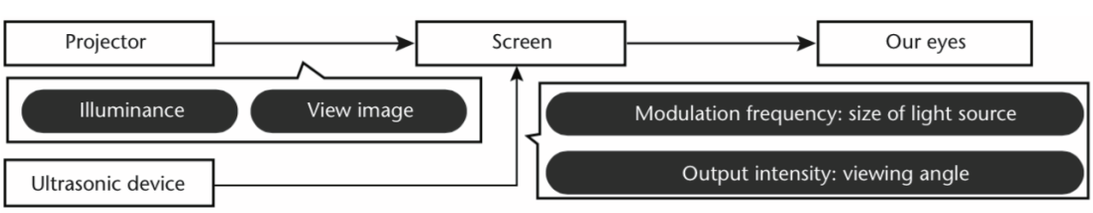


Figure 2.24: Diagrams our system.


Figure 2.25: Sample results for four reflective states from five viewing angles. The red circle shows the reflective spot from the mirror state

- *The diffuse state.*

With 20-Hz modulation, the display gleamed slightly. At 800 Hz, large bright spots moved with the viewing angle's change, appearing as a metallic luster. These spots show a different texture, which implies that we can change the appearance by changing the frequency while keeping the luminance value the same.

### 2.8.4. Evaluation for Material Display

We conducted experiments to evaluate our display's reflectance, stability, and realism.

#### 2.8.4.1. Human Tests

Study participants viewed an image on an LCD screen and an image on our display and indicated which looked more like the real material, which in this case was aluminum foil. Most participants found our display's image to be more realistic.

Then, we showed the participants two sheets of aluminum foil; sheet A had the shiny side visible, and sheet B had the dull side visible (see Figure 2.20). We asked them to select which one of several images projected on our display was most like each sheet. The participants stated that 20- or 60-Hz modulation looked more like sheet A

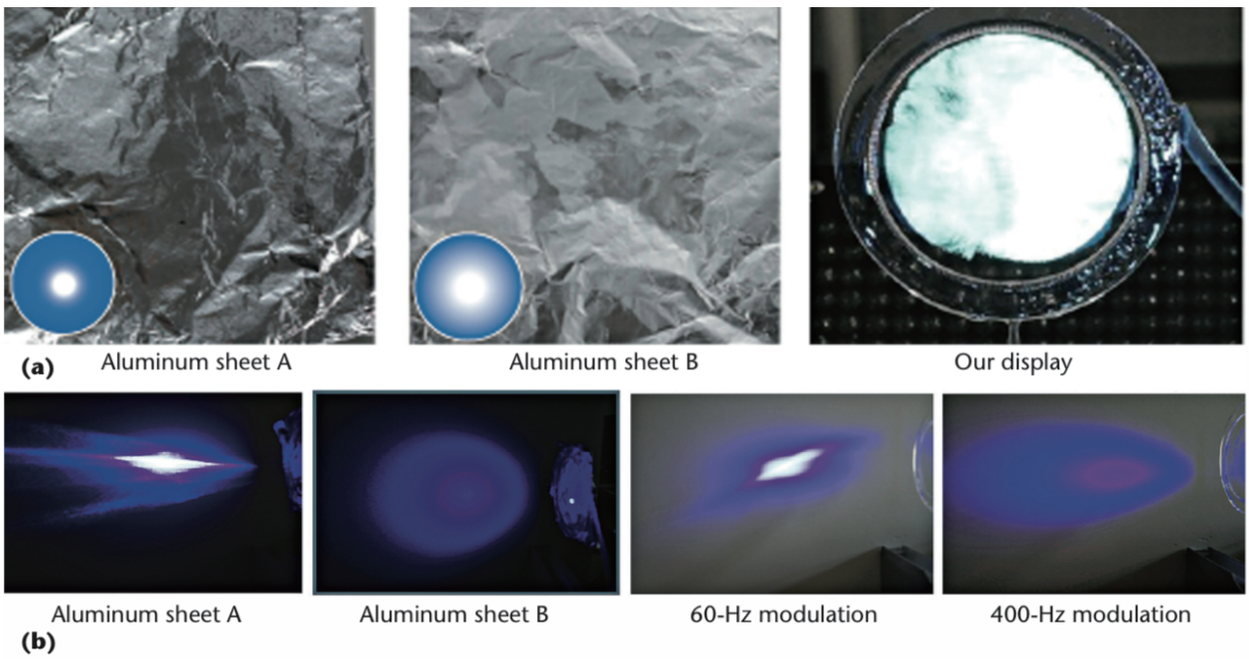


Figure 2.26: Comparing our display to two sheets of aluminum foil. (a) The two sheets and an aluminum-like image on our display. Sheet A had the shiny side visible; sheet B had the dull side visible. The insets in the first two images illustrate the size of reflection spots. (b) Laser reflection on the two sheets and on our display at 60- and 400-Hz modulation. Note the similarities between sheet A and 60-Hz modulation and between sheet B and 400-Hz modulation.

and that 400-Hz modulation or the diffuse state looked more like sheet B.

#### 2.8.4.2. Further Laser Tests

For comparison, we performed a laser test on regular paper to illustrate diffuse reflection (see Figure 2.27.d). We then performed laser tests on sheets A and B; Figure 2.27.e and Figure 2.27.f show the brightness graphs. As you can see, the results for sheet A were similar to those for 60-Hz modulation, and the results for sheet B were similar to those for 400-Hz modulation and the diffuse state. Moreover, the laser reflection images for our display resembled those for the real material (see Figure 2.26).

This implies that the intensity of the reflection pattern in the brightness graphs for our display is similar to that of the real material and that our results are therefore considerably realistic.

#### 2.8.4.3. Practical Use of the Display

One practical use of this technology is to obtain a dynamic reflection reference for materials (for example, dynamic sampling of printing, furniture, metal, and fabric).

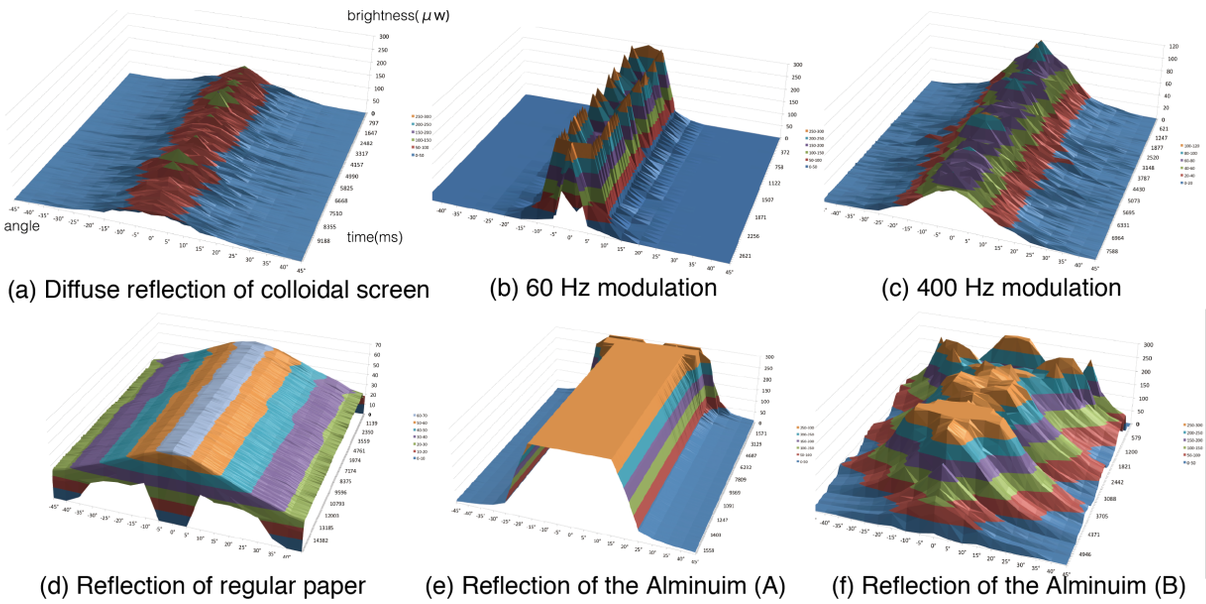


Figure 2.27: How brightness changed with modulation frequency, for tests with a laser. (a) Diffuse reflection on our display. (b) The reflection with 60-Hz modulation on our display. (c) The reflection with 400-Hz modulation on our display. (d) Diffuse reflection of regular paper. (e) The reflection of aluminum sheet A (f) The reflection of aluminum sheet B

This is useful for people choosing materials for products. Moreover, employing this technology to parameterize an object's reflectance is useful for people who want to design a product's appearance, predict the appearance of coatings, or discuss appearance in a consistent way.

## 2.9. Discussion

Here we examine our display's limitations and potential uses.

### 2.9.1. Soap Film Limitations

The soap film's durability depends on the ultrasound device's power and the soap itself. Furthermore, a small disturbance such as a breeze or humidity change will affect it. We can increase the soap film's life span by using a pump that continuously provides the soap solution to the frame. We also found a glue-like substance that helps the film last more than a day.

### 2.9.2. Optical-Property Limitations

When turning transparent soap film into an opaque display, we found that certain spots can't be covered and remain transparent. The coverage area is roughly 95 per-

(a) (b) (c)

Figure 2.28: Differences in View Angles (a)87.5 deg (b) 45 deg (c) 0 deg

cent. Typically, the outer rim is transparent because the frame blocks the ultrasound waves.

### 2.9.3. Limitation on View Angles

We achieved a maximum view angle of 175 deg. Our screen is slightly curved by acoustic radiation pressure because of that, we can see the image from 175 deg point(Figure 2.28). The view angle changes according to the intensity, the waveform of amplitude modulation, and the frequency of the ultrasound. If the view angle is too small, only the light is shown and not the content of the projected image because it is too acute for human eyes. However, we used this to our advantage and displayed three different images from different angles (we applied it to the perspective screen and material display).

### 2.9.4. Entertainment Computing

A soap bubble is a unique material that users can insert their fingers into. Moreover, soap bubbles generate a lot of joy by their beauty and in our making and seeing them. Soap bubbles are used in the entertainment industry on occasions such as party events, and in theme parks and science museums. This technology can be applied in these industries to enable video projections on the bubbles. In this way, it

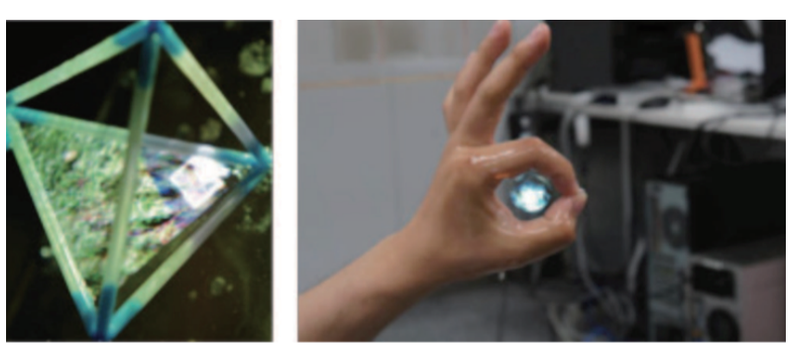

Figure 2.29: Polygon frame and hand frame

can contribute to the expansion of the entertainment computing field.

## 2.10. Conclusion and Future Work

In this project, we proposed an innovative first step to dynamically altering the brightness, shape, and view angle of colloidal screens by Computational Acoustic Fields. Especially we utilize capillary waves on colloidal films and acoustic radiation pressure to deform the screen.

Many future potential projects are envisioned. One potential project is a dynamic 3D model with a minimal view angle and various images projected from different angles. This would be more cost effective than other methods such as holographic viewers. Furthermore, it would be interesting to see a 3D model made out of soap film on a polygon shaped frame (Figure 2.29) with several ultrasonic speakers. Many 3D models, such as those in games, tend to use the same models with different textures to create new enemies. The same concept can be applied to this display. Another usage for this display is to utilize its interesting interactive properties such as inserting and popping. For example, a game in which the player has to cut the screen to kill an enemy can be facilitated. In general, if we are able carry this concept to a bigger scale; it would open up many possibilities for the future of the entertainment computing industry.

In multimedia, it's important to show digital content that's as realistic as possible. Our system contributes to this goal by controlling reflectance in real time. However, properties other than reflectance are also important. Examples include an image's color and smoothness (that is, the projected image might be pixelated). We're investigating how to show the bidirectional surface-scattering reflectance distribution function, which will allow images to be vivid and realistic.

# 3.Project on Haptic Modification

*In this chapter, we describe a method to change the haptic state of physical material pasted on transducers by computational time-division 2D acoustic field. Especially we utilize squeeze film effect to change the friction on real material. This project is aimed to realize malleability on haptic texture of real world object like computer graphics in the digital world by applying computational acoustic fields.*

## 3.1.Introduction

The representation of texture is a major concern during fabrication and manufacture in many industries. Thus, the manner of fabricating everyday objects and the digital expression of their textures have become a popular research area [56]. It is not easy to change the texture of objects in the real world although it is easy in the digital world (i.e. just setting texture parameters). Recently, computer graphics are getting to be used in the real world. For example, digital fabrication technologies are employed widely from laboratories to consumer uses. The fabricated (3D-milled, 3D-printed, etc.) objects represent their specific textures. There are some methods to modify their textures after fabrication. For design and other industrial applications, it would be useful if the fabricated objects are malleable [56] like computer graphics in the digital world. In the human computer-interaction and graphics communities, the following concepts have been proposed: Programmable matter [10], radical atoms [12], etc[13]. In this chapter we aim to transform the haptic textures of re-


Figure 3.1: (Left) System overview (right) real material surfaces.

al-world objects.

Two steps are required to transform real-world textures. The first step is to reduce the original texture and the second is to rewrite the texture. There are many different types of haptic textures in the real world and it is necessary to reduce them as preprocessing. It is then possible to rewrite the textures. In this project, we focus on the first step and we introduce a technique named “Diminished Haptics” (Figure 3.1). This technique reduces and transform the degrees of real-world haptic textures using ultrasonic vibration based on a squeeze film effect [64]. By applying this technique, we can adjust the haptic texture of real world object. This technology is applicable to the situation when we choose texture material samples in shopping or ordering.

This chapter is structured as follows. First, a brief overview and background were provided in the introduction.  Then, related work and the principle are shown. Finally, the equipment used for the implementation and the results of experiments related to haptic textures are presented. This technology will facilitate new relationships between people and textures in the real world.

## 3.2.Related Work

There have been several related studies on haptic texture representation. One approach is wearable devices to provide additional vibration to users’ fingers [63]. The other is haptic displays add haptic feedback on their smooth surfaces. The technologies employed in the latter approach include ultrasonic vibrations [57][58] and elec-

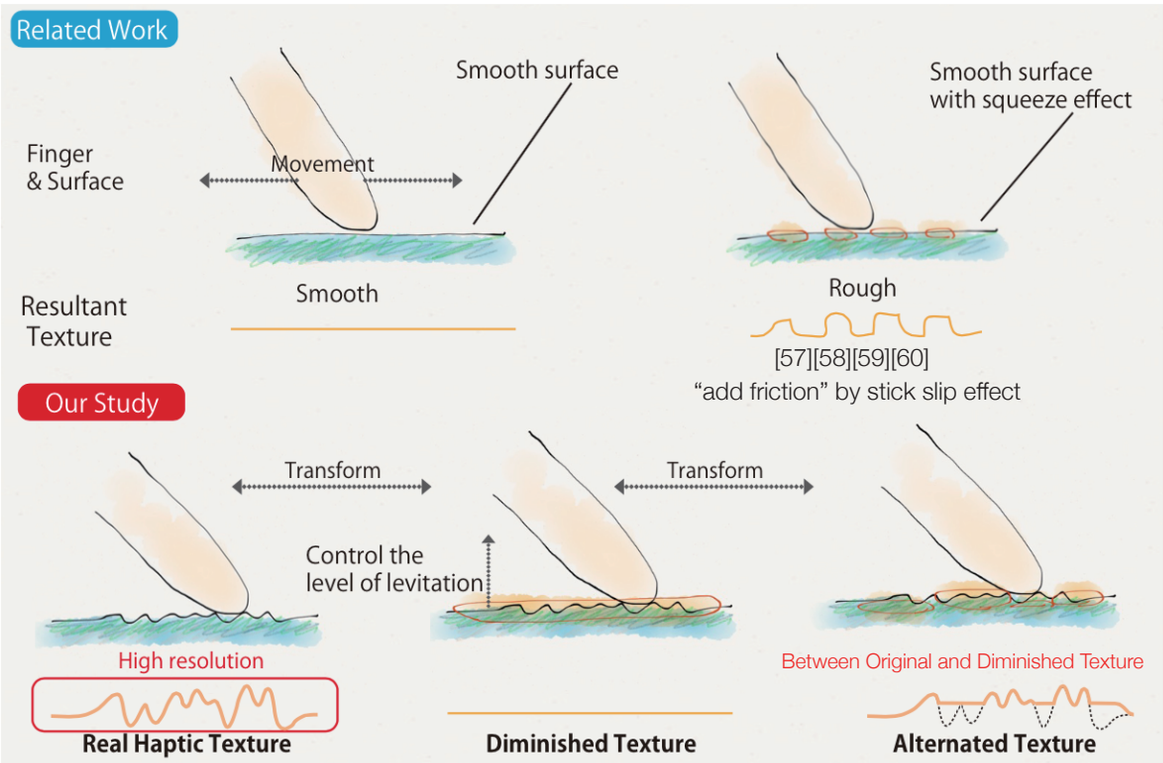


Figure 3.2: Basic idea (top) conventional studies (bottom) our approach

trostatic forces [59]. These technologies have been applied to trackpads [60], pointing devices [61], and augmented reality (AR) systems [62]. The ultrasonic technology utilizes a squeeze film effect to reduce the friction of a flat surface and reproduces the texture by modulating the ultrasonic vibration (as shown in Figure 3.2, top). The electrostatic technology also adds textures to smooth surfaces.

In this project, we aim to achieve the opposite effect, i.e., we reduce the texture of a real material using a squeeze film effect. We focus on the transformation of real textures and we employ a real material as the surface of haptic display (Figure 3.2, bottom). We consider that the reduction process has an important role as a preprocessing step in the transformation of real-world textures. Our approach is also ap-

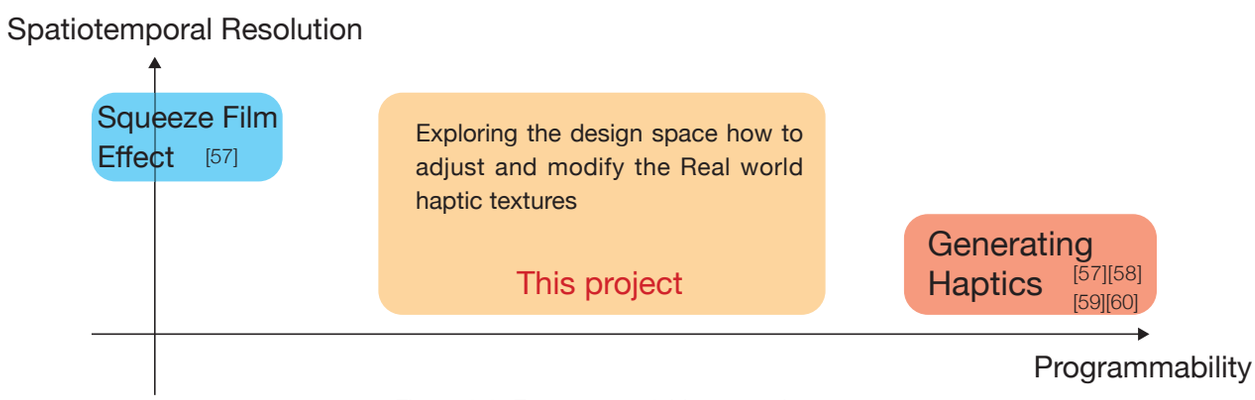


Figure 3.3: Focus area of this research

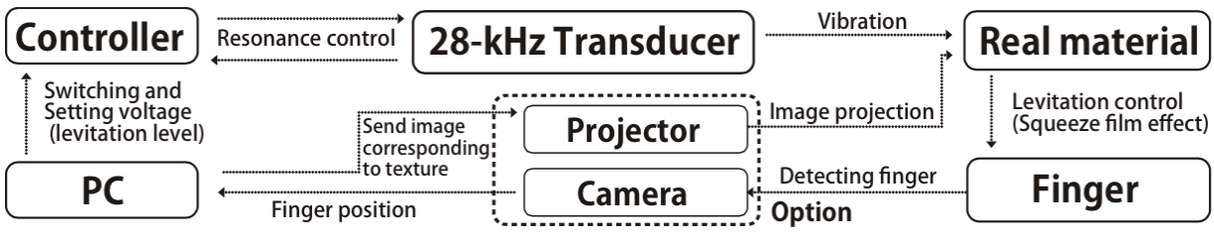


Figure 3.4: System components; computer,ocuognthropllearp, 28kHz

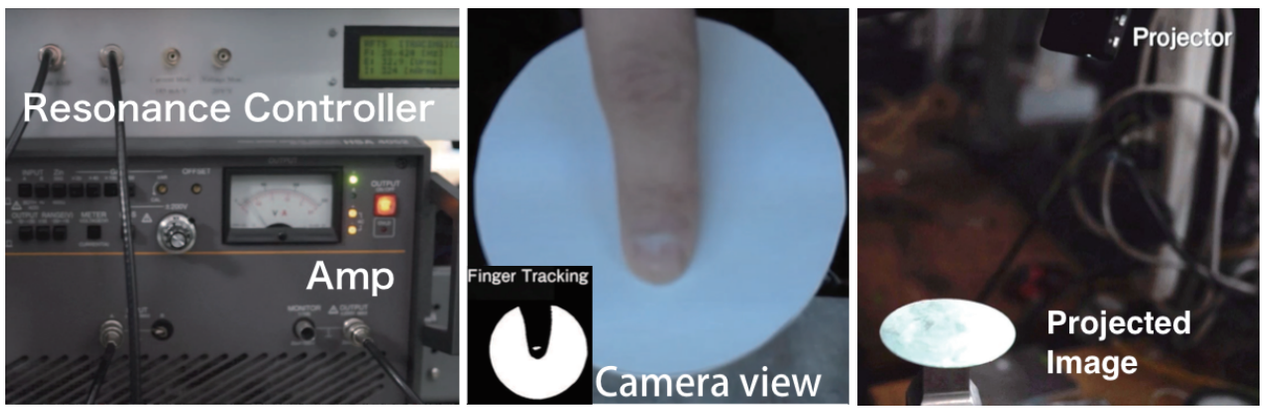


Figure 3.5: (Left) finger tracking, (right) image projection.

plicable to other purposes such as increasing textures and expanding conventional technologies by reducing the original haptic textures.

In Figure 3.3 we show the focus area of this research. In [57] squeeze film effect was reported. This project is aimed to explore the design space around adjusting real world haptic textures. In conventional studies, they did not adjust the haptic texture of external material. We focus how to change the haptic texture of real world material by external forces.

This technology is applicable to adjust real world haptic texture when one chooses materials. Conventional studies did not focus on how to change or to adjust the haptic texture of real world material.

## 3.3.Design & Implementation

Our approach aims to transform the haptic textures of real materials. In particular, our method transforms real textures by utilizing ultrasonic vibration. We employ ultrason-

ic vibration to reduce and erase the haptic textures of real-world objects based on the squeeze film effect. Using our system, the texture obtained is inherently high resolution and the altered textures are felt without lateral movement of fingers because real material has its own texture (Figure 3.1, right). These features are different from those obtained using previous methods [57][58][59][60]. Figure 3.4 shows a diagram of our system, which has four components: The host computer, the resonance controller, the ultrasonic transducer, and real material textures. Users can touch the real material with their bare fingers. The height of levitation by the squeeze film effect is controlled to transform the textures.

The process operates as follows. The computer sends a start signal to the controller, which adjusts the resonance frequency of transducer and attached material. Next, the controller generates the input signal to the transducer. The amplitude of the input signal determines the levitation height of the finger relative to the material surface based on the squeeze effect. We paste papers of various real textures (Figure 3.1, right) onto a metallic plate that is acoustically coupled to the 28-kHz transducer. Resonance control (adjusting the frequency of the input signal figure 3.5 top) is necessary for this use because the resonance of transducer changes when user touches the transducer.

In further applications, we also employ a projector, a camera, and other equipment. These are optional components which are connected to the computer for the application purpose (Figure 3.5). A finger tracking system with a camera is shown in Figure 3.5 (left). A camera (640 × 480 pixels) is set above the material's surface. Because the finger moves only two-dimensionally,  tracking with a binary image is enough to detect the finger position. Thanks to this finger-tracking, multiple textures can be provided on the same material by altering the ultrasonic vibration according to the finger position (the additional waveform overlapped in 28kHz signal). In addition, a projector is set above the material's surface, which projects an image onto the surface to transform the visual appearance of the material. By utilizing ultrasonic vibration and projection, our system can transform the real material in terms of haptic and visual characteristics.

Here we describe the overview of our systems. In next section 3.4, we introduce our resonance tracking methods in detail. Resonance tracking has important role to vibrate the material continuously. Because of the touch of users, the resonance frequency of material can be changed. Then we have to track the resonance frequency in order to vibrate the material in high amplitude. Without resonance tracking, the squeeze film effect would not appear appropriately.

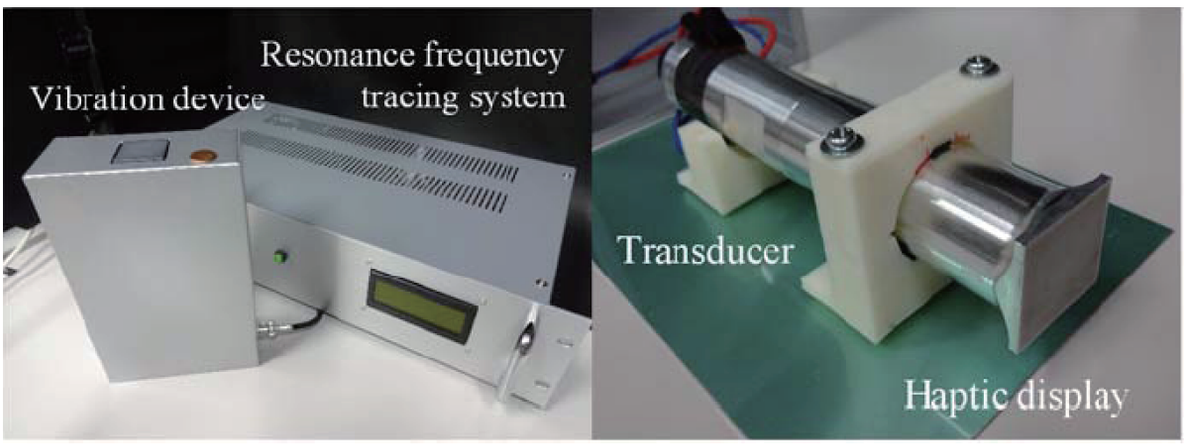


Figure 3.6: (left) resonance frequency tracing system (right) transducer and haptic display

## 3.4.Resonance Tracking

### 3.4.1. Implementation

Figure 3.6 (right) shows the vibration device. The device has a bolt-clamped Langevin-type transducer with a horn. At a vibration node, the transducer and horn is mounted to a casing with rubber block. The tip of the horn is square shape with sides of 30 mm. Real materials (e.g. sandpaper, wallpaper, etc.) were glued on the tip as the surface of haptic display. User can touch the real material with their bare fingers.

The resonance frequency of the bolt-clamped Langevin-type transducer is changed according to the various reason when a finger contact with the real material texture. The difference of the vibration performance is shown in Figure 3.7. When the finger was contacted with the haptic display, the admittance loop was small. Additionally,

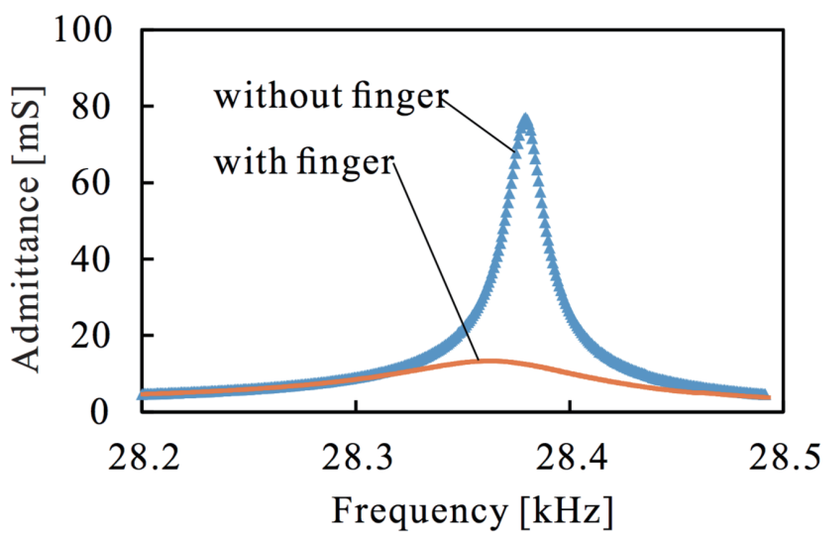


Figure 3.7: Admittance of transducer with/without finger

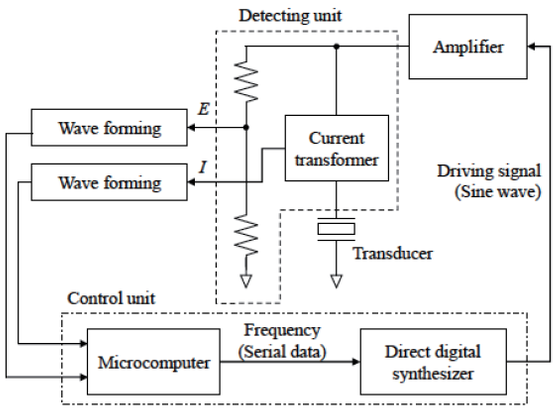


Figure 3.8: Overview of Resonance frequency tracing system

to generate strong vibration, the transducer has high Q factor. Therefore, in order to keep strong vibration, resonance frequency should be traced during the diminished texture.

This resonance frequency tracking is one of the key factor to realize our concept. In conventional studies they did not have to vibrate the material with high amplitude because their focus is how to generate the haptic feedback on planer surface by stick slip effect. We have to change the thickness of squeeze film. Then we have to keep the thickness of squeeze film when user touch the tactile display surface. Then we need the resonance frequency tracing to obtain the enough amplitude.

In this project, we used a resonance frequency tracing system based on current phase measurement. Overview of the resonance frequency tracing system is illustrated in Figure 3.8. The system consists of a microcomputer, a direct digital synthesizer, an amplifier, voltage and current detecting unit and two wave forming circuit. These components are packaged in a portable casing. The system is tracing the resonance frequency by measuring the phase difference between the applied voltage and current [65]. To measure the phase difference, amplified driving voltage was supplied to the ultrasonic transducer through a detecting unit. In the following experiments, we used this resonance frequency tracing system.

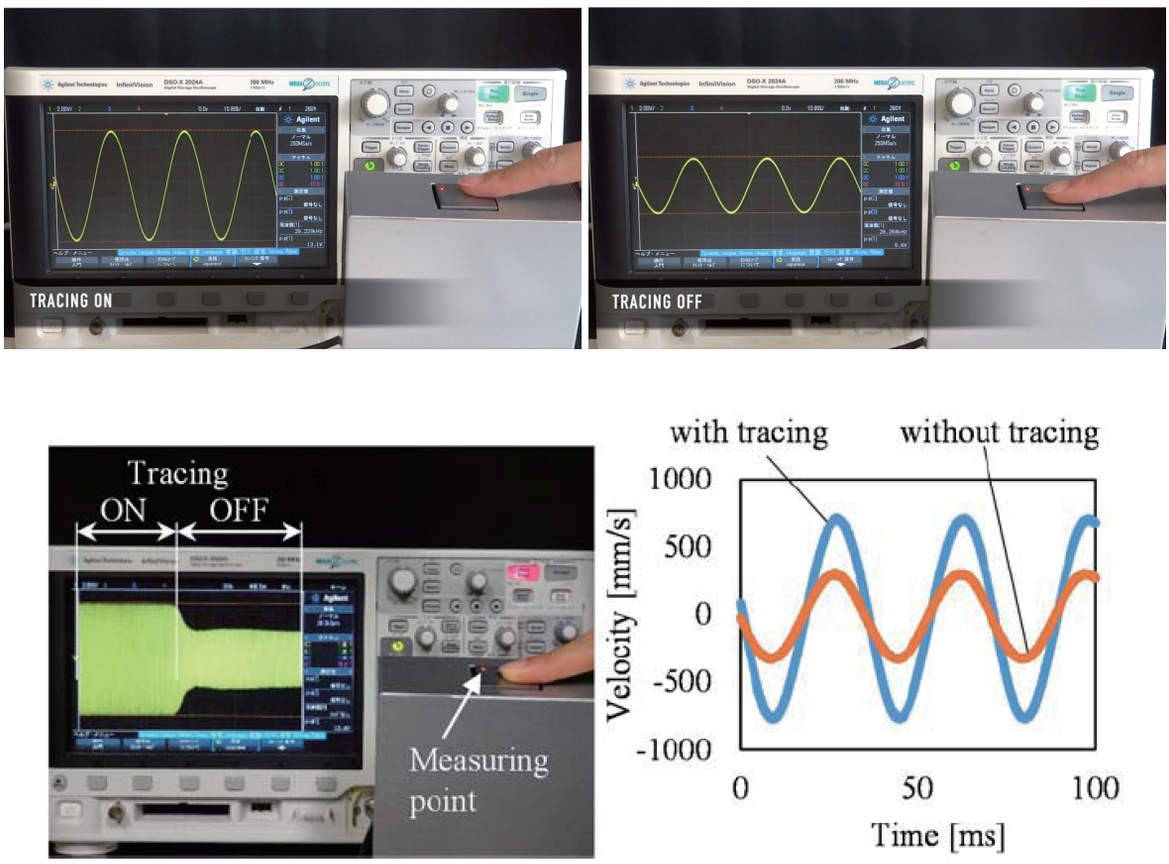


Figure 3.9: (top-left) result waveform with resonance tracing system (top-right) without resonance tracing system (bottom-left) result waveform shown in different time duration (bottom-right) Vibration velocity at haptic display with or without resonance frequency tracing

| Tracing | Finger | Vibrationvelocity [mm/s] |
|---|---|---|
| OFF | Without | 850 |
| OFF | With | 387 |
| ON | With | 818 |

Table 3.1: Vibration velocity of on/off tracing and with/without finger

### 3.4.2. System Evaluation

To show the effectiveness of the resonance frequency tracing system, the vibration velocity of the haptic display was measured. The vibration velocity was measured by using laser Doppler vibrometer. The overview of the experiment and the measured velocity are shown in Figure 3.9. Applied voltage was 13.5 Vrms. The decreasing of velocity was occurred when the tracing was off. This result shows that the squeeze

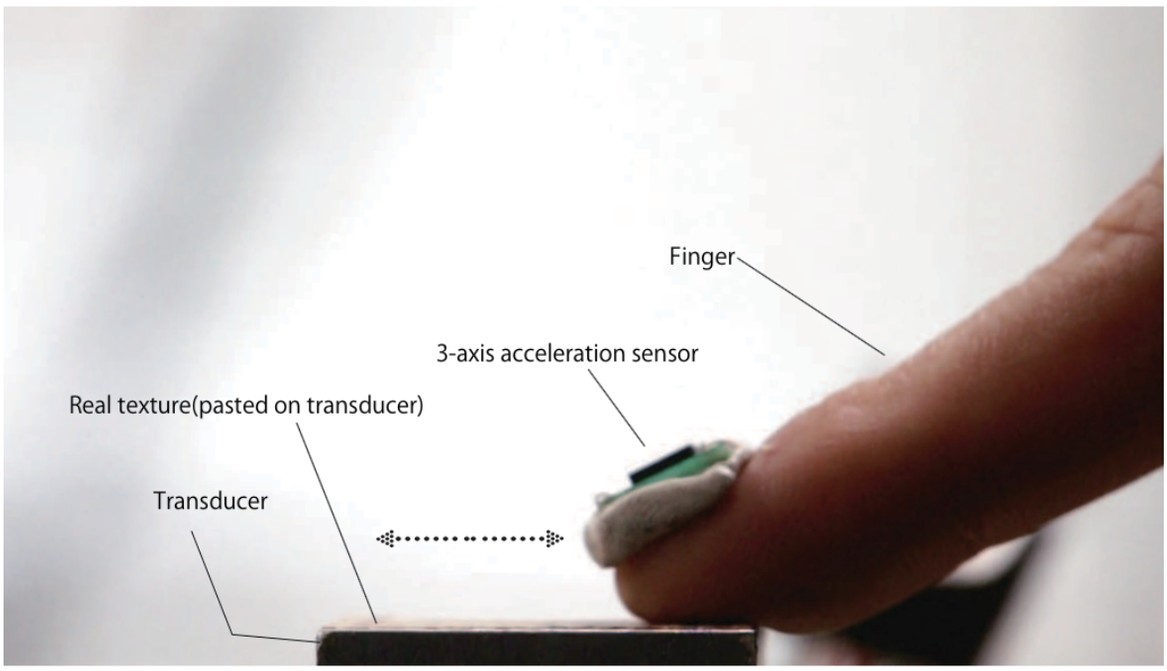


Figure 3.10: Experiment overview: 3-axis accelerometer attached to the nail and finger trace the texture on the transducer.

film effect was decreased, i.e., the transform of textures was changed when a finger contacted with the display. Therefore, the resonance frequency tracing system is essential equipment for the diminished haptics. Additionally, the reducing the real haptic texture was obtained by using this system. The degree of reduction was changed with or without tracing system.

## 3.5.Evaluation with material and touch

In this section, we describe the experimental evaluation of our approach. Our evaluation involved a quantitative evaluation based on a three-axis accelerometer and interviews with subjects. First, we describe the experimental design and we provide an overview of the results, which are followed by a description of the quantitative evaluation and interviews.

### 3.5.1. Design and Results Overview

To evaluate the alteration of the haptic texture, we focused on the high-frequency

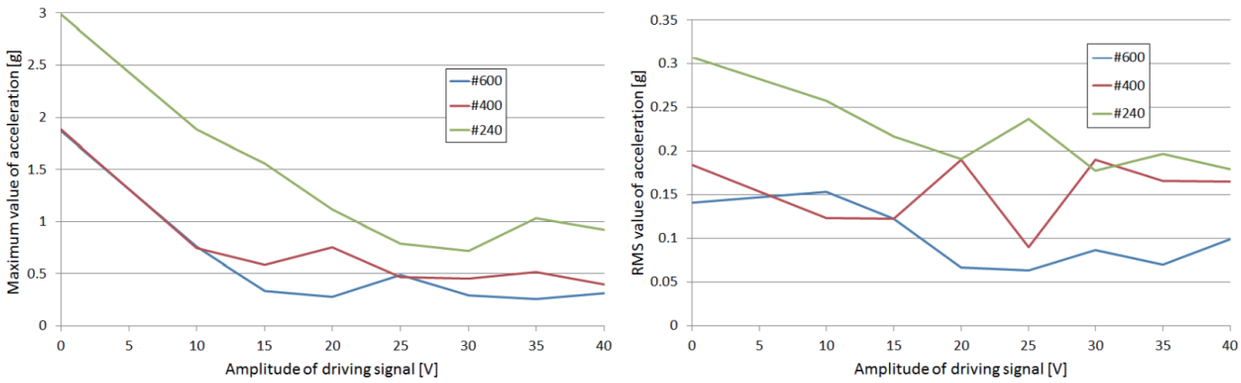


Figure 3.11: (Left) maximum value of acceleration #600 vs #400 vs #240 (right) RMS value of acceleration #600 vs #400 vs #240 (Horizontal Axis) Amplitude of driving signal to transducer (V) (Vertical Axis) Maximum value of accleration (g).

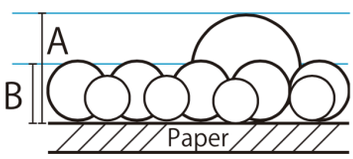


| Number of sandpaper | Max particle size (μm)(A) | Average diameter (μm) (B) | Height of bump (μm) (A)-(B) |
|---|---|---|---|
| #600 | ≦53 | 20.0±1.5 | 33±1.5 |
| #500 | ≦63 | 25.0±2.0 | 38±2.0 |
| #400 | ≦75 | 30.0±2.0 | 45±2.0 |
| #320 | ≦98 | 40.0±2.5 | 58±2.5 |
| #280 | ≦112 | 48.0±3.0 | 64±3.0 |
| #240 | ≦127 | 57.0±3.0 | 70±3.0 |

Table 3.2: Sandpaper number grades, the diameters of the particles, and height of bump

components of the finger vibration when a finger was traced on the surface. Using a three-axis accelerometer (KXR94-2050) attached to a fingernail, we measured the degree of haptic texture reduction (as shown in Figure 3.10). Graphs were obtained for the accelerometer in two states: transducer active (levitated) and inactive (not levitated), where the shapes of the graphs contained waves that exhibited changes in the high frequency components (transducer's frequency (28kHz) is much higher than sampling frequency). When the transducer was inactive, the friction was not altered and the high frequency components of the graphs were evident. When the transducer was active, the friction was decreased and the high frequency components of the graphs were reduced.

In this experiment, the area of the touch surface was 2 $cm^2$ and the finger movement was regulated to 4 cm/s. The accelerometer could measure ± 2 × g and the output data were captured using an oscilloscope.

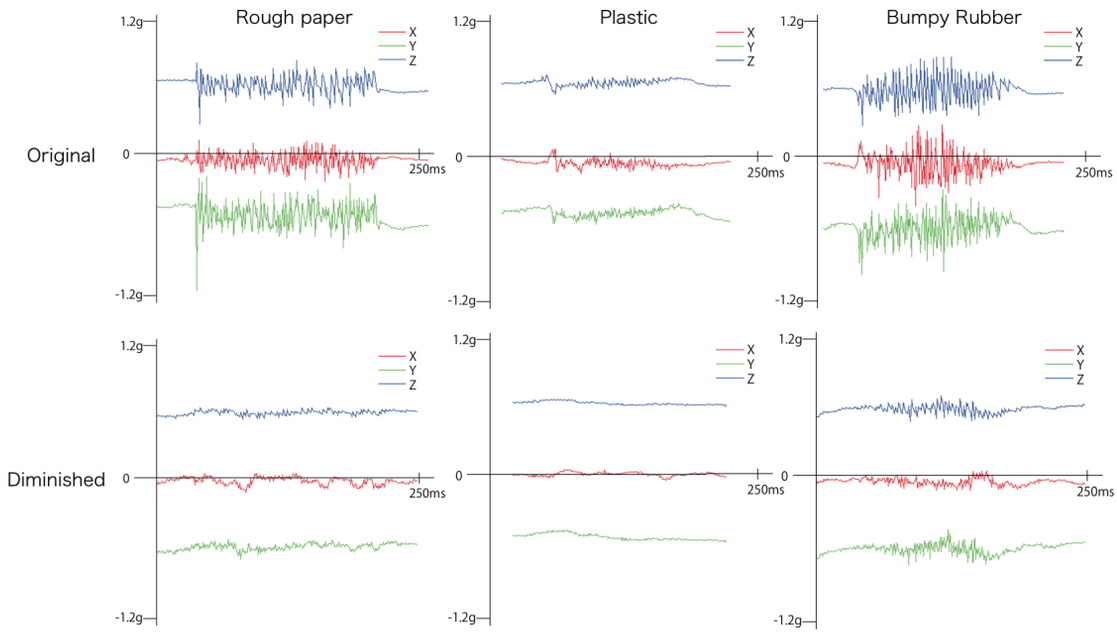


Figure 3.12: Results (30 V RMS) on several materials (left) rough paper, (center) plastic, (right) bumpy rubber.

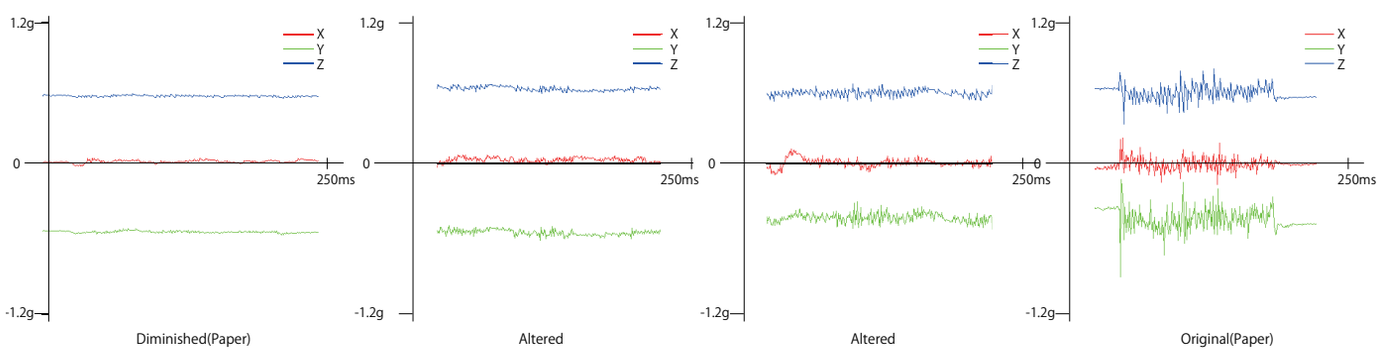


Figure 3.13: Results on altered texture between Original and Diminished textures

### 3.5.2. Roughness and Levitation

In these experiments, we investigated the reduction of haptic textures based on a quantitative evaluation. We used sandpaper as the surface. We cut sandpaper into pieces that measured 2 $cm^2$ and pasted them onto the transducer. The sandpaper grades ranged from #600 (smooth) to #240 (rough), i.e., #600, #500, #400, #320, #280, and #240. The diameters of the particles on the sandpaper surfaces are shown in Table 3.1. The particles were attached to the surface of the sandpaper and

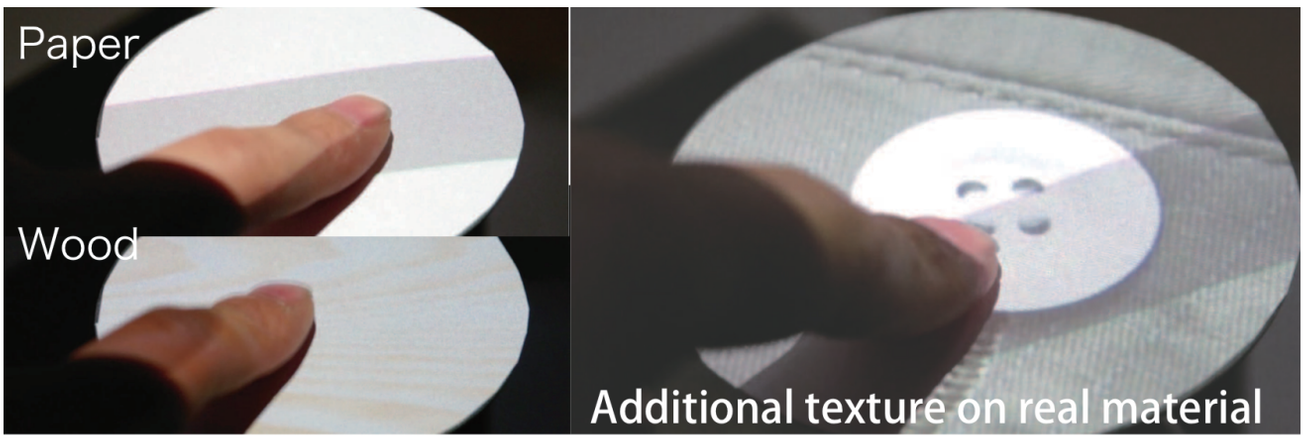


Figure 3.14: Application: spatiotemporal control with projection

their diameters determined the roughness of the sandpaper. We adjusted the output voltage from 0 V to 40 V (5 V steps). The squeeze film effect began to occur at 10 V. If the output exceeded 40 V, the subjects felt heat on their finger. The graph obtained using the three-axis accelerometer is shown in Figure 3.11. The RMS and maximum value of acceleration were reduced with high amplitude.

### 3.5.3. Real Materials

In these experiments, we investigated the reduction in the haptic textures of several materials: sticky plastic, rough paper, copy paper, metal, bumpy rubber, and double-sided tape. We cut the materials into pieces that measured 2 $cm^2$ and pasted them onto the transducer (30 V RMS). Each subject traced the textures on the transducer with a finger. The three-axis accelerometer was attached to a fingernail. The examples of the results are shown in Figure 3.12. It is confirmed that the textures are effectively reduced and transformed to different textures.

### 3.5.4. Interviews

We have interviews with four subjects. They have tried tactile display system utilizing conventional actuation ways[58]. After the experience of tactile display system by conventional actuated ways they tried our system. We asked their comments. Four subjects stated that: “The texture changed,” “I did not feel the vibration,” “The tex-

ture became smooth but it was slightly jagged," "It is very high resolution," etc. The ultrasonic vibration was sufficiently high frequency not to be detected by the human sensory system.

If the squeeze film was not sufficiently thick to levitate the finger from the material, the subjects felt a jagged sensation from the tops of the geometry of rough materials. All subjects (age; 23, 26, 33,41, ) recognized the texture transformation.

## 3.6.Application

Examples of possible applications of the proposed method are as follows. Our technology aimed at transformation of real world textures. Then we focus on how to adjust the haptic texture of base material. Moreover the characteristic of our system has selectivity of base material and we can change it easily because we vibrate it by external forces.

### 3.6.1. Haptic transformation:

The proposed method controls the magnitude of the texture using a squeeze film effect. While the texture is eliminated when the squeeze film is sufficiently thick, the texture is reduced when the squeeze film is thinner than the height of the texture peaks.

This application inherently provides high resolution haptic texture because it never generate the haptic texture but adjust real world textures. This application is applicable to the catalog of sample materials which is usually used in the case we choose furniture, new coating of housing, etc.

### 3.6.2. Combine with Spatiotemporal Control

The proposed method can provide multiple areas of different textures on the same material (Figure 3.13) based on levitation control. According to the finger position. Switching the squeeze film effect can also provide additional textures on a real material.

We tested with functional generator combined with resonance tracing system. It can adjust the different texture at different points and different timings.

Real materials are employed and their textures are reduced in the proposed method, the presented textures are inherently high resolution. Additionally they can be felt from the onset of the touch (without lateral movement). Moreover the proposed

method can be combined with projection to provide visual and haptic textures at the same time (Figure 3.13).

## 3.7.Discussion, Conclusion, and Future work

In this chapter, we developed a method that allows the haptic transformation of real textures by Computational Fields. This method reduces the haptic texture of a real material using the squeeze film effect generated by ultrasonic vibration.

We discussed several related methods that use ultrasonic haptic systems. Our approach is different from these approaches because it reduces the texture of surfaces. We also implemented and evaluated the proposed method. The textures generated by this method are inherently high resolution. We conducted evaluations using a three-axis accelerometer and we confirmed that our prototype system operated successfully.

In future research, we will apply this method to 3D-printed objects by applying ultrasonic vibration at adequate frequency. Resonance analysis is needed because the resonance frequency is different depending on the shape of the object.

# 4.Project on Acoustic Levitation

*In this chapter, we describe a method to change the three dimensional position of physical material levitated by computational 3D acoustic-potential field. This project is aimed to realize malleability on 3D position and animation of real world object like computer graphics in the digital world by applying computational fields. In this chapter we utilize standing waves in computational acoustic field and the standing wave is generated at focal points of ultrasonic phased array. We computationally calculate and generate the focal points in three dimensional position.*

## 4.1. Introduction

Interaction with real-world objects is a popular topic in research related to real-world-oriented interactive technologies. In the context of display technologies, analog installations with real objects are still very popular (Figure 4.2(b)) in many situations, such as window displays, shops, and museums. Our research in this paper is motivated by the digital control of analog objects in mid-air, i.e., real objects that are suspended and moved in mid-air without physical support, such as posts, rods, and strings (Figure 4.2 (a)).

Because of growing interest in the materialization of computer graphics, digital fabrication technologies have recently emerged as one of the most important application fields in real-world-oriented computer graphics. These technologies are rapidly expanding from research laboratories to commodity markets for personal use. Fabrication technologies bring computer graphics to the real world. However, two missing and desirable functionalities in digital fabrication are the controllability of spatial position and animation. In the digital world, the spatial position of graphical models is freely controllable by merely setting the coordinates. The ability to do the same in the real world is also desirable for digital fabrication.

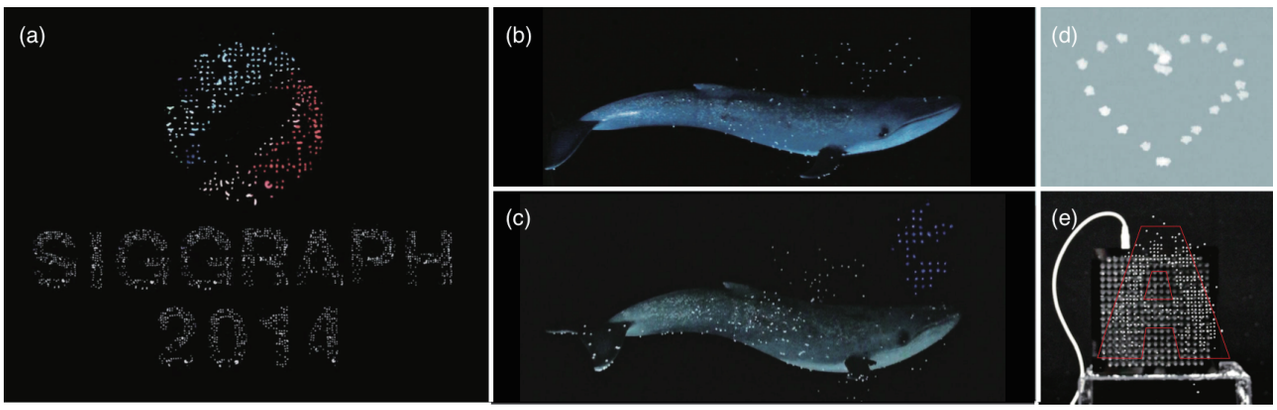


Figure 4.1: Application images of Pixie Dust. These are levitated and manipulated objects in graphic metaphors. (a) Floating screen with projection (showing 'S','I','G','G','R','A','P','H','2','0','1','4',and SIGGRAPH logo separately and mixed into one image) . (b-c) Whale (hung by string) with surrounding particles and projected spout. (d) Physical vector graphics (showing “heart”). (e) Physical raster graphics (showing “A” by shooting off other particles from plane levitation). These details are descirebed in Section 4.5.

We propose in this paper a method to control the spatial position and 3D animation of small objects by utilizing a noncontact manipulation technology. With this method, we can employ real objects as graphical components, such as display pixels (static control) and vector graphics (dynamic control). We believe that a new avenue in the field of computer graphics will be opened if fabricated models can be moved by noncontact manipulation.

In this project acoustic manipulation method has been extended to 3D manipulation [75]. In this chapter, we describe both how to expand acoustic manipulation method in 3D and how to expand it to graphical Application. By using and extending 3D acoustic manipulation technology, we create an acoustic-potential field (APF). Compared to magnetic levitation, air jets, and other noncontact levitation technologies, acoustic manipulation and APF have the following advantages: these can be used with a wide variety of available materials, these provide satisfactory refresh rate, and these have sufficient spatial resolution. While our technology is limited in terms of the size and density of the objects that are controllable, it contributes to computer graphics by allowing levitated small objects to be used in graphical metaphors, such as the pixels of raster graphics, moving points of vector graphics, and animation.

To discuss various noncontact manipulation technologies in a unified manner, here we introduce a concept called “computational potential field” (CPF). CPF is one of the sub-domain of Computational Fields. We have gathered from literature in the area that conventional studies on noncontact levitation/manipulation are based on potential fields determined by various physical quantities, such as sound pressure in acoustic levitation

and magnetic fields in magnetic levitation [33]. Levitated objects can be manipulated by spatially and temporally controlling the potential fields. When the field is controlled by a computer, we call it a CPF.

The contributions of this project are as follows. First, we describe the design of our graphics system. We present the details of the ultrasonic-phased array and discuss its advantages and disadvantages. Second, we report the performance measurements of our system, including the measurements of the spatial resolution, stability, speed of movements, and size and weight of the levitated objects. Finally, we investigate the applications of our system. In addition to the examples of APF-based graphics applications, we also discuss the implementation of 3D interaction. By integrating a motion-capture system into our graphics system, we facilitate interaction between the levitated objects and the user. Although our investigation is performed using acoustic levitation, our results and discussions can also be useful in designing other CPF-based graphics using other principles of mid-air levitation.

## 4.2. Background and Related Work

In this section, we introduce our motivation for our project and cite related works on non-contact manipulation. Following this, we introduce the concept of CPF to discuss various noncontact manipulation technologies in a unified manner. We then cite related works on acoustic manipulation, passive mid-air screens, and volumetric displays.

### 4.2.1. Motivation

Controlling objects in the real world is a popular topic in the computer graphics (CG) and human-computer interaction (HCI) communities. Various ideas to realize this have been proposed – e.g., programmable matter [10], radical atoms [12], actuation interfaces [11], and smart material interfaces [13]. These proposals focus on controlling real objects through a computer and generating physically programmable material. These concepts will play very important roles in future interactive CGs because they expand the range of graphics from “painted bits” to the real world [5].

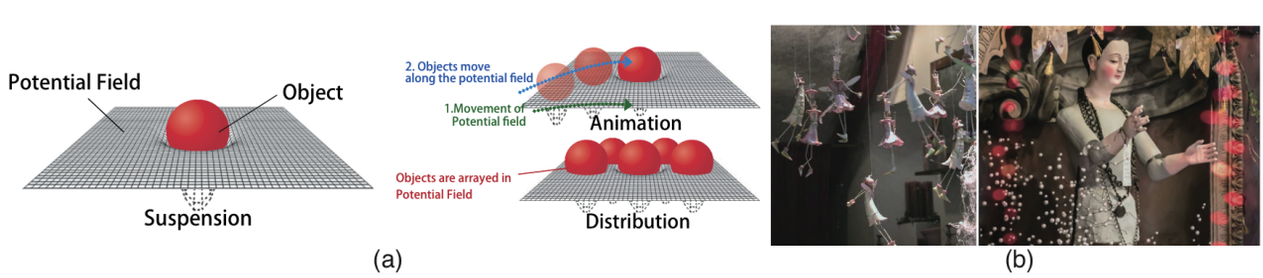


Figure 4.2: These figures show the concept of computational potential field. (a) Sketch of computational potential field: Objects are trapped in local minima of the potential field. (b) Window installation with objects supported in mid-air.

Table 4.1: Comparative table of manipulation methods.

| Physical quantity | Material parameters | Mechanism | Spatial resolution |
|---|---|---|---|
| Sound [88] | Density & volume | Ultrasonic transducers | Wave length |
| Airflow [71] | Density & surface area | Air jets | Spread of air jets |
| Magnetism [18] | Weight & magnetism | Electromagnet & XY stage | Size of magnet |

Two methods are currently available to control objects in the real world. In one, objects actuate themselves, whereas they are actuated by their surroundings in the other. The latter method is divided into two types of actuation: contact and noncontact. We address the noncontact approach.

### 4.2.2. Manipulation in Interactive Techniques

Several related studies have aimed at noncontact manipulation in the context of interactive techniques. For example, ZeroN [18] was proposed to manipulate a 3D object by controlling the magnetic field and using it as a floating screen and an input user interface (UI). The levitated object is limited to a single magnetic sphere in this proposal. Noncontact manipulation can be also achieved by using air-jets [71], i.e., an airflow field. While the research is limited to 2D manipulation, it can be extended to 3D. Air-cannons [32] have a possibility to be used in the similar manner. Sound is also utilized to manipulate objects in air. Both of standing waves (acoustic levitation/manipulation) and traveling waves (e.g., Ultra-Tangibles [21]) are available. A comparison of these manipulation methods is shown in Table 4.1.

### 4.2.3. Computational Potential Field

We propose a new implementation concept – computational potential field (CPF). We use the term “potential field” in a narrow sense: a scalar field that gives a force vector field working on a given object. Then CPF is defined as a potential field determined by some physical quantities controlled by a computer that can suspend and move objects in the real world. To the best of our knowledge, all conventional research on noncontact manipulation can be classified as CPF. All studies in the area employ CPFs as “invisible strings” to manipulate real objects. In these implementations, the objects have no actuators and only float in air according to the spatiotemporal changes of the CPF.

### 4.2.4. Acoustic Manipulation

Several studies have been conducted on manipulation using ultrasonic waves. For example, Ultra-Tangibles [21] utilizes the acoustic radiation pressure of traveling waves from

the surrounding ultrasonic-phased arrays. Marshall et al. demonstrated 2D manipulation of lightweight spherical objects. Another method – acoustic levitation/manipulation – utilizes ultrasonic standing waves. A bolted Langevin transducer (BLT) is used together with a reflector to trap objects in water and levitate them in air [71][79]. Opposite BLTs were used to manipulate objects in a 1D direction along the acoustic beam [71][77]. Acoustophoretic transport [80] and lapillus bug [23] move the object along a 2D plane with a transducer array and a reflector plate. Here we extended acoustic manipulation methods to move objects in a 3D space with opposite transducer arrays and propose the application of this method.

In this project, we aim to describe the extension and application of acoustic levitation and manipulation to the fields of CG and HCI. One difference between our proposal and conventional methods in the area is that we control the shape of the beams. Furthermore, multiple objects can be levitated and manipulated together in a 3D space using our method. Our system can also make a dot matrix display in mid-air. These differences from related research are depicted in Figure 4.3. The limitations of our system are described in Section 4.6.

### 4.2.5. Passive Mid-air Screens

Studies that have been conducted on dealing with mid-air screens are listed. Many image-projection technologies have been investigated. The systems proposed by [46][47] use fog as a screen and the one by [82] uses dust-like particles as a screen. These technologies display images in air by utilizing the diffusion property of fog and dust. [49] has developed a screen that uses falling water drops in air. Utilizing their lens-like property, images are able to be projected onto them. Multilayer water-drop screens are created in air and images corresponding to the spatial position of the water drops are projected by synchronizing the projector with the water bulbs. In the aspect of passive floating display using water, there is [83]which is the display aimed to realize ambient display. Our study

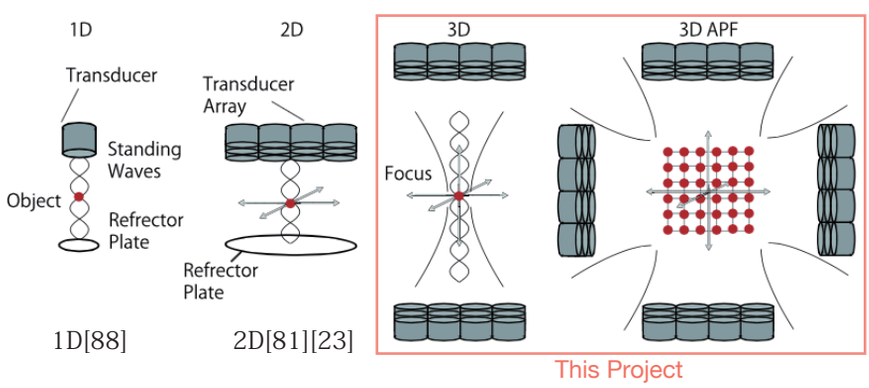


Figure 4.3: The differences in acoustic manipulation approaches. (Conventional Approaches) (a) Simple standing wave levitation. (b) 2D manipulation of small particles with transducer array. (Our approaches) (c) 3D manipulation using opposite phased arrays. (d) 3D manipulation and deformation of Acoustic- Potential Field

differs from these studies in the spatial control and selectivity of the available material, and can also expand these passive screen approaches.

### 4.2.6. Volumetric Displays and Screens

Studies directed toward controlling the spatial position of an active screen and display are also being actively pursued. There are two kinds of the studies; one aimed to achieve multi-perspective 3D image and the other aimed to realize deformation of planner screens for haptic and/or other purposes. Multi-perspective 3D display is a popular topic in computational display areas. We would like to cite several researches from the viewpoint of volumetric display. [84] constructs 3D images with a rotated mirror and projection. [85] achieves 3D images by rotating a vertical diffuser plate and projection. [86] is glasses-free light field display using volumetric attenuators. On the other hand, there are researches that focus on the dynamic deformable screen and display. For example, the deformable actuated screen “Project FEELEX” [9] constructs 3D forms on the screen surface using an actuator array set under the screen. LUMEN, proposed by [44], is comprised of actuated dot-matrix light-emitting diode (LED) – physical pixels showing RGB and H (height). [15] has proposed an interactive deformable screen, called ”inForm,” that handles and/or interacts with other objects. A noncontactly-actuated deformable screen (we described chapter 2) [22] employs an ultrasonic-phased array to deform a colloidal screen. This project differs from these screens and displays in that it allows for 3D manipulation and levitation. Moreover, we can use various materials as volumetric pixels. While there is a 3D solution [87] that uses a plasma 3D volumetric display, our approach is different from it because of the fact that volumetric pixels are touchable in our approach.

## 4.3. Acoustic-Potential Field Generator

In this section, we describe the theory of our acoustic-potential field generator. It consists of ultrasonic-phased arrays surrounding the workspace. First, we explain how to make a focal point/line with an ultrasonic-phased array. Then, we describe the distribution of the ultrasonic-acoustic-potential field.

### 4.3.1. Ultrasonic-Phased Array

The acoustic-potential field generator consists of multiple modules of ultrasonic-phased array. Each module has hundreds of ultrasonic transducers and controls each separately with adequate time (or phase) delays. We employ a similar setup both to levitate and

manipulate small particles and to generate the potential distributions. In this project, we use this setup to generate not only a single focal point, but also other distributions of ultrasound, e.g., multiple focal points [68] and a focal line. In the following sections, we explain how to generate the focal point and focal line. Their spatial distributions are also shown.

#### 4.3.1.1. How to Generate Focal Point

A focal point of ultrasound is generated as follows. The time delay $\Delta t_{ij}$ for the (i, j)-th transducer is given by:

$$\Delta t_{ij} = (l_{00} - l_{ij}) / c \quad (4.1)$$

where $l_{00}$ and $l_{ij}$ are the distances from the focal point to the (0, 0)th (reference) and the (i, j )-th transducers, respectively. c is the speed of sound in air. The focal point can be moved by recalculating and setting the time delays for its next coordinates.

It has been theoretically and experimentally shown that the spatial distribution of ultrasound generated from a rectangular transducer array is nearly sinc-function-shaped [29]. The width of the main lobe w parallel to the side of the rectangular array is written as

$$w = \frac{2\lambda R}{D} \quad (4.2)$$

where λ is the wavelength, R is the focal length and D is the length of the side of the rectangular array (Figure 4.4). This equation implies that there is a trade-off between spatial resolution and the array size.

#### 4.3.1.2.How to Generate Focal Line

A focal line of an ultrasound is generated in a similar manner with variation in the target

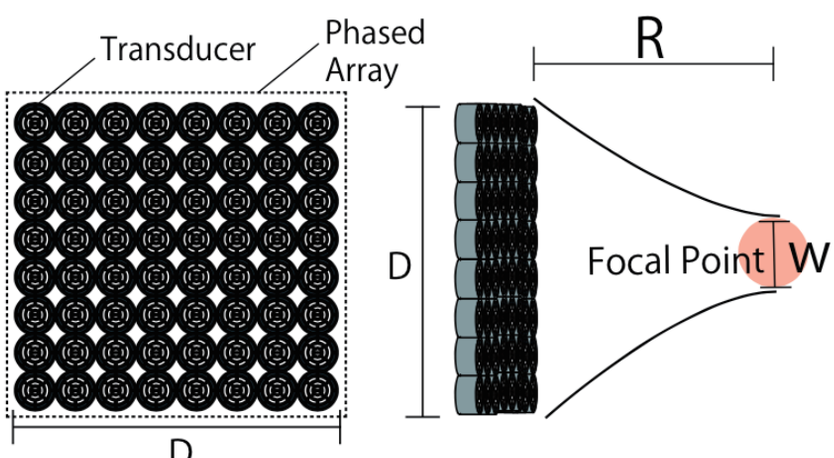

Figure 4.4: Phased array with side length D and focal length R.

coordinates. In this case, the time delay $\Delta t_{ij}$ for the (i, j)-th transducer is given by:

$$\Delta t_{ij} = (l_{0j} - l_{ij}) / c \qquad (4.3)$$

where $l_{0j}$ and $l_{ij}$ are the distances from the j-th focal point to the (0, j )-th and the (i, j )-th transducers, respectively, i.e., each column targets its own focal point (Figure 4.6). The thickness of the focal line is w, as defined in Eq. (4.2) above. The peak value of the amplitude of the focal line is lower than that of the focal point because the acoustic energy is distributed over a broader area.

### 4.3.2. Acoustic-Potential Field

The principle of acoustic levitation was mathematically explained by [70] and [74]. When a small sphere is in an acoustic field, the potential energy U [J/m$^3$] of an ultrasonic standing wave is expressed as

$$U = -B\langle K_a \rangle + (1-\gamma)\langle P_a \rangle \qquad (4.4)$$

$K_a$ and $P_a$ here are the kinetic and potential energy densities of ultrasound, respectively. <> is the time average. B is given by $3(\rho - \rho_0)/(2\rho + \rho_0)$, where $\rho$ and $\rho_0$ are the densities of a small sphere and the medium, respectively. $\gamma$ is given by $\beta/\beta_0$ where $\beta$ and $\beta_0$ are the compression ratios of the small sphere and the medium, respectively. The force F [N] acting on a sphere of volume V is given by $F = -V \nabla U$ . In the following, we show the potential fields for a focal point and a focal line.

#### 4.3.2.1.Focal Point

A narrow beam of standing wave is generated in the vicinity of a focal point when two phased arrays are set opposite each other and generate the common focal point (Figure 4.5). The length of the standing wave depends on the focal depth.

We assume an ultrasonic standing wave along the z-axis. Its sound pressure p is written as

$$p = \sqrt{2} A g(x,y) \cos\left(\frac{2\pi z}{\lambda}\right) e^{-j\omega t} \qquad (4.5)$$

where A is the root mean square (RMS) amplitude, g(x, y) is the normalized cross-sec-

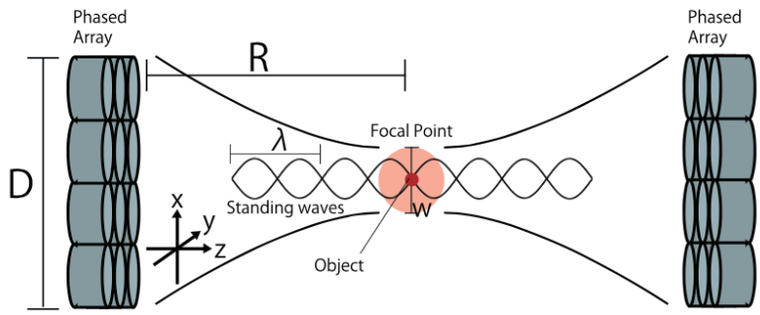


Figure 4.5: Opposite phased arrays, focal points, and standing wave.

tional distribution of the ultrasonic beam, and ω is the angular velocity. By definition, $K_a \equiv \frac{p^2}{2\rho c^2}$ and $P_a \equiv \frac{\rho u^2}{2}$ where $u = \frac{1}{\rho c}\frac{\partial p}{\partial z}$ is the particle velosity. In the beam of standing wave, Then U is written as

$$U = g(x,y)^2 \frac{A}{\rho_0 c^2}\left\{-B + (B+1-\gamma)\cos^2\left(\frac{2\pi z}{\lambda}\right)\right\} \quad (4.6)$$

As we mentioned above, it has been theoretically determined that the distribution of the focal point g(x, y) generated by a rectangular transducer array can be approximated by a sinc function [29].

$$g(x,y) \simeq \mathrm{sinc}\left(\frac{2\pi x}{\omega}, \frac{2\pi y}{\omega}\right) \quad (4.7)$$

where the two-dimensional sinc function sinc(x,y) is defined as sin(x)sin(y)/xy.

Figure 4.7 shows the potential energy distribution based on Eqs. (4.6) and (4.7) for y = 0. It is assumed here that the sphere is made of polystyrene and the medium is air. Hence, $\rho = 1 \times 10^3$ kg/m$^3$, $\rho_0 = 1.2$kg/m$^3$, $\beta = 2.5\times10^{-10}$ Pa$^{-1}$, and $\beta_0 = 7.1\times10^{-6}$Pa$^{-1}$ acoustic axis of the ultrasound beam at its nodes. Figure 4.7 (b) and (c) show the particles levitated and animated in this potential field.

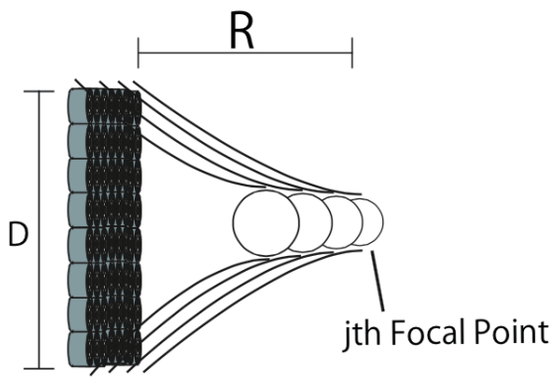

Figure 4.6: Generation of focal line.

#### 4.3.2.2.Focal Line

A sheet beam of standing wave is generated in the vicinity of a focal point when four phased arrays surround the workspace and generate focal lines at the same position. This acoustic field is described as two beams of standing waves that overlap perpendicular to each other.

We assume an ultrasonic standing wave parallel to the x and z axes. Its sound pressure p is written as:

$$p = \sqrt{2}A\mathrm{sinc}\left(\frac{2\pi y}{\omega}\right)\left\{\cos\left(\frac{2\pi x}{\omega}\right)+\cos\left(\frac{2\pi z}{\omega}\right)\right\}\mathrm{e}^{-j\omega t} \quad (4.8)$$

Then U is written as:

$$U = \mathrm{sinc}^2\left(\frac{2\pi y}{\omega}\right)\frac{A^2}{\rho_0 c^2}\left\{-B\left[\cos\left(\frac{2\pi x}{\omega}\right)+\cos\left(\frac{2\pi z}{\omega}\right)\right]\right. \quad (4.9)$$
$$\left.+(1-\gamma)\left[\cos\left(\frac{2\pi x}{\omega}\right)+\cos\left(\frac{2\pi z}{\omega}\right)\right]^2\right\}$$

Figure 4.8 shows the potential energy distribution based on Eq. (4.9) for y = 0 under the same conditions as in Section 4.3.2.1. The potential field has equally spaced local minima. This is used to create a dot matrix of small particles.

### 4.3.3. Setup Variations

The intensity of the suspending force depends on the direction of the acoustic beam relative to gravity. Here, we derive and compare two extreme situations of a narrow beam: a vertical and a horizontal setup. The axial force $F_z$ counters gravity in the vertical setup (Figure 4.9 (a)) and the radial force $F_x$ in the horizontal setup (Figure 4.9(b)). For simplicity,

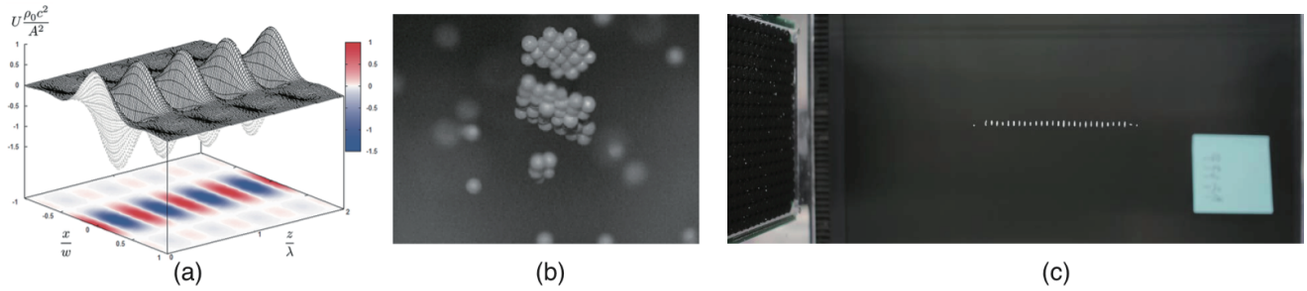

Figure 4.7: (a) Potential field in the vicinity of the focal point of the ultrasonic beam. (b) Small particles captured by 4000-fps high speed camera (200x magnified). (c) Small particles trapped in potential field.

we assume B ≈ 3/2 and γ ≈ 0, because ρ>>$\rho_0$ and$\beta<<\beta_0$ for our case.

First, the radial force $F_x$ parallel to the x-axis through the center of a node is obtained as:

$$F_x \equiv -V\frac{\partial U}{\partial x}\Big|_{(y,z)=(0,\frac{\lambda}{4})} \simeq \frac{A^2V}{\rho_0 c^2}\frac{6\pi}{\omega}\left[\frac{\sin(\frac{2\pi x}{\omega})\cos(\frac{2\pi x}{\omega})}{(\frac{2\pi x}{\omega})^2}-\frac{\sin^2(\frac{2\pi x}{\omega})}{(\frac{2\pi x}{\omega})^3}\right] \quad (4.10)$$

The maximum value of $F_x/V_g$ is 5×10 kg/m at x≈–0.2ω, where g = 9.8 m/s$^2$ is the gravitational acceleration and A = 5170 Pa. This means that a material can be levitated by $F_x$ if its weight density is smaller than this value. For example, the weight density of polystyrene is approximately 1 × 10$^3$ kg/m$^3$. Second,the axial force $F_z$ along the z-axis is obtained as:

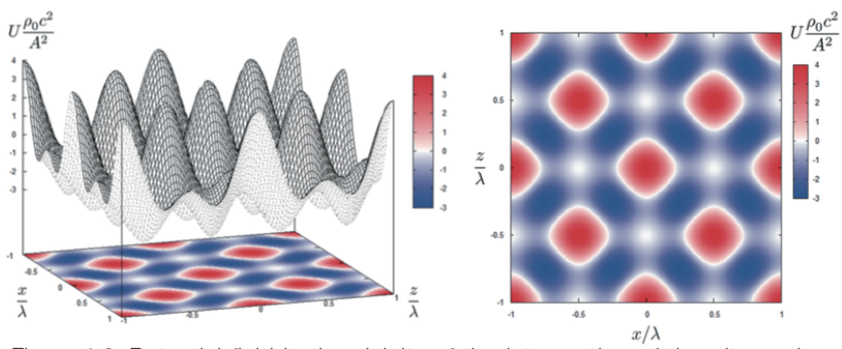

Figure 4.8: Potential field in the vicinity of the intersection of the ultrasonic sheet beams.

$$F_z \equiv -V\frac{\partial U}{\partial x}\Big|_{(x,y)=(0,0)} \simeq \frac{A^2V}{\rho_0 c^2}\frac{10\pi}{\lambda}\sin(\frac{2\pi z}{\lambda})\cos(\frac{2\pi z}{\lambda}). \quad (4.11)$$

The maximum value of $F_z/V_g$ is $3.63\times10^4$ kg/m$^3$ at, for example, $z = \lambda/8$. The maximum value of $F_z$ is 7.3 times larger than that of $F_x$, as derived above. This estimation agrees with the report that lateral restoring forces are approximately 10in the direction of the main sound beam [88], and explains why $F_z$, rather than $F_x$, was primarily used in conventional studies.

In this project, we can also utilize $F_x$ to levitate objects because we have sufficient high-amplitude ultrasound owing to phased arrays. Note that not only the weight density but also the size and shape of the objects are important factors to determine if they can be trapped in the nodes.

### 4.3.4. Frequency and Size of Floated Objects

The node size depends on the frequency of the ultrasound and determines the allowable size of the floated objects (Figure 4.10 (a)). The interval between the nodes is λ/2 and the size of the node is λ/2 by the width of the ultrasonic beam w. For example, λ/2 = 4.25 mm when we select 40 kHz. The frequency should be determined according to the intended application. Note that this is a rough standard, and that objects larger than the node size can be levitated if the protrusion is small/light enough to be supported by the suspending force (Figure 4.10 (b)). By animating the focal point, we can animate object

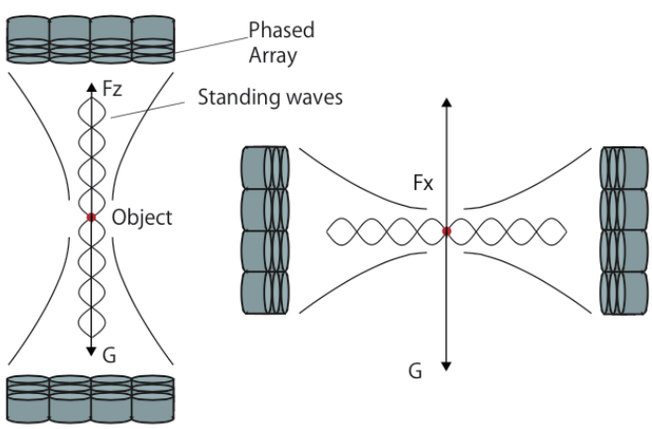


Figure 4.9: The force against the gravity. (a) Vertical setup. (b) Horizontal setup.

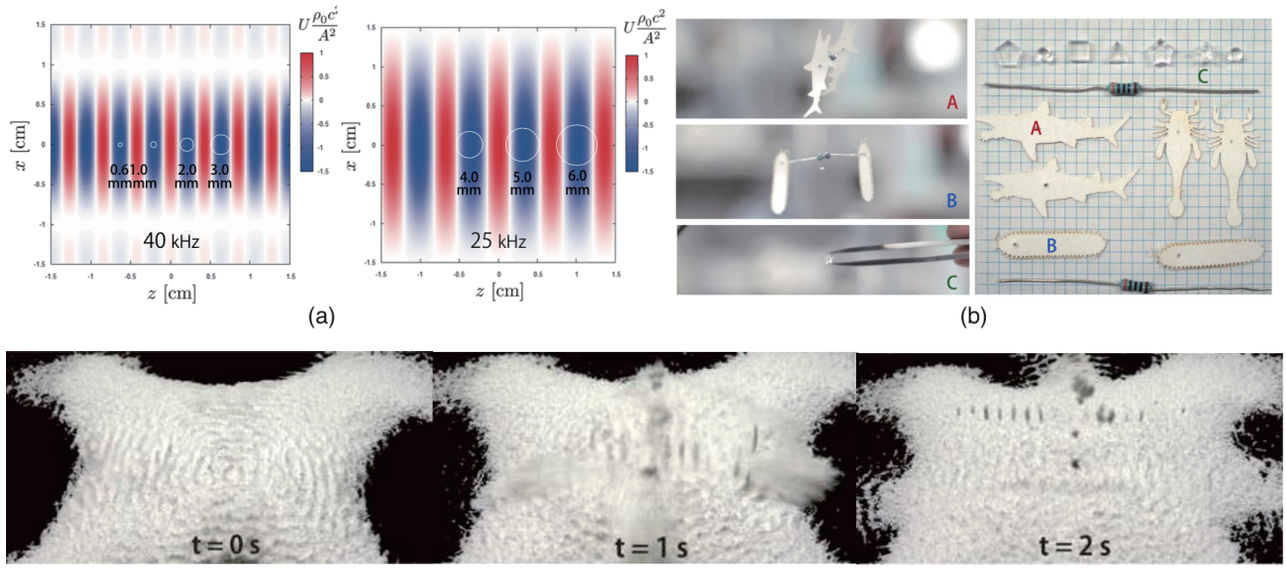


(a) (b) (c)

Figure 4.10: (a) Node size vs. frequency of ultrasound. White circles show particles in various diameter. (b) Floating paper models fabricated by laser cutter. (c) Scoop up and vertical manipulation of particles

trapped in standing waves (Figure 4.10(c)).

### 4.3.5. Shape of Potential Field

We have discussed two types of potential fields above: a focal point and focal line. Note that phased arrays control transducers individually and can generate other distributions of potential fields, such as multiple beams. The arrangement of the phased arrays can be used to design the shape of the potential field. Figure 4.11 shows examples of the computational acoustic-potential field, where the particles indicate the local minima (nodes) of

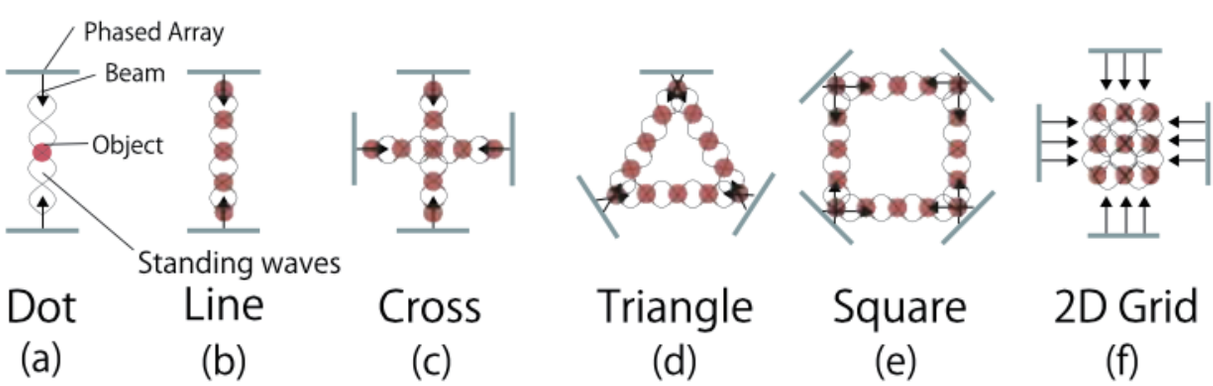


Figure 4.11: Multiple beams and different shapes of potential field. (a) Dot by a pair of phased arrays. (b) Line by a pair of phased arrays. (c) Cross by two pairs of phased arrays. (d) Triangle by three phased arrays. (e) Square (with multiple beams) and (f) dot-matrix (with wide beams: focal line described in 4.3.2.2) by two pairs of phased arrays.

the potential fields.

## 4.4. Implementation and Evaluation

In this section, we describe the implementation of the acoustic potential field generator that consists of phased arrays. We then show the results of the experiments and the measurements of the acoustic-potential field generator.

### 4.4.1. Phased Array Modules

We developed our manipulation system with four modules of phased array [55], as shown in Figure 4.12. The surrounded area is 520 × 520 $mm^2$. We placed the phased arrays facing each other. We have two options of phased arrays with different frequencies (40 and 25 kHz; Table 2). The position of the focal point is digitally controlled with a resolution of 1/16 of the wavelength (approximately 0.5mm for the 40-kHz ultrasound) and can be refreshed at 1kHz. The 40-kHz phased array consists of 285 transducers (10mm diameter, T4010A1, Nippon Ceramic Co., Ltd.) arranged in a 170 × 170 $mm^2$ area. The sound pressure at the peak of the focal point is 2585 Pa RMS (measured) when the focal length R = 200 mm. The 25-kHz phased array consists of 100 transducers (16-mm diameter, T2516A1, Nippon Ceramic Co., Ltd.). The sound pressure at the peak of the focal point is 900 Pa RMS (estimated) when the focal length R = 200 mm. Using 25-kHz

Table 4.2: 40-kHz and 25-kHz ultrasonic phased arrays.

| | 40 kHz | 25 kH |
|---|---|---|
| Number of transducers | 285 pcs | 100 pcs |
| Sound pressure | 2585 Pa RMS (measured) | 900 Pa RMS (estimated) |
| Size of nodes | 4.25 mm | 6.8 mm |

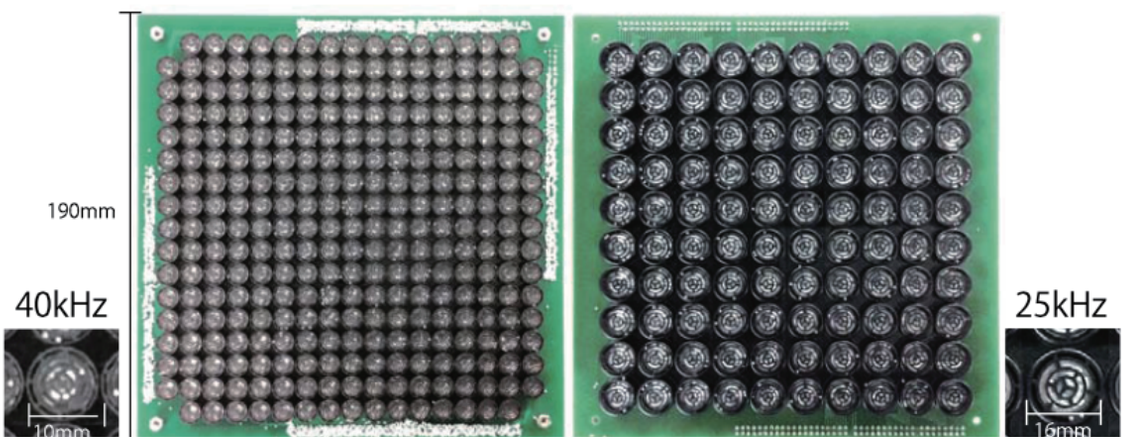


Figure 4.12: Phased arrays. (Left) 40 kHz and 285 pcs. (Right) 25 kHz and 100 pcs.

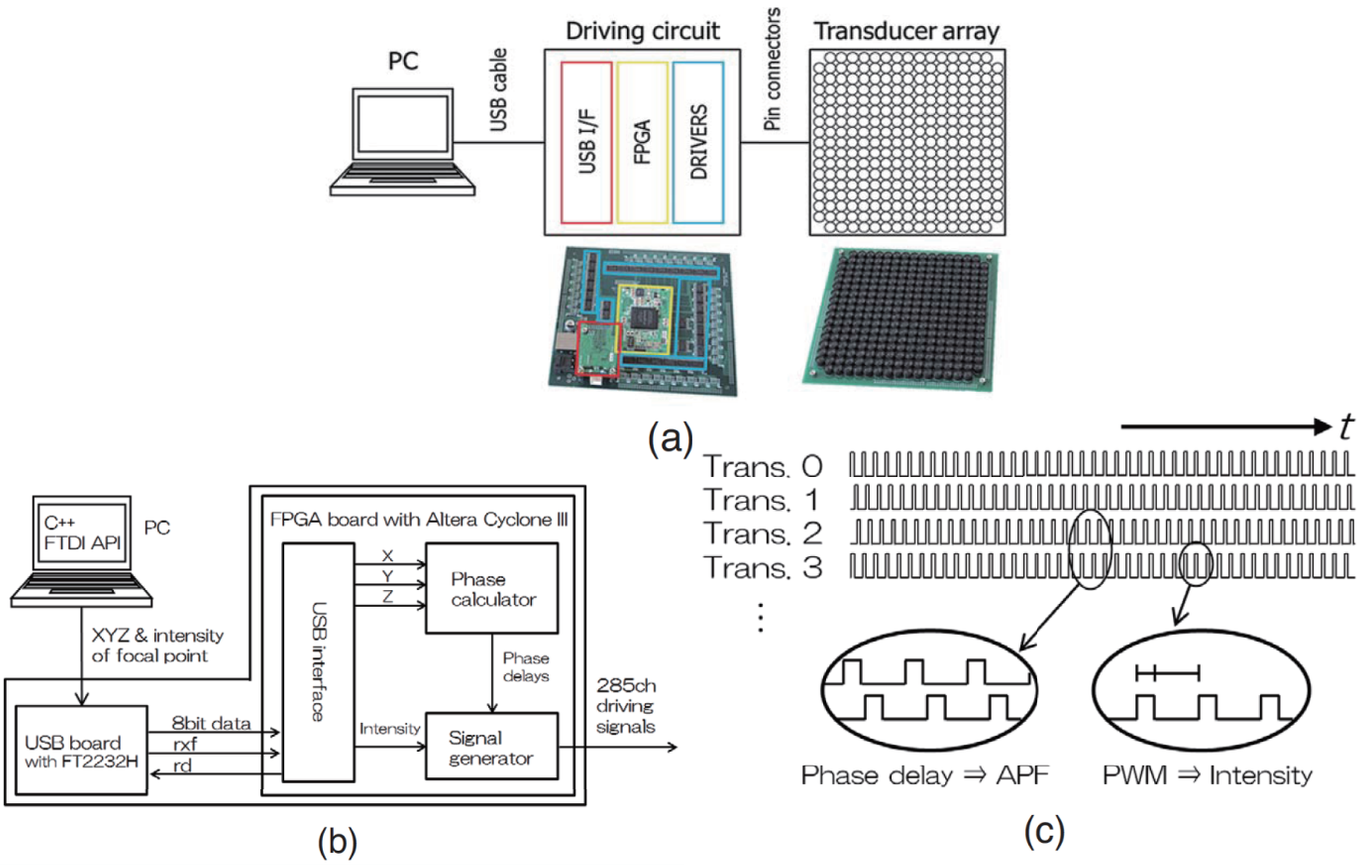


Figure 4.13: (a) System overview. (b) Diagram of data-flow. (c) Control of focusing (or distribution of acoustic potential field) and output intensity.

phased arrays, the suspending force is much smaller while the size of the focal point is larger. In this study, we primarily use 40-kHz phased arrays to obtain a larger suspending force.

The size and weight of a single phased array are 19×19×5 $cm^3$ and 0.6 kg, respectively. It consists of two circuit boards. One is an array board of ultrasonic transducers and the other is a driving board, including an FPGA and push-pull amplifier ICs. These boards are connected to each other with pin connectors. The phased array is controlled by a single PC via USB. The control application is developed in C++ on Windows (Figure 4.13). The PC sends the data, including the coordinates of the focal point and output intensity, to the driving board. The driving board receives the data, calculates adequate time delays for each transducer based on Eqs. (4.1) or (4.3), and generates the driving signals. The driving signals are sent to the transducers via the amplifiers. Modifying the time-delay calculation algorithm changes the distribution of the acoustic-potential field. The output intensity is varied using pulsewidth modulation (PWM) control of the driving signal.

### 4.4.2. Control Methods

We detail here our control method using the APF to manipulate levitated objects. The narrow beams, or sheet beams, of standing wave are generated in the vicinity of a single target point in our current setup. The APF changes according to the movement of this target point and then moves the levitated objects. Note that all the levitated objects are moved together in the same direction in this control method.

The movement of the target point should be as continuous as possible to keep the objects levitated. If the distance between the old and new target points is large, the levitated objects cannot follow the change in the APF. Note that although the APF generator has a 0.5-mm spatial resolution and a 1-kHz refresh rate, the inertia of the levitated objects limits the speed of their movement. This capability is investigated in Section 4.3.2.

### 4.4.3. Experimental measurements

#### 4.4.3.1.Visualization of Beams

Here, we visualize the acoustic field by placing dry ice near it. The air inside the ultrasonic beam is cooled and the moisture is frozen and visible. The micro-particles of ice gather at the local minima of the acoustic-potential field. Figure 4.14 shows the ultrasonic beams of standing waves of 25 kHz and 40 kHz. In both cases, the interval between the nodes is $\lambda/2$.

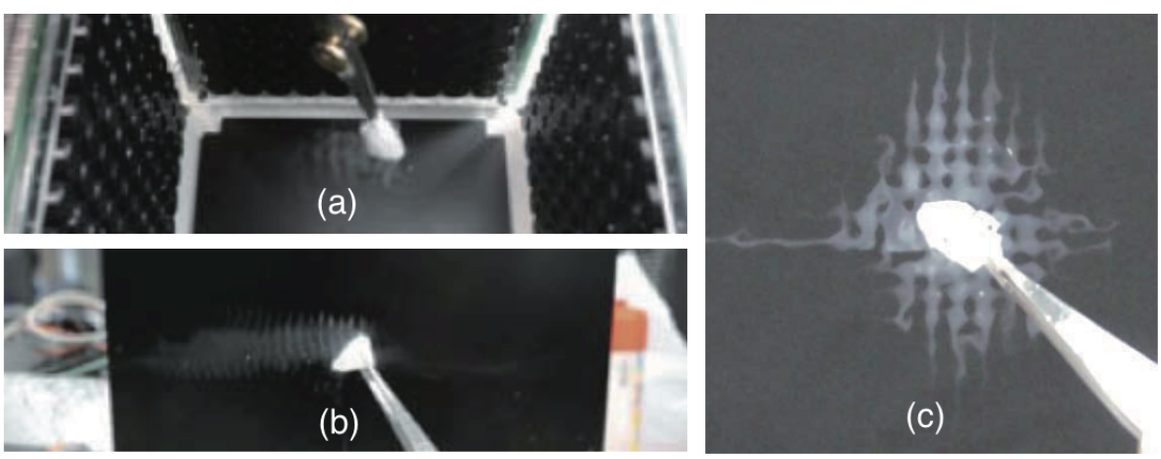


Figure 4.14: Visualization of ultrasonic beams by dry ice. (a) 25 kHz, (b) 40 kHz, and (c) 2D grid of 40 kHz.

#### 4.4.3.2.Speed of Manipulation

We examined the speed of manipulation attained by the current setup by measuring the duration of the cyclical movement at different frequencies. The test was conducted using expanded polystyrene spheres of diameters 0.6 mm and 2 mm. In each trial, a single particle was set at the third node from the intersection of the ultrasound beams along one of the acoustic axes (x-axis). All the directions of movement (i.e., x along an acoustic axis in which the particle is trapped, z along the other axis, and y perpendicular to both the axes) were tested. The focal length was set at 260 mm (Figure 4.15 (a)). The sound pressure was set to 70% of the maximum. The amplitude of the cyclic movement was 15 mm. Figure 4.15 (b)–(d) shows the results. The points on the graph indicate the average floating time for the different frequencies, and the bars indicate the maximum and minimum values. It can be observed that manipulation along the y-axis was more stable than along the other axes. We speculate that manipulations along the x and z axes tend to induce discontinuity in the ultrasound to change the focal length. Moreover, the graph shows that particles with diameter 0.6 mm are more stable than those with diameter 2 mm at higher frequencies. This suggests that larger particles tend to fall from the nodes of a standing wave.

#### 4.4.3.3.Workspace

We examined the size of the workspace in which the particles are suspended. The experiment begins with the center position. Each beam has 14-19 nodes that are occupied by the particles. The experimental setup is shown in Figure 4.16. Figure 4.16 shows how a particle falls when the focal point moves to a more distant position. The x-axis shows the distance from the center and the y-axis shows the number of nodes that include particles with a 0.6-mm diameter.

The workspace was studied next. In the case of movement along one of the acoustic axes, the manipulated particles could approach the ultrasound array to within 60 mm, but dropped when the distance became smaller. In the case of movement perpendicular

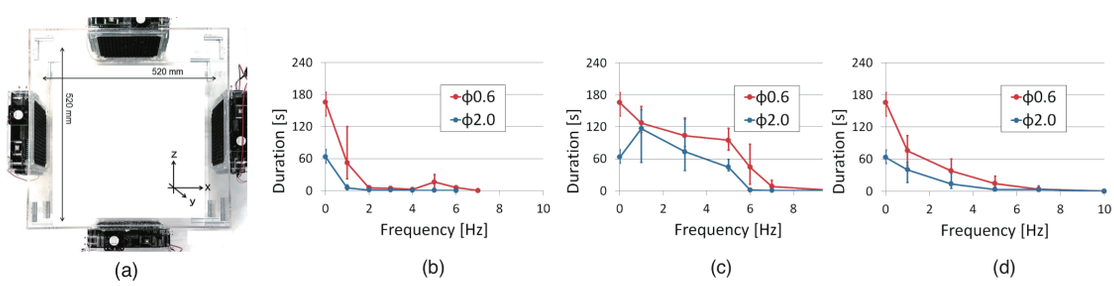


Figure 4.15: (a) Experimental setup and results on speed of manipulation. (b) Parallel to x-axis. (c) Parallel to y-axis. (d) Parallel to z-axis.

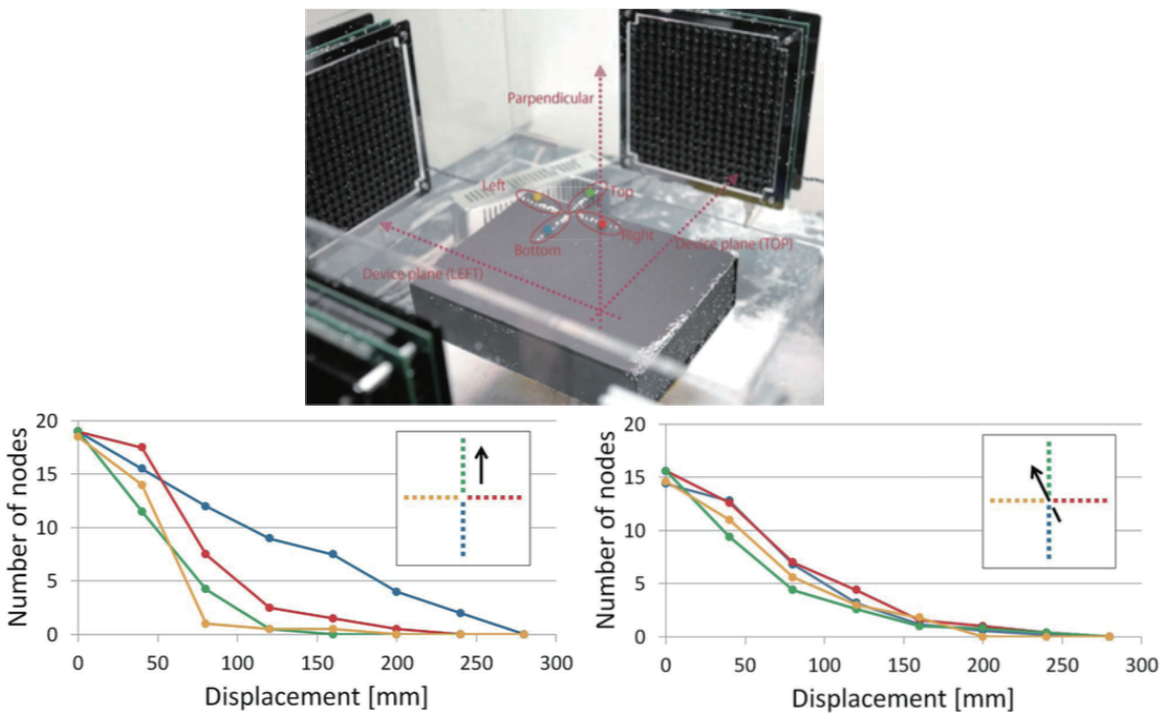


Figure 4.16: Experimental results on size of workspace. Left graph shows movement along acoustic axis and right graph shows movement perpendicular to device plane.

to the acoustic axes, the particles at the more distant nodes dropped earlier when they moved away from the center of the system. A particle at the intersection of the ultrasound beams dropped when it came to within 330 mm of the center.

#### 4.4.3.4.Weight Capability

We examined the capability of levitation with various materials. We employed nuts made of several materials and sizes. We levitated them in the center of the node in the vertical and horizontal setup. The results are shown in Figure 4.17. The weight capability is calculated from the size and density: vertical Fz can hold up to 1.09 g and horizontal $F_x$ can hold up to 0.66 g. The relationship between the amplitude of the ultrasound and mass is also plotted in Figure 4.17.

While we concluded that our system can suspend up to 1.09 g and 0.66 g, there are other factors to be considered in addition to the weight of objects – namely, the shape of objects, the intensity of the ultrasound, and the geometry of the APF.

## 4.5. Applications and Results

In this section, we discuss the application of the proposed method. First, we describe the characteristics of the method. We then outline the possible applications: graphics

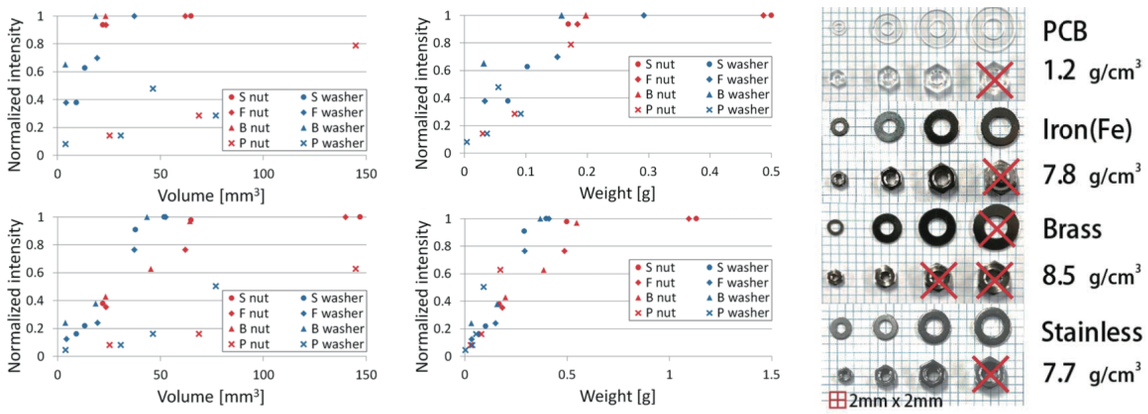


Figure 4.17: Experimental results (nuts and ring washers). (Left) The horizontal axis shows the volumes and weights of objects. The vertical axis shows the normalized intensity of ultrasound. The upper and lower graphs show horizontal and vertical setup, respectively. The labels S, F, B, and P are Stainless, Iron (Fe), Brass, and PCB, respectively. (Right) Levitated objects (the objects marked with "x" were not levitated).

and interactions based on the acoustic potential field (APF) of wide/narrow ultrasonic beams.

### 4.5.1. Characteristics

The levitation and manipulation method used in our study has several characteristics that can prove useful in graphics applications. These include

*1. Simultaneous levitation and manipulation of multiple objects by modification of APF*

*2. Rapid manipulation of levitated objects resulting in the production of persistence of vision*

*3. Only dimension and density limitations on levitating objects*

In this project we introduced two options, wide and narrow beams. The wide beam is used for projection screens and raster graphics, whereas the narrow beam is used for the levitation of various objects and vector graphics. Furthermore, other applications – animation of real objects, interaction with humans, particle effects, and pseudo high-screen resolution – can be implemented. Figure 4.18 shows a map of the applications placed according to their speed of motion.

### 4.5.2. Graphic Application with grid-like APF

In this application, a 2D grid APF generated by wide beams, depicted in Figure 4.19, is used as a projection screen floating in mid-air. Moreover, raster graphics images are gen-

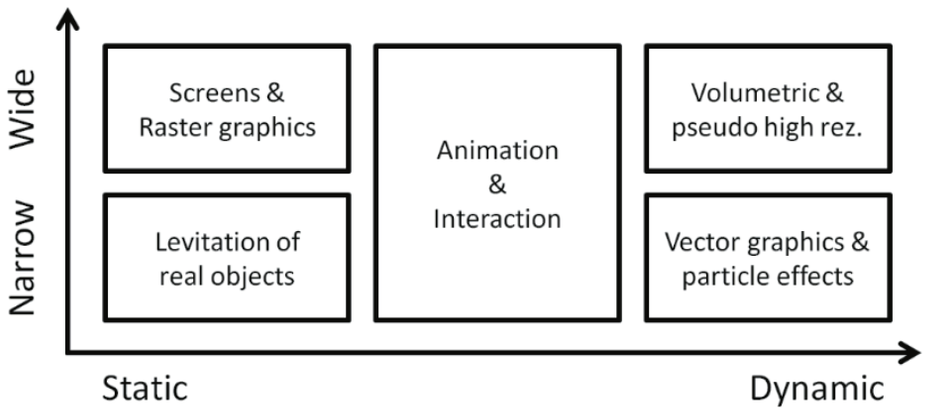


Figure 4.18: Application domain.

erated when adequate particles are blown off.

#### 4.5.2.1.Projection Screen

Figure 4.19 shows a floating screen, with the 2D grid APF suspending small particles in all the nodes. The movement of the screen has a high refresh rate and high spatial resolution. In our current prototype, the maximum control rate is 1 kHz, the distance between the particles is 4.25 mm, and 85 × 85 particles are held at the maximum. This kind of mid-air floating screen is applicable for use in areas such as entertainment, show windows, and interior displays.

Conventional proposals include fog screens [46], water drop screens [49], and fog-filled bubble screens [51]. However, these are mid-air, passive projector screens. Our proposed system differs from these in that the spatial position of our screen is controllable and the screen objects can be selected according to usage (e.g.. spatial interaction with screen, adjusting focus) (Figure 4.20 (b)). Our system can also expand conventional systems by, for instance, suspending water drops, holding fog particles, and controlling soap bubbles in the air.

Furthermore, the screen can be moved three-dimensional as well as manipulation and animation applications. There are two types of effects: The movement vertical to the screen results in volumetric expression and that parallel to the screen achieves pseudo high resolution.

#### 4.5.2.2.Levitated Raster Graphics

Figure 4.20 (c) shows an example of raster graphics display. First, the APF suspends small particles in all nodes to the same extent as in Section 4.5.2.1. The system then


Figure 4.19: Mid-air screen with projection (showing SIGGRAPH logo, S, I, G, G, R, A, P, and H). This figure is taken separatedly and after that we merged into one figures. This figure is realized by floating screen filled with particles (particle is floating in dark part of this figure) and we projected image on it.

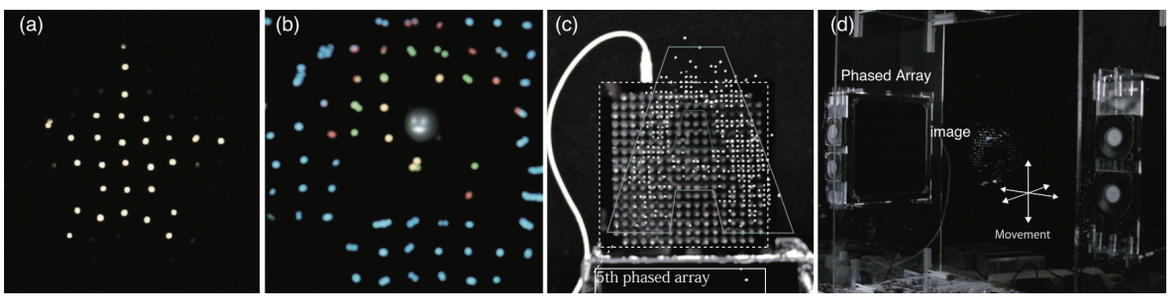


Figure 4.20: (a) Mid-air screen with another projection (“Star”). (b) Mixture of objects of different sizes (a detailed image is projected on larger particle). (c) Physical raster graphics (showing “A”). (d) Setup of mid-air screen and physical raster graphics.

adequately blows off some of the particles and generates a raster image. This process is performed by an additional phased array, or air jet (automatic type or hand manipulated). These additional device can shooting down the particle in plain levitated screen. The accuracy of dropping particles is approximately 2 cm by phased array and a single pixel by air jet at close range. The control rate of movement and spatial resolution of pixels are the same as in Section 4.5.2.1. It took 30 seconds to generate the raster graphics in Figure 4.20(c) by hand manipulated air-jet shooter.

There are several studies that focus on mid-air displays. For example, [87] is a 3D volumetric display based on laser-excited plasma that generates an image consisting of luminous points. Our system differs from this to the extent of non-luminous and physical-material pixels. A projector or laser plasma projector is not necessarily needed and the natural appearance of a real object is used as an expression. The availability of a non-luminous mid-air display in addition to a conventional luminous mid-air display is useful for design contents and installation.

### 4.5.3. High-Speed Animated APF

We focus here on a cross APF generated by the narrow beams shown in Figure 4.11 (a)–(c). By changing the spatial position of the nodes of the APF (either points or lines), the

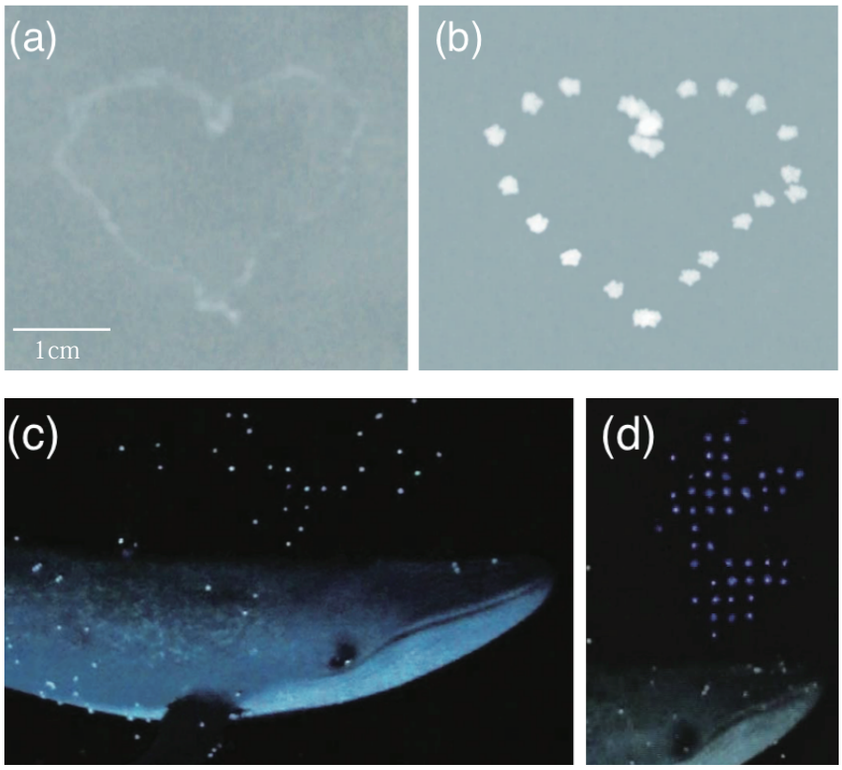


Figure 4.21: (a) Physical vector graphics (“heart”). shutter speed 1/20 (b) Physical vector graphics (“heart”) with 60 Hz strobe light. shutter speed 1/20 (c) Whale (hung by string) and surrounding particles. (d) Whale (hung by string) with projected spout.

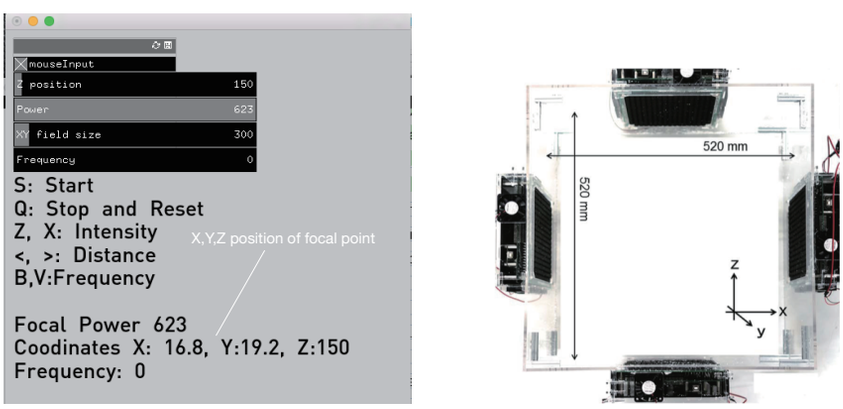


(a) (b)

Figure 4.22: (a) Manipulation Interfaces (b) coordinates

levitated objects are moved. The movement is fast enough to turn the trajectories of the objects into vector graphics based on persistence of vision.

#### 4.5.3.1.Physical Vector Graphics

By moving particles quickly, a vector graphics display is achieved based on persistence of vision. We used two types of particles as moving particles: 1-mm luminous paint-

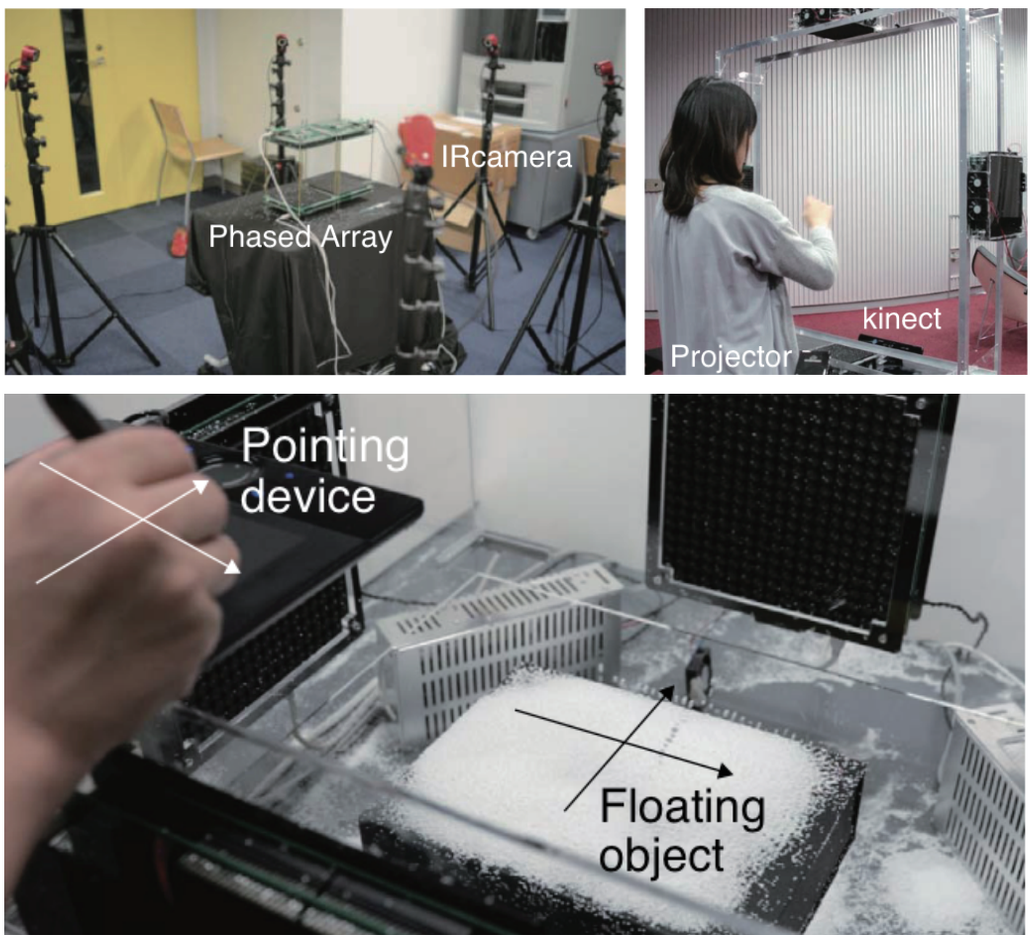


Figure 4.23: Animation and Interaction. (Left) With IR based motion capture system. (Middle and right) interaction with floated materials.

ed balls and 1-mm polystyrene particles. In the case of the luminous painted balls, we first irradiated light onto the balls and then manipulated them quickly mid-air. The trajectories are designed as a series of coordinates of control points, which are set up to 1,000 points-persecond (operation frequency). As the results of the above experiments showed, the maximum speed of movement was 72 cm/s. This speed is enough to produce persistence of vision. Figure 4.21 (a) and (b) show the results.

Research has been conducted on long-exposure photographs of LED lights [78] and LED-decorated quad-copters [66]. However, our study differs from them in that vector graphics in mid-air are rendered in real time and non-luminous images are obtained with polystyrene balls. One of the merit of our approach can be available to operate in a short distance with human.  Laser-excited plasma [87] is dangerous to human body.

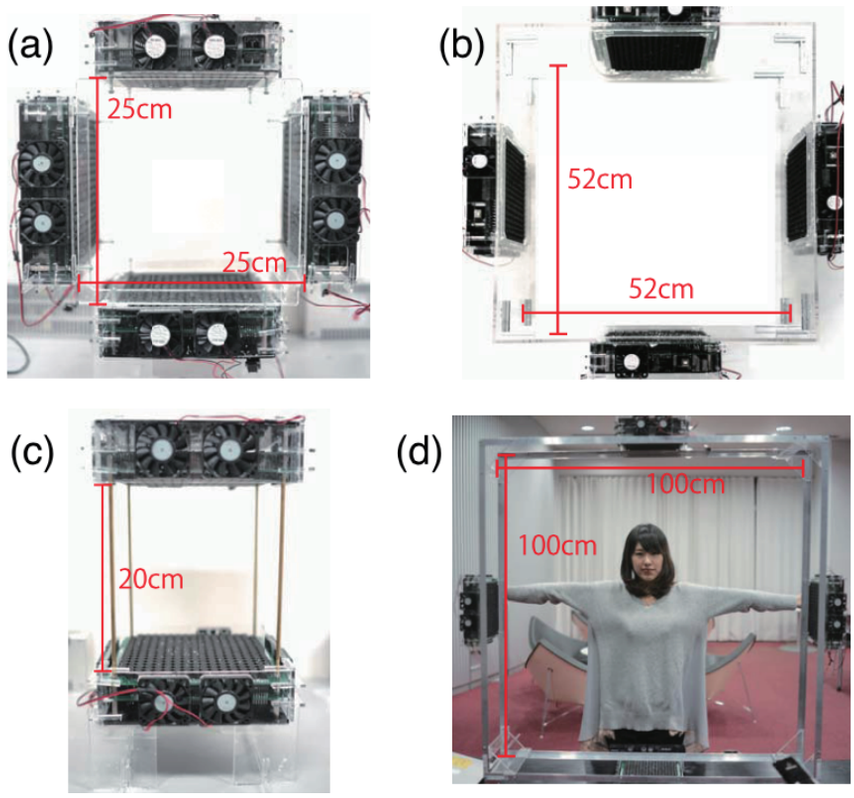


Figure 4.24: Setup variation. (a) 25 cm × 25 cm. (b) 52cm × 52 cm. (c) 20cm × 20 cm. (d) 100 × 100 cm.

#### 4.5.3.2.Physical Particle Effects

The movement of the APF produces not only vector graphics, but also particle effects in the real world (Figure 4.21 (c)). The temporal change in the APF affects the trajectories of falling particles, and the trajectory changes of multiple particles visualize the APF change. The speed of the movement is the same as in Section 4.5.3.1.

### 4.5.4. Animation and Interaction

Both 2D grid and cross APFs offer animation of levitated objects and/or interaction between users and levitated objects. Our study animates “passive” and “real-world” objects based on a noncontact manipulation method (Figure 4.23). We combined our levitation and manipulation setup with an IR-based motion capture system. When we levitated and manipulated small retro-reflective balls, all the balls were tracked by the motion capture system. Results are shown in Figure 4.23 (Left), in which we used a single 1-mm retro-reflective ball and levitated it.

Another motion capture setup was developed with Kinect. In this setup, users are detected without any attachments on their bodies and the levitated objects are controlled

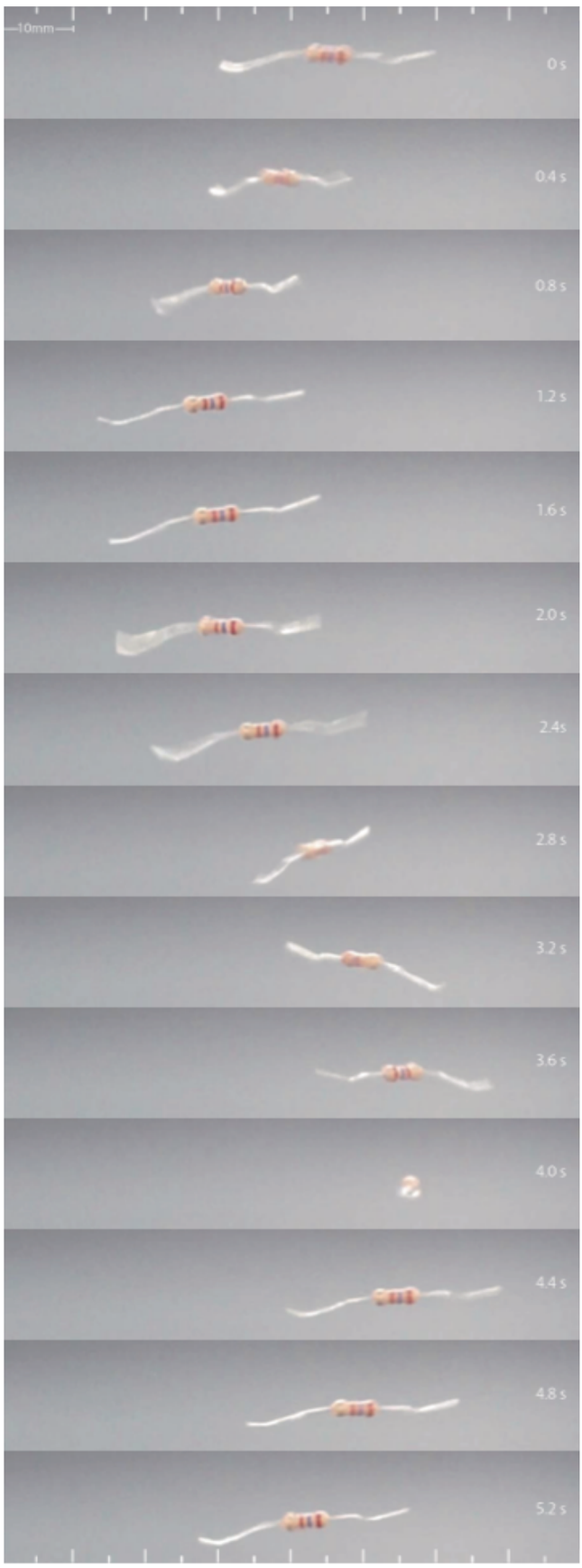


Figure 4.25: Time-series photographs of animation of a floated ob- ject (0.25-W carbon resistor).

according to the motion of the users' hands. An illustration of its use is given in Figure 4.23 (Right).

## 4.6. Discussions

### 4.6.1. Limitations

#### 4.6.1.1.Material Limitation

There are two factors to consider when choosing objects to manipulate: dimension and density. The allowable dimension is determined by the geometry of the APF and the allowable density of the material is related to the intensity of ultrasound. In Section 4.4, the maximum density of a levitated object is theoretically derived as $5 \times 10^3$ kg/m$^3$. Examples of materials that satisfy this condition include light metals and liquids. As described in Section 3, the size limitation (the size of nodes) is determined by the frequency of ultrasound: 4.25 mm for 40 kHz and 6.8 mm for 25 kHz. A lower frequency leads to larger size. Internal force is also an important factor in selecting the material. For example, the electrostatic force determines the maximum number of particles that can be trapped in a single node. The surface tension of the fluid determines the size of the droplets that can be levitated. Further, the shape of the levitated object is limited by the shape of the node.

#### 4.6.1.2.Sustainability of Suspension

Three factors determine the sustainability of the suspension: the heat condition of ultrasonic devices, oscillation of objects inside the nodes, and acceleration in vector graphics. In this section, descriptions of the factors and the ways to cope with them are provided.

The difference in the heat condition of the ultrasonic devices causes a single standing wave to affect the sustainability of the suspension. The temperatures of devices are equivalent prior to them being turned on. When they are turned on, their temperatures gradually increase because of the heat generated by amplifier ICs whose characteristics are not fully equivalent. When there is a difference in temperature, the operating frequencies of the controlling circuits differ. The frequency difference causes transportation of the nodes and the levitated objects fall off when they reach the edge of the localized standing wave. The cooling and maintenance of the temperature balance of the devices is one treatment. Another is to adjust phase delays based on feed-forward or visual feedback control.

Oscillation of levitated objects is another factor to be considered. When some kind of fluctuation occurs on the object, it suffers the restoring force from the potential field. If the intensity of the ultrasound is too high, the oscillation grows and finally exceeds the node of the potential field. The oscillation is restrained by decreasing the intensity of the

ultrasound keeping it suspended.

When moving levitated objects, the acceleration acts to throw them off the nodes. This determines the possible shapes and sizes of the physical vector graphics. Increasing the intensity of ultrasound at sharp curves would elongate the drawing time and expand the variation of physical vector graphics.

In practice, it is acceptable in many cases to refill objects into the APF if necessary.

### 4.6.2. Scalability

In this sub-section, we discuss the scalability of our method in terms of the weight and size of objects, the speed of movement, and the number of control channels.

*Weight*

The intensity of the ultrasound radiated from a single phased array is in proportion to the number of transducers. More transducers enable us to levitate heavier objects. Increasing the number of transducers results in other benefits in addition to higher intensity. One such benefit is a larger workspace keeping the size of the focal point. Another is smaller dispersion of the phase delay characteristics, which leads to more accurate generation and control of the acoustic field.

*Size*

In Section 6.1, we stated that the size of the object is limited by the frequency. In order to retain its non-audible property, an ultrasonic wave down to 20 kHz (the maximum frequency that humans can sense) is available. We then have a scalability limit of up to 8 mm.

*Speed*

The maximum manipulation speed of physical vector graphics is 72 cm/s, as mentioned above. Because the workspace is fixed, the acceleration needed to accelerate the object to a given speed is available with a higher intensity of ultrasound.

*Multiple controls*

In a single wide/narrow acoustic beam of a standing wave, all the levitated objects are manipulated together. Multiple beams are generated, for example, by separating a single phased array into several regions and controlling them individually. In this way, we can also control multiple clusters of objects individually.

*Degree of Freedom*

Our manipulation system and floating screen system can manipulate in 3DOF. We can bring particles or floating screen to three dimensional position. However we can not rotate the particles or floating screen and we can not generate the complex graphics using only four phased arrays (making raster graphics requires additional equipments to shoot down the particles)

### 4.6.3. Setup Variations

Our system has a wide range of setup variations at this stage, from 20×20 $cm^2$ to 100 $cm^2$. Larger setups will be possible in the future with larger ultrasonic devices. Figure 4.24 shows the setup variations.

### 4.6.4. Computational Potential Field

In Section 2.3, we introduced the concept of Computational Potential Field (CPF), which is the source of a noncontact force. This concept not only explains various noncontact forces (such as acoustic, magnetic, and pneumatic) in a unified manner but also serve as a platform for discussing and designing noncontact manipulation in the future. This frees us from specific physical parameters, such as sound pressure, magnetism, and airflow, and allows for discussions based on the divergence, the rotation, the response speed, and the wave/diffusion characteristics of the CPF.

## 4.7. Conclusion and Future Work

In this chapter, we reported on a study conducted to expand “graphics” from the digital world to the real world. In the study, 3D acoustic manipulation technology is used to turn real objects into graphical components. The method has wide-ranging applications, such as mid-air projection screen, raster graphics, vector graphics, and real-object animation, with millimeter-sized objects. We implemented these applications using the current version of ultrasonic phased arrays, conducted experimental evaluations, and demonstrated the capabilities of the system. To aid in the explanation of our approach, we also introduced the concept of “computational potential field,” which has the ability to unify all the noncontact manipulation technologies.

# 5.Discussion

*The implementation of programmable matter by Computational Acoustic Fields provides both advantages and drawbacks. In this section, we discuss the results, trade-offs, and limitations of Computational Acoustic Fields, and present some ideas for future work.*

## 5.1. Implementation Result

The implementation results are reasonable, and they agree with our theoretical expectations. In conventional studies, a single field is used for each purpose. We believe it is important to select from a variety of fields according to the specific purpose. Specifically, in acoustic fields, we can utilize several characteristics such as radiation pressure, standing waves, capillary waves, and squeeze film effects.

In this research, we employed an acoustic generator to actuate light materials (e.g., soap bubbles, material sticker, plastic beads). If we need to actuate heavier materials, this should be replaced by a magnetic or other generator.

In chapters 2 and 4, we employed a noncontact method for actuation, and in chapter 3 we employed a semi-contact method. The noncontact method provides less force than the contact technique. We must therefore choose the means of actuation

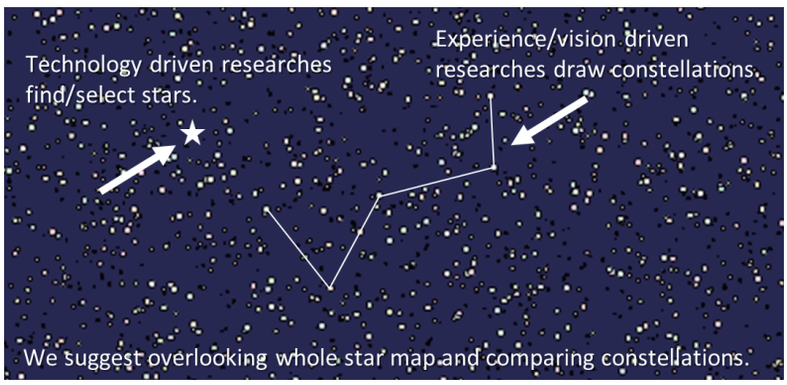


Figure 5.1:Metaphor of this research

carefully.

## 5.2. Notations in the Use of Computational Fields

In conventional studies, the computational magnetic field was employed in tangible applications. Theoretically, the computational magnetic field requires intermediate objects to be used as UIs, because humans are not sensitive to magnetic fields. The magnetic field can provide powerful actuation, and this means the design of objects has a large degree of freedom, from iron sand to metallic balls.

In this thesis, we employed computational acoustic fields. In such fields, we must take account of the audible sounds that radiate from the envelopes of ultrasound waves. In addition, high-amplitude ultrasound can be harmful to human ears. These

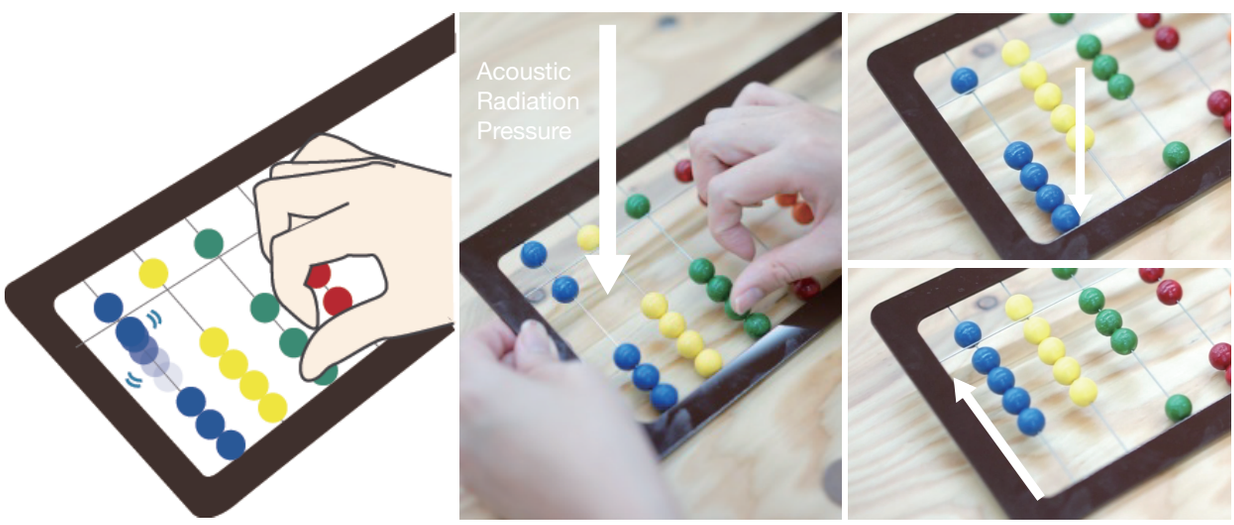


Figure 5.2: Calm actuation of abacus by separated acoustic phased arrays

issues should be considered in the design of applications.

## 5.3. Calmness of Field Oriented Actuation

Our concept of Computational Fields covers noncontact and semi-contact actuation technologies that conceal the actuators from human sight and increase the programmability of the actuation of matter. We believe this is a worthy contribution the realization of Calm Technologies.

We believe field-oriented programmable matter is a useful concept in the development of Calm Technologies from the aspect of interface selectivity. We employed non-digital materials to bring about actuation (modifying the haptic texture and levitating objects in the air in chapters 3 and 4, respectively). These are examples in which non-digital materials turn into programmable matter.

One of the drawbacks of noncontact actuation is that the efficiency of energy transmission is lower than that of conventional contact-based methods. In spite of this, the absence of bulky mechanical systems in the workspace is a large advantage of the noncontact actuation technologies from the viewpoint of calmness (Figure 5.2).

## 5.4. Drawbacks and Advantages

As we have pointed out above, one of the drawbacks of Computational Fields is the inefficiency of energy transmission. Another drawback is the interference among neighboring systems due to excessive radiation.

The advantages are the programmability and calmness. Applications that combine a Generator and Matter are reusable in future systems that use the same combination. Moreover, users naturally concentrate on Matter, because Fields are invisible and Generators are hidden or remote from the users.

## 5.5. Contribution of this framework

This thesis proposes a long-term vision of Computational Fields, and has described three prototypes that utilize Computational Acoustic Fields. Conventional studies on interactive techniques usually report new methods or results based on various different technologies. Our concept provides a framework to compare these studies

(Figure 5.1). Furthermore, our framework potentially includes all fields, other than noncontact or semi-contact forces, from odor distributions to gravity, for when future technologies have matured. A mutual understanding and interaction between various technologies and phenomena may provide us with new insights (Figure 5.1). The contribution of this study is similar to the exploration of a new star map in which to study, compare, define, and design things. It will also reduce the time consumed in designing, implementing, and theoretically describing new studies by referring to previous knowledge described in the common manner of Computational Fields.

# 6.Conclusion

In this thesis, we applied Computational Fields to realize the malleability of Computer Graphics (e.g., programmability of optical states, shapes, haptic states, and 3D positions) in real-world objects. The common feature of these studies is that actuated objects do not have actuators and are driven by Computational Fields. These are examples of how to implement field-oriented programmable matter in the pursuit of a graphics-based approach.

This thesis has a three-layered hierarchical structure. At the top layer, we introduced the concept of Computational Fields, in which fields of physical quantities are controlled by computers to alter the real world. This concept is useful to summarize research on field-oriented programmable matter (environmental actuation).

In the middle layer, we focused on noncontact actuation technologies that have not been discussed from the viewpoint of fields. We listed and compared noncontact actuation technologies.

In the bottom layer, we implemented three prototype systems for noncontact actuation based on acoustic fields: Optical Control of Colloidal Screen (chapter 2), Haptic Transformation (chapter 3), and Acoustic Manipulation (chapter 4). These prototypes expand current graphics approaches, and can be applied in UIs, displays, computer graphics, and entertainment computing.

In chapter 1, we introduced the concept of Computational Fields to summarize related work on environmental programmable matter. Then, we provided a survey of related work and a formulation of actuation methods. After that, we introduced Computational Acoustic Fields and described their characteristics. Computational Acoustic Fields have no limitation on the selectivity of actuation material, and have an

actuation range on the μm–cm order. For these reasons, we chose Acoustic Fields to realize programmable matter via environmental actuation.

In chapter 2, we described an optical programmable screen whose view angle is programmable from 2–175°. Conventional studies on screens with dynamic optical properties have not explored applications combined with projected images. Our results overcome the limitations on screen characteristics, enabling us to change the optical characteristics and shape of the screen. Our results are applicable to various expressions (e.g., 3D expression, BRDF material expression) by controlling the view angle dynamically.

In chapter 3, we developed a haptic modification system that can modify uneven surfaces by up to 50 μm by controlling the thickness of the squeeze film effect. This project explored the design space around the haptic modification of real world textures via the squeeze film effect. For this purpose, we developed a transducer and a resonance tracing system that matches the amplitude of vibration against the user's touch. This technology is applicable to new material samples that can modify their haptic characteristics.

In chapter 4, we presented an acoustic levitation method that can levitate objects of up to 1 g (7.8 g/cm$^3$). This method can move particles and small objects at up to 72 cm/s. We expanded standing wave-based acoustic manipulation to 3D manipulation by employing ultrasonic phased arrays instead of a single transducer. The manipulation workspace was expanded to one million times that of conventional studies. We explored the design space of this manipulation method with an emphasis on graphics applications. Our results are applicable to levitated displays and the animation of physical objects.

In chapter 5, we described the general drawbacks and limitations on the use of Computational Acoustic Fields. We discussed the calmness of our actuation methods and the contribution of the proposed framework.

We believe that these prototype systems and methods obtained by Computational Acoustic Fields will contribute to expanding graphics expressions, and will be applicable to UIs, displays, computer graphics, and entertainment computing.

# References

[1] Sutherland, I. E. The ultimate display. Proc. IFIP Congress (1965), 506-508. 1965

[2] Rekimoto, J. and Nagao, K. The world through the computer: Computer augmented interaction with real world environments. Proc. UIST, ACM (1995), 29-36. 1995

[3] Weiser, M. and Brown, J.S. The coming age of calm technology. Beyond Calculation (1997), 75-85. 1997

[4] Weiser, M. The Computer for the 21st Century. Scientific American 265, 3 (1991), 66-75. 1991

[5] Ishii, H. and Ullmar, B. Tangible bits: Towards seamless interfaces between people, bits and atoms. Proc. CHI, ACM (1997), 234-241. 1997

[6] Raskar, R., Welch, G., Low, K.-L., and Bandyopadhyay, D. Shader lamps: Animating real objects with image-based illumination. Proc. 12th Eurographics Workshop on Rendering Techniques, Springer (2001), 89-102. 2001

[7] Feiner, S., Macintyre, B., and Seligmann, D. Knowledge-based augmented reality. Commun. ACM 36, 7 (1993), 53-62. 1993

[8] Azuma, R. T. A survey of augmented reality. Presence: Teleoperators and Virtual Environments 6, 4 (1997), 355 - 385. 1997

[9] Iwata, H., Yano, H, Nakaizumi, F., and Kawamura, R. Project FEELEX: Adding haptic surface to graphics. Proc. SIGGRAPH, ACM (2001), 469-476. 2001

[10] Goldstein, S.C., Campbell, J.D., and Mowry, T.C. Programmable matter. Computer 38, 6 (2005), 99-101. 2005

[11] Poupyrev, I., Nashida, T., and Okabe, M. Actuation and tangible user interfaces: The Vaucanson duck, robots, and shape displays. Proc. TEI, ACM (2007), 205-212. 2007

[12] Ishii, H., Lakatos, D., Bonanni, L., and Labrune, J.B. Radical atoms: Beyond tangible bits, toward transformable materials. Interactions 19, 1 (2012), 38-51. 2012

[13] Vyas, D., Poelman, W., Nijholt, A., and Bruijn, A.D. Smart material interfaces: A new form of physical interaction. Ext. Abstracts CHI, ACM (2012), 1721-1726. 2012

[14] Blackshaw, M., DeVincenzi, A., Lakatos, D., Leithinger, D., and Ishii, H. Recompose: Direct and gestural interaction with an actuated surface. Ext. Abstracts CHI, ACM (2011), 1237-1242. 2011

[15] Follmer, S., Leithinger, D., Olwal, A., Hogge, A., and Ishii, H. inFORM: Dynamic physical affordances and constraints through shape and object actuation, Proc. UIST, ACM (2013), 417-426. 2013

[16] Yao, L., Niiyama, R., Ou, J., Follmer, S., Silva C.D., Ishii, H. PneUI: Pneumatically actuated soft composite materials for shape changing interfaces, Proc. UIST, ACM (2013), 13-22. 2013

[17] Patten, J. and Ishii, H. Mechanical constraints as computational constraints in tabletop tangible interfaces, Proc. CHI, ACM (2007), 809-818. 2007

[18] Lee, J., Post, R., and Ishii, H. ZeroN: Mid-air tangible interaction enabled by computer controlled magnetic levitation, Proc. UIST, ACM (2011), 327-226. 2011

[19] Kono, M. and Kakehi, Y. Tamable looper: Creature-like expressions and

interactions by movement and deformation of clusters, Proc. SIGGRAPH, ACM (2012), Posters article no. 25. 2012

[20] Weiss, M., Wacharamanotham, C., Voelker, S., and Borchers, J. FingerFlux: Near-surface haptic feedback on tabletops, Proc. UIST, ACM (2011), 615-620. 2011

[21] Marshall, M.T., Carter, T., Alexander, J., and Subramanian, S. Ultra-tangibles: Creating movable tangible objects on interactive tables, Proc. CHI, ACM (2012), 2185-2188. 2012

[22] Ochiai, Y., Oyama, A., Hoshi, T., and Rekimoto, J. Poppable display: A display which enables people to interact with popping, breaking, and tearing, Proc. GCCE, IEEE (2013), 124-128. 2013

[23] Kono, M., Kakehi, Y., and Hoshi, T. Lapillus bug, Proc. SIGGRAPH Asia, ACM (2013), Art Gallery. 2012

[24] Ochiai, Y., Hoshi, T., and Rekimoto, J. Pixie dust: Graphics generated by levitated and animated objects in computational acoustic-potential field, ACM Trans. Graphics 33 (2014), article no. 85. 2014

[25] Chubb, E.C., Colgate, J.E., Peshkin, M.A. ShiverPaD: A glass haptic surface that produces shear force on a bare finger, IEEE Trans. Haptics 3, 3 (2010), 189-198. 2010

[26] Ochiai, Y., Hoshi, T., Rekimoto, J., and Takasaki, M. Diminished haptics: Towards digital transformation of real world textures. Proc. Eurohaptics (2014). 2014

[27] Gershun, A., The Light Field, Moscow, trans. by P. Moon and G. Timoshenko, J. Math. and Physics, vol. 18, 1939, pp. 51-151. 1936

[28] Bau, O., Poupyrev, I., Israr, A., and Harrison, C. TeslaTouch: Electrovibration for touch surfaces. Proc. UIST, ACM (2010), 283-292. 2010

[29] Hoshi, T., Takahashi, M., Iwamoto, T., and Shinoda, H. Noncontact tactile display based on radiation pressure of airborne ultrasound. IEEE Trans. Haptics 3, 3 (2010), 155-165. 2010

[30] Kodama, S. and Takeno, M. Sound-responsive magnetic fluid display. Proc. INTERACT, IOS (2001), 737-738. 2001

[31] Suzuki, Y. and Kobayashi, M. Air jet driven force feedback in virtual reality. IEEE Computer Graphics and Applications 25, 1 (2005), 44-47. 2005

[32] Sodhi, R., Poupyrev, I., Glisson, M., and Israr, A. AIREAL: Interactive Tactile Experiences in Free Air. Trans. Graphics 32, 4 (2013), article no. 134. 2013

[33] Brandt, E.H. Levitation in physics. Science 243, 4889 (1989), 349-355. 1989

[34] Awatani, J. Studies on acoustic radiation pressure. I. (general considerations), J. Acoust. Soc. Am. 27, 2 (1995), 278-281. 1995

[35] Hasegawa, T., Kido, T., Iizuka, T., and Matsuoka, C. A general theory of rayleigh and langevin radiation pressures, Acoust. Sci. and Tech. 21, 3 (2000), 145-152. 2000

[36] Thompson, M.T. Eddy current magnetic levitation, IEEE Potentials 19, 1 (2000), 40-44. 2000

[37] Ochiai, Y., Oyama, A., and Toyoshima, K., A colloidal display: Membrane screen that combines transparency, BRDF and 3D volume. In ACM SIGGRAPH 2012 Emerging Technologies (SIGGRAPH'12). ACM, New York, NY, USA, Article 2, 1 page. 2012

[38] Raffle, H., Joachim, W. M., and Tichenor, J., Super cilia skin: An interactive membrane. In CHI '03 Extended Abstracts on Human Factors in Computing Systems (CHI EA '03). 808-809. 2003

[39] Coelho, M., and Maes, P., Sprout I/O: A texturally rich interface. In Proceedings of the 2nd international conference on Tangible and embedded interaction (TEI '08). 221-222. 2008.

[40] Furukawa, M., Uema, Y., Sugimoto, M., and Inami, M., Fur interface with bristling effect induced by vibration. In Proceedings of the 1st Augmented Human International Conference (AH '10). Article 17, 6 pages. 2010.

[41] Hullin, B. M., Hendrik, P., Lensch, A., Rasker, R., Seidel, H., and Ihrke, I., A dynamic BRDF display. In ACM SIGGRAPH 2011 Emerging Technologies (SIGGRAPH '11). Article 1, 1 page. 2011.

[42] Koike, T., and Naemura, T., BRDF display. In ACM SIGGRAPH 2007 posters (SIGGRAPH '07).Article 116. 2007.

[43] Cholewiak, R., and Sherrick, C., A computer-controlled matrix system for presentation to skin of complex spatiotemporal pattern. Behavior Research Methods and Instrumentation, 13(5), 667-673. 1981.

[44] Poupyrev, I., Nashida, T., Maruyama, S., Rekimoto, J. and Yamaji, Y., Lumen: Interactive visual and shape display for calm computing. ACM SIGGRAPH 2004 Emerging Technologies. 2004.

[45] Leithinger, D., Lakatos, D., Devincezi, A., Blackshaw, M., and Ishii, H., Direct and gestural interaction with relief: A 2.5D shape display. In Proceedings of the 24th annual ACM symposium on User interface software and technology (UIST '11). 541-548. 2011.

[46] Rakkolainen, I., Diverdi, S., Olwal, A., Candussi, N., Hoellerer, T., Laitinen, M., Piirto, M., and Palovouri, K., The Interactive FogScreen. ACM SIGGRAPH 2005 Emerging Technologies. 2005.

[47] Lee, C., Diverdi, S., and Hoellerer, T., Depth-fused 3D imagery on an immaterial display. IEEE Transactions on Visualization and Computer Graphics, 15(1), 20–33. 2009.

[48] Sugihara, Y., Hashimoto, H., and Yamamoto, K., A proposal of water display. In Proceedings of the seventh International Conference on Artificial Reality and Tele-Existence, 63-70. 1997.

[49] Barnum, P. C., Narasimhan, S. G., and Kanade, T., A multi-layered display with water drops. ACM Trans. Graph. 29, 4, Article 76 (July 2010), 7 pages. 2010.

[50] Suzuki, T. Water Canvas 2004-2013

[51] Nakamura, M., Inaba, G., Tamaoki, J., Shiratori, K., and Hoshino, J., Bubble cosmos. In ACM SIGGRAPH 2006 Emerging Technologies (SIGGRAPH '06). Article 3. 2006.

[52] Hirayama, S., and Kakehi, Y., Shaboned display: An interactive substantial display using soap bubbles. In ACM SIGGRAPH 2010 Emerging Technologies (SIGGRAPH '10). Article 21, 1 page. 2010.

[53] Suzuki, R., Suzuki, T., Ariga, S., Iida, M., and Arakawa, C., “Ephemeral melody”: Music played with wind and bubbles. In ACM SIGGRAPH 2008 posters (SIGGRAPH '08). Article 80, 1 page. 2008.

[54] Lamb, H. Hydrodynamics (6th ed.). Cambridge University Press. ISBN 978-0-521-45868-9, 1994

[55] Hoshi, T., Compact ultrasound device for noncontact interaction. In Proceedings of ACE 2012, pp. 502-505. 2012

[56] Hullin, M.B., Ihrke,I., Heidrich, W., Weyrich,T., Damberg,G., Fuchs,M., State of the Art in Computational Fabrication and Display of Material Appearance, EUROGRAPHICS 2013 Stateof-the-Art Report (STAR), 2013.

[57] Biet, M., Casiez, G., Giraud, F., Lemaire-Semail, B., Discrimination of Virtual Square Gratings by Dynamic Touch on Friction Based Tactile Displays, Proc. 2008 Symposium on Haptic Interfaces for Virtual Environment and Teleoperator Systems, pp. 41-48, 2008.

[58] Winfield, L., Glassmire, J., Colgate, J.E., Peshkin, M., T-PaD: Tactile Pattern Display through Variable Friction Reduction, Proc. Second Joint EuroHaptics Conference and Symposium on Haptic Interfaces for Virtual Environment and Teleoperator Systems, pp. 421-426, 2007.

[59] Bau, O., Poupyrev, I., Israr, A., Harrison, C., TeslaTouch: Electrovibration for Touch Surfaces, Proc. 23nd Annual ACM Symposium on User Interface Software and Technology, pp. 283-292, 2010.

[60] Amberg, M., Giraud, F., Lemaire-Semail, B., Olivo, P., Casiez, G., Roussel,N. , STIMTAC, a Tactile Input Device with Programmable Friction. Adjunct Proc. UIST'11, pp. 7-8, 2011.

[61] Casiez, G., Roussel, N., Vanbelleghem, R.,Giraud, F., Surfpad: Riding Towards Targets on a Squeeze Film Effect, Proc. CHI'11, pp. 2491-2500, 2011.

[62] O. Bau, I. Poupyrev, M.L. Goc, L. Galliot, M. Glisson: REVEL: Tactile Feedback Technology for Augmented Reality. ACM Trans. Graphics, vol. 34, no. 1, pp. 89-100, 2012.

[63] Ando,H., Miki,T., Inami,M., Maeda, T., SmartFinger: Nail-Mounted Tactile Display, Proc. ACM SIGGRAPH 2002, p. 78, 2002.

[64] Watanabe, T., Fukui,S., A Method for Controlling Tactile Sensation of Surface Roughness Using Ultrasonic Vibration, Proc. IEEE International Conference on Robotics and Automation, vol.1, pp.1134-1139, 1995.

[65] Takasaki, M., Maruyama,Y., Mizuno, T., Resonance Frequency Tracing System for Langevin Type Ultrasonic Transducer, Proc. IEEE International Conference on Mechatronics and Automation, pp. 3817-3822, 2007.

[66] Aigenbauer et al. http://www.aec.at/spaxels/en/, accessed JAN 22, 2014, 2013.

[67] Anton,N., Leonardo,G., Andrea,M., Patrizia,M., “Smart material interfaces: A material step to the future.” In Proceedings of the 1st workshop on Smart Material Interfaces: A Material Step to the Future (SMI '12). ACM, New York, NY, USA, Article 1, 3 pages. DOI: 10.1145/2459056.2459057 http://doi.acm.org/10.1145/2459056.2459057. 2012.

[68] Carter,T., Seah,A.S., Long, B., Drinkwater,B., Subramanian,S., UltraHaptics: Multi-Point Mid-Air Haptic Feedback for Touch Surfaces. UIST'13. 2013.

[69] Cholewiak, R., Sherrick, C., “A computer-controlled matrix system for presentation to skin of complex spatiotemporal pattern.” Behavior Research, 1981.

[70] Gor'kov, L. P., “On the forces acting on a small particle in an acoustical field in an ideal fluid.” Sov. Phys. Dokl. 6, 773–775. 1962.

[71] Iwaki, S., Morimasa, H., Noritsugu, T., Kobayashi, M., “Contactless manipulation of an object on a plane surface using multiple air jets.” Proc. ICRA 2011, 3257–3262, 2011.

[72] Kozuka, T., Yasui, K., Tuziuti, T., Towata A., Iida, Y., “Noncontact acoustic manipulation in air.” Jpn. J. Appl. Phys. 46, 4948–4950. 2007.

[73] Marshall, M., Carter, T., Alexander, J., Subramanian, S., “Ultra-tangibles: Creating movable tangible objects on interactive tables.” In Proceedings of the SIGCHI Conference on Human Factors in Computing Systems (CHI '12). ACM, New York, NY, USA, 2185–2188. DOI: 10.1145/2207676.2208370 http://doi.acm.org/10.1145/2207676.2208370. 2012

[74] Nyborg, W. L. 1967. “Radiation pressure on a small rigid sphere.” J. Acoust. Soc. Am. 42, 497–952. Zellweger, P.T.,

[75] Ochiai, Y. Hoshi, T., Rekimoto, J., "Three-dimensional mid-air acoustic manipulation by ultrasonic phased arrays." ArXiv e-print, arXiv:1312.4006. 2013.

[76] Ochiai, Y., Oyama, A., Hoshi, T., REKIMOTO, J., "Poppable display: A display which enables people to interact with popping, breaking, and tearing." Proc. IEEE GCCE 2013. 124-128. 2013.

[77] Skinner, L, B., Benmore, C, J., Tumber, S., Lazareva, L., Neuefeind, J., Santodonato, L., Du, J., Parise, J. B. 2012. J. Phys. Chem. B 116, 13439.

[78] TOCHIKA. 2013. http://tochika.jp, accessed Sep 18, 2013.

[79] Weber, R. J. et al. 2012. “Acoustic levitation: Recent developments and emerging opportunities in biomaterials research.” Eur. Biophys. J. 41, 397–403. 2012.

[80] Xie, W. J., Cao, C. D., Lu, Y. J., Hong, Z. Y., AND Wei, B., “Acoustic method for levitation of small living animals.” Appl. Phys. Lett. 89, 214102. 2006.

[81] Foresti, D., Nabavi, M., Klingauf, M., Ferrari, A., Poulikakos, D., Acoustophoretic contactless transport and handling of matter in air. Proceedings of the National Academy of Sciences. 2013.

[82] Perlin, K., Han, J., Volumetric display with dust as the participating medium, Feb. 14. US Patent 6,997,558. 2006.

[83] Heiner, J. M., Hudson, S. E., Tanaka, K., The information percolator: Ambient information display in a decorative object. In Proceedings of the 12th Annual ACM Symposium on User Interface Software and Technology, ACM, New York, NY, USA, UIST ’99, 141–148.1999.

[84] Jones, A., Mcdowall, I., Yamada, H., Bolas, M., Debevec, P. Rendering for an interactive 360° light field display. ACM Trans. Graph. 26, 3 (July). 2007.

[85] Cossairt, O., Napoli, J., Hill, S., Dorval, R., Favalora, G., Occlusion-capable multiview volumetric threedimensional display. Applied Optics 46, 8, 1244–1250. 2007.

[86] Wetzstein, G., Lanman, D., Heidrich, W., Rasker, R. Layered 3d: Tomographic image synthesis for attenuation-based light field and high dynamic range displays. ACM Trans. Graph. 30, 4 (July), 95:1–95:12. 2011.

[87] Kimura, H., Aasano, A., Fujishiro, I., Nakatani, A., Watanabe, H. True 3d display. In ACM SIGGRAPH 2011 Emerging Technologies, ACM, New York, NY,

USA, SIGGRAPH '11, 20:1–20:1. 2011.

[88] Whymark, R., Acoustic field positioning for containerless processing. Ultrasonics 13, 6, 251 – 261. 1975.

[89] Inoue, S., Koseki J., Kobayashi, K., Monnai, Y., Hasegawa, K., Makino,Y., Shinoda, H., HORN: the hapt-optic reconstruction. In ACM SIGGRAPH 2014 Emerging Technologies (SIGGRAPH '14). ACM, New York, NY, USA, , Article 11 , 1 pages. DOI=10.1145/2614066.2614092 http://doi.acm.org/10.1145/2614066.2614092, 2014.

# Publications

**[Journals]**

1. Yoichi Ochiai, Takayuki Hoshi, and Jun Rekimoto: Three-dimensional Mid-air Acoustic Manipulation by Ultrasonic Phased Arrays, Plos One 9:5 (2014) e97590. (pre print ArXiv e-print, arXiv:1312.4006)

2. Yoichi Ochiai, Takayuki Hoshi, and Jun Rekimoto: Pixie Dust: Graphics Generated by Levitated and Animated Objects in Computational Acoustic-Potential Field, ACM Transactions on Graphics, 33 (2014) article no. 85

3. Yoichi Ochiai, Alexis Oyama, Takayuki Hoshi, and Jun Rekimoto: Colloidal Metamorphosis: Time Division Multiplex of Colloidal Screen Reflection, IEEE Computer Graphics and Applications, pp.42 - 51, July-Aug. 2014, DOI=10.1109/MCG.2014.41.

4. Yoichi Ochiai, Alexis Oyama, Takayuki Hoshi, and Jun Rekimoto: Colloidal Display: an ultra-thin transparent display with controllable surface state and dynamic properties, VRSJ Journal 18(3), pp. 277-286, 2013. [CiNii] (In Japanese)

**[Conference Proceedings]**

1. Daisuke Yamaguchi, Yoichi Ochiai, Takayuki Hoshi, Jun Rekimoto, Masaya Takasaki: Driving System of Diminished Haptics: Transformation of Real World Textures, Proc. AsiaHaptics 2014, B-18, Tsukuba (Japan), 18-20 Nov., 2014

2. Yoichi Ochiai, Takayuki Hoshi, Jun Rekimoto, and Masaya Takasaki: Diminished Haptics: Towards Digital Transformation of Real World Textures, Proc. Eurohaptics 2014, Poster Article No.53, Versailles (France), 24-27 Jun., 2014.

3. Yoichi Ochiai, Alexis Oyama, Takayuki Hoshi, and Jun Rekimoto: Theory and Application of the Colloidal Display: Programable Bubble Screen for Computer Entertainment, Proc. 10th International Conference on Advances in Computer Entertainment Technology (ACE 2013), pp. 198-214, Twente (Netherlands), 12-15 Nov., 2013.

4. Yoichi Ochiai, Alexis Oyama, Takayuki Hoshi, and Jun Rekimoto: Poppable Display: A Display Which Enables People to Interact with Popping, Breaking, and Tearing, Proc. 2nd 2013 IEEE Global Conference on Consumer Electronics (GCCE 2013), pp. 124-128, Makuhari (Japan), 1-4 Oct., 2013.